Virtual Reaction Chambers as a tool for DNA sequencing

Dissertation
zur Erlangung des Grades
der Doktorin der Naturwissenschaften
der Naturwissenschaftlich-Technischen Fakultät
der Universität des Saarlandes

von

Ana V. Almeida

Saarbrücken

2017

Tag des Kolloquiums: 16.10.2017

Dekan: Univ.-Prof. Dr. rer. nat. Guido Kickelbick

Mitglieder des Prüfungsausschusses:
- Gutachter (Betreuer): Prof. Dr. Andreas Manz
- Gutachter (nicht Betreuer): Prof. Dr. Ralf Seemann
- Vorsitzenden: Prof. Dr.-Ing. Georg Frey
- Promovierter akad. Mitarbeiter: Dr. Gao Haibin

Bitte unterschrieben als Einzelblatt einreichen
und in die Arbeit eingebunden, ebenfalls unterschrieben.

Eidesstattliche Versicherung

Hiermit versichere ich an Eides statt, dass ich die vorliegende Arbeit selbstständig und ohne Benutzung anderer als der angegebenen Hilfsmittel angefertigt habe. Die aus anderen Quellen oder indirekt übernommenen Daten und Konzepte sind unter Angabe der Quelle gekennzeichnet. Die Arbeit wurde bisher weder im In- noch im Ausland in gleicher oder ähnlicher Form in einem Verfahren zur Erlangung eines akademischen Grades vorgelegt.

Ort, Datum

_____

Unterschrift

_____

Abstract

The topic of this thesis refers to the contribution of genetic variations, in which single nucleotide polymorphisms (SNP) can be included, to the manifestation and cause of disease. The facilitation of the treatment and cure of such conditions is done through identification and study of the cascade of biological mechanisms and processes; however the achievement of such goals is hampered by the formidable complexity and scale of the data sets involved in nucleic acid and protein analysis and thus the development of faster and cheaper methods is desirable. An intuitive trajectory for this development is the miniaturization of analytical methods with the incorporation of microfluidics which entails the manipulation of fluid analytes through channels and chambers on the microscale. This young field is projected to be instrumental in the realization of low temporal and financial cost analytical techniques.

This thesis demonstrates the application of open-surface microfluidics to sequence DNA with the use of pyrosequencing. This method facilitates a reduction in instrument complexity and size and thus allows for functional integration or device disposability. Following incubation of the DNA with superparamagnetic particles, it was placed on a hydrophobic glass substrate. The DNA was then moved through microliter-volumes of mineral oil-coated water droplets via manipulation of the nanoparticles using a magnetic field; thus, these droplets could then be used either for pyrosequencing or for washing of the DNA strands. The reaction performance was determined, using the resequencing protocol with a 34 base pair (bps) of single-stranded DNA, to be highly linear for all 4 homopolymers events tested. *De novo* sequencing was performed with 51 and 81 bps while it was also verified that up to 7 homopolymers could be determined. This method displays full compatibility with previously demonstrated open surface steps for sample preparation and so confirms PCR on a flat glass substrate as an integrated sample-to-answer protocol.

All assays were based on primer extension via DNA polymerase. A microfluidic device consisting of microliter-volume droplet-to-droplet DNA transport via manipulation of magnetic particles was used in this work. The

difference in reaction kinetics for matched and mismatched configurations at the 3'-ends of the primer-template complex was employed in sample differentiation. The assay combined pyrosequencing technology with a sequence-by-synthesis bioluminometric DNA sequencing probe on one common microfluidic platform. Base-by-base sequencing was performed to obtain accurate single nucleotide polymorphism (SNP) scoring data with microliter volumes. The application of magnetically actuated beads to facilitate virtual chamber reactions for chip based DNA analysis was presented. Single base incorporation was seen to be detectable with the use of this pyrosequencing assay.

Keywords: DNA sequencing, single nucleotide polymorphisms, superparamagnetic particles, open surface microfluidics, magnetic actuation.

Zusammenfassung

Mit Abschluss des Humangenomprojekts verlagert sich der Fokus darauf, zu verstehen, wie genetische Variationen, wie z. B. Einzelnukleotid-Polymorphismus (SNP, single nucleotide polymorphism), zu Erkrankungen führen. Die enorme Menge an Sequenzinformationen müssen mit schnelleren, wirtschaftlicheren und leistungsfähigeren Technologien für die Analyse von RNA, DNA und Proteinen analysiert werden, um die die biologischen Mechanismen lebender Organismen zu verstehen und zu kontrollieren. Ein Ansatz ist die Miniaturisierung analytischer Methoden durch die Anwendung der Mikrofluidik, wobei Ströme in Kanälen auf der Mikrometer-Skala manipuliert werden. Es wird erwartet, dass Fortschritte in der Mikrofluidik-Chip-Technologie eine wichtige Rolle bei der Entwicklung wirtschaftlicher und schneller DNA-Analysemethoden spielen werden.

In dieser Doktorarbeit wird die Anwendung von Mikrofluidik an offenen Oberfläche für die Sequenzierung von DNA mittels Pyrosequenzierung demonstriert. Dies bietet Vorteile bezüglich der Instrumentengröße, der Einfachheit, Verfügbarkeit und Funktionsintegration, insbesondere in Kombination mit den vielfältigen und flexiblen Möglichkeiten der Mikrofluidik an offenen Oberflächen. Die DNA wurde auf superparamagnetischen Partikeln inkubiert und auf ein Glassubstrat mit hydrophobischer Schicht platziert. Die Partikel mit gebundener DNA wurden mithilfe von Magnetkraft über Tropfen in Mikroliter-Größe, beschichtet mit Mineralöl zur Verhinderung von Verdunstung, bewegt. Diese Tropfen dienten als Reaktionsstationen für die Pyrosequenzierung sowie als Waschstationen. Das Sequenzierungsprotokoll mit 34 Basenpaaren (bps) einzelsträngiger DNA wurde zur Bestimmung der Reaktionsleistung verwendet und zeigte eine ausgezeichnete Linearität für alle 4 Homopolymere. Diese De-novo-Sequenzierung wurde mit 51 und 81 bps durchgeführt. Wir haben außerdem geprüft, dass bis zu 7 Homopolymere bestimmt werden können. Dieses Verfahren ist vollständig mit bisher verwendeten Schritten zur Probenvorbereitung an offenen Oberflächen kompatibel. Daher kann eine PCR als vollständig integriertes System von der

Probe bis zum Ergebnis auf einem flachen Glassubstrat zusammengestellt werden.

In dieser Doktorarbeit werden Mikrofluidik-Anwendungen für verschiedene Genotypisierungsassay vorgestellt. Das übergeordnete Ziel ist die Kombination des Potentials des Chiplabor-Konzepts der Mikrofluidik mit Biochemie, um Verfahren für die DNA-Analyse zu entwickeln uns derzeit verfügbare Verfahren zu verbessern. Drei Genotypisierungsassays werden hier mithilfe von miniaturisierten Mikrofluidik-Methoden überprüft.

Alle Assays basieren auf der Verlängerung von Primeren durch DNA-Polymerase. Ein Mikrofluidik-Instrument mit Handhabung von Tropfen zu Tropfen für Magnetpartikel für Volumen im Mikroliterbereich wurde in diesen Studien verwendet. Das Mikrofluidik-Verfahren nutzt die Vorteile der unterschiedlichen Reaktionskinetik für komplementäre und nicht-komplementäre Konfigurationen am 3‘-Ende des Primer-Template-Komplexes. Insgesamt beinhalteten die Assays die Anpassung der Pyrosequenzierungstechnologie, eines bioluminometrischen DNA-Sequenzierungsassays basierend auf Sequenzierung durch Synthese, an dieselbe Mikrofluidik-Plattform. Basenweise Sequenzierung wurde in einem Mikrofluidik-Instrument durchgeführt, um genaue SNP-Scoring-Daten für Volumina im Mikroliterbereich zu erzielen. In dieser Doktorarbeit wird die Anwendung virtueller Reaktionskammern von Partikel, die magnetisch ausgelöst werden, für die Chip-basierte DNA-Analyse präsentiert. Die Inkorporation von einzelnen Basen mithilfe der Pyrosequenzierungsreaktion wurde auf diesen Partikel beobachtet.

Stichworte: DNA-Sequenzierung, Einzelnukleotid-Polymorphismus, Superparamagnetischpartikel, offene Mikrofluidik, Mikrosystem, magnetische Betätigung

Acknowledgments

I would like to thank everyone who has contributed to this thesis and has made these last few years so enjoyable.

I am especially grateful to:

Andreas Manz for accepting me as a PhD student and for being a true visionary with a fantastic skill for attracting good people.

Pavel Neuzil, Microfluidics group leader, for his guidance during this scientific journey.

My colleagues, fellow students and friends not only in KIST-Europe but overall in Saarbrücken and beyond:

Zeynep and Mark: the shorty-spicy-lady and the tally-gentleman. Wouldn't think of better companions to start this journey with. You guys rock!

Matthias: starting off with the labs and kicking off with the projects on a fresh group and becoming a permanent member of my family…so much to say and so little space. Because of you, Saarland will always be home to me. Thank you for all the inspiring and fruitful discussions on microfluidics and life in general, for being so enthusiastic and, last but not least, for being you.

Jang Mi: my favorite power Frau! Determination and fantastic energy to keep all of those boys under control.

Jukyung and Seung Jae…such a long jurney! Thank you for being part of it!

Tijmen: my climbing partner and honeybear!

Thomas: no bull**** modus operandi and one of the fairest people I know.

Marc: my chuchu! For life! Let's keep on growing and getting distracted with Life.

André and Eric: Perhaps one day I'll be as cool as you.

Leon Abelmann: To prove me on a daily basis that Science is a playground for our curious hearts.

Everyone in KIST-europe: for interesting discussions on a variety of subjects (some of which involved science…) and for the very funny and moments; for being great and enthusiastic colleagues and friends …

KIST-europe for hosting me for these years, to introduce me to such different and beautiful culture and enabling me in Science.

All collegues, former and present, at KIST-Europe for being so nice and helpful and for contributing (everyone in his or her own special way) to the fantastic atmosphere of this place. I feel very privileged to have had the opportunity to get to know you and to work with you, and even if all names aren't listed, you are in my heart.

My friends, in and out of science, for being such great persons and for all the good times we have shared.

My family for always being there for me with good advice, skype calls full of affection or whatever will do the trick to keep me motivated

My parents for endless support and encouragement and for believing in me and wishing me happiness whatever I do. They are my giants ("*The reason why I am seeing so far, it is because I am standing on the shoulders of giants"*, Isaac Newton).

Ferdia, the love of my life, my life-partner, for loving me and being my rock in stormy weather. We made it!

Table of contents

List of abbreviations

Abbreviation	Description
A	adenine
AIDS	acquired immuno defficiency syndrome
AMASE	apyrase-mediated allele-specific extension
ARMS	amplification refractory mutation system
ASA	allele specific amplification
ASPCR	allele-specific PCR
ATP	adenosine triphosphate
AuNPs	gold nanoparticles
bp	base pairs
BSA	bovine serum albumin
C	cytosine
CBC	complete blood count
CCD	charge coupled device
CE	capillary electrophoresis
COC	cyclic olefin copolymer
Cys	cysteine
DASH	dynamic allele specific hybridization
dATP	deoxyadenosine triphosphate
dCTP	deoxycytosine triphosphate
ddC	dideoxycytosine
ddG	dideoxyguanine
ddNTP	dideoxynucleotide
ddT	dideoxythymine
dGTP	deoxyguanine triphosphate
DI	deionized
dNTP	nucleoside triphosphates
dsDNA	double-stranded deoxyribonucleic acid
dTTP	deoxythymine triphosphate
EWOD	electrowetting on dielectrics

FRET	fluorescence resonance energy transfer
G	Guanine
GFP	green fluorescent protein
His	Histidine
HIV	human immuno deficiency virus
Ile	Isoleucine
IPA	isopropyl alcohol
LCR	ligase chain reaction
Leu	Leucine
LNA	locked nucleic acid
LOC	lab-on-a-chip
MEMS	Microelectromechanical
Met	Methionine
MPs	magnetic particles
OLA	oligonucleotide ligation assay
OSM	open surface microfluidics
PASA	PCR amplification of specific alleles
PC	poly(carbonate)
PCR	polymerase chain reaction
PDMS	polydimethylsiloxane
PMMA	poly(methyl methacrylate)
POC	point-of-care
PPi	pyrophosphate
PTFE	polytetrafluoroethylene
RCA	rolling circle amplification
SBE	single base extension
SBH	sequencing-by-hybridization
SBS	sequencing-by-synthesis
Ser	Serine
Ser	Serine
SNP	single-nucleotide polymorphism
SPP	superparamagnetic particles
SSB	single-stranded DNA-binding protein

ssDNA	single-stranded deoxyribonucleic acid
SU-8	epoxy-based negative photoresist
T	thymine
Thr	threonine
TNP	triple-nucleotide polymorphisms
Tyr	tyrosine
UV	ultraviolet
Val	valine
μTAS	miniaturized total analysis systems

Chapter 1

Introduction: DNA

The human body consists of approximately $3{,}72 \times 10^{13}$ cells[1], most containing the hereditary information of the genome in the form of 6×10^{9} base pairs of deoxyribonucleic acid (DNA).[2] DNA molecules are the libraries in living cells where the information required for building a cell and an organism are stored.

This subchapter **1.1** briefly describes relevant information over DNA and corresponding sequencing technologies and the microfluidics field, emphasing the inter-relation between both topics.

1.1 Chemical structure of DNA and organization

DNA is a linear polymer composed of single chemical units called nucleotides.[3-4] The number of nucleotides in a cellular DNA molecule can exceed a hundred million.[2] A nucleotide has three parts: a phosphate group, a deoxyribose and an organic base. The bases are adenine, guanine, cytosine and thymine; abbreviated A, G, C and T, respectively.[4] When the nucleotides polymerize to form DNA, the hydroxyl group attached to the 3' carbon of the sugar group of one nucleotide forms an ester bond to the phosphate attached to the 5' carbon of another nucleotide. This dictates the extremely important property of the orientation of the polynucleotide strand.[5] DNA consists of two associated polynucleotide strands forming a double helix. The sugar-phosphate backbones are on the outside of the double helix and the bases project into the interior. The orientation of the two strands is antiparallel and complementary to each other. The strands are held together by the cooperative energy of many hydrogen bonds in addition to hydrophobic interactions.[6-7] The opposite strands are held in precise register by a regular base pairing between the two strands: A is paired with T by two hydrogen bonds and G is paired with C by three hydrogen bonds.[7]

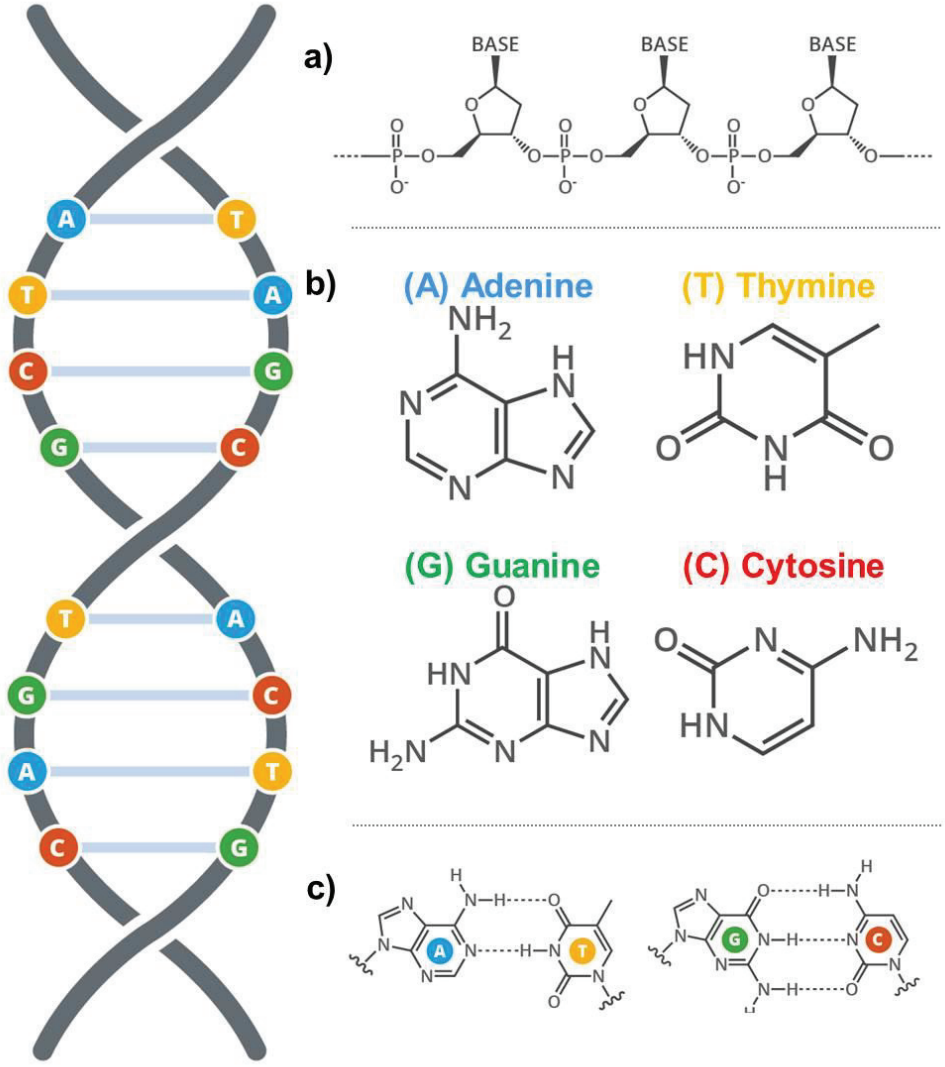

Figure 1: *Chemical structure of DNA. DNA stores and transmits genetic information in all multicellular life forms. The sequences formed by the bps code for proteins which execute a wide range of physiological functions. a) The "backbone" made up of phosphate sugars which support the subunits of the polymer, each nucleotide consists of a phosphate group, a sugar group and a base. b) Adenine, thymine, guanine and cytosine are the bases present in DNA. c) These bases form base pairs (bps) with the second strand in the double helix; Adenine (A) always pairs with Thymine (T), whilst guanine (G) always pairs with cytosine (C).*

1.2 Genomic variations

This DNA is arranged into *n* chromosomes or in a plasmid depending on the organism (**Figure 2**) and the composition of the DNA bases within these macromolecules determines the genotype and contributes to the phenotype of an individual[8] (**Figure 1**). Consequently, alterations in chromosomes may lead to genetically related diseases (**Figure 3**). Cells are constantly exposed to agents and events that can be harmful to the DNA. Depurination, deamination, oxidation and methylation of bases are endogenous events that can change the base composition of DNA, while exogenous agents such as UV light, ionizing radiation and genotoxic substances may damage DNA by creating pyrimidine dimers, double strand breaks and adducts.[9-14] Several different gatekeeper and DNA repair systems exist to maintain DNA integrity, but occasionally these backup systems fail and mutations arise.

1.2.1 Mutations

Mutations can be divided into two classes; **gross alterations** and **subtle alterations**. Gross alterations involve changes in chromosome number, partial deletions of chromosomes, chromosomal translocations and gene duplications, while subtle alterations comprise of single base substitutions, insertions and deletions.[15-16] Mutations are common events in cancer and the ability to monitor them is therefore of great interest for diagnostic and prognostic purposes as well as in understanding gene function.[17]

Therefore, detecting genomic variations is fundamental in genetic research. For example, in cancer research, mutation detection is vital for diagnosis but also gives insight into gene function[18]. Strains of microorganisms can also be identified by point variations in their genome, and, in recent years, the pharmaceutical companies have shown a rising interest in single nucleotide variations to be able to use “the right drug for the right patient”.[19]

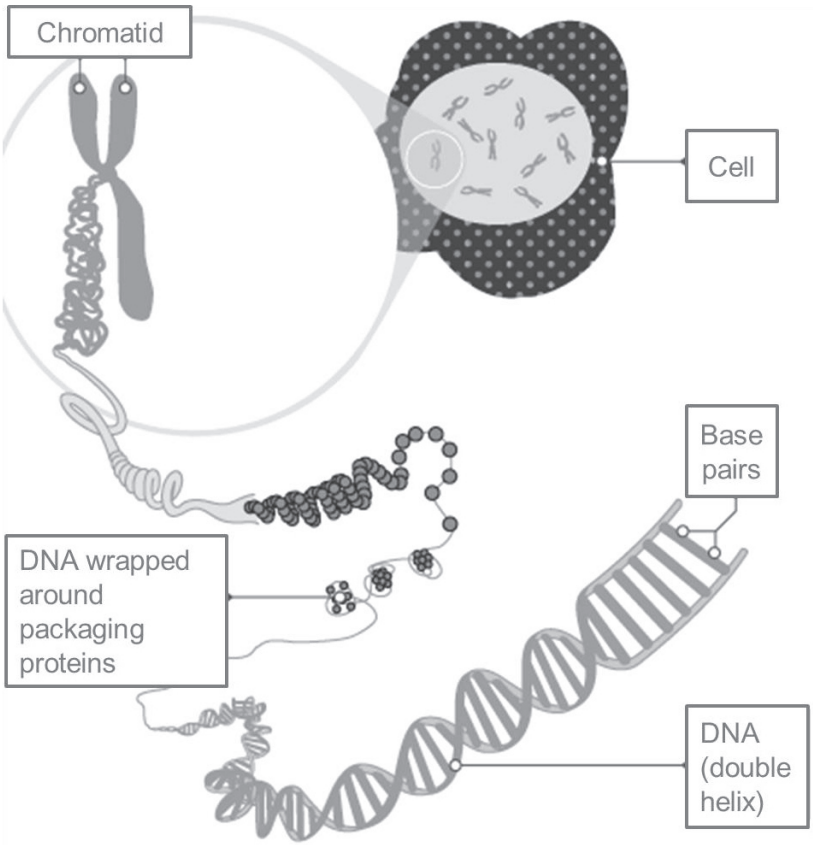

Figure 2: *DNA configuration. DNA is contained within the cells of every living thing though its organization varies within different life form. A binary distinction can be made between the two main DNA organizational conformations with organisms being either prokaryotes or eukaryotes. a) Prokaryotes. Bacteria are prokaryotic cells. They do not exhibit membrane-bound nucleus with their DNA, instead existing freely in the cytoplasm. Their monochromosomal DNA sequence, which is circular in aspect and located at the center of the cell, contains the genetic information required to support all cellular functions. Additional rings of bacterial DNA known as plasmids. Certain genes within these plasmids can code for antibiotic resistance which increases the probability of survival. Interbacterial exchange of plasmids is also possible through hair-like extensions from each cell's surface known as pili. b) Eukaryotes: animal, plant and fungi cells are eukaryotes. All contain a membrane-bound nucleus in which the cell's chromosomes are linear. Chromosomal DNA is tightly coiled around special proteins, known as histones, shown below. (adapted from http://www.bbc.co.uk/education/guides/z36mmp3/revision/2).*

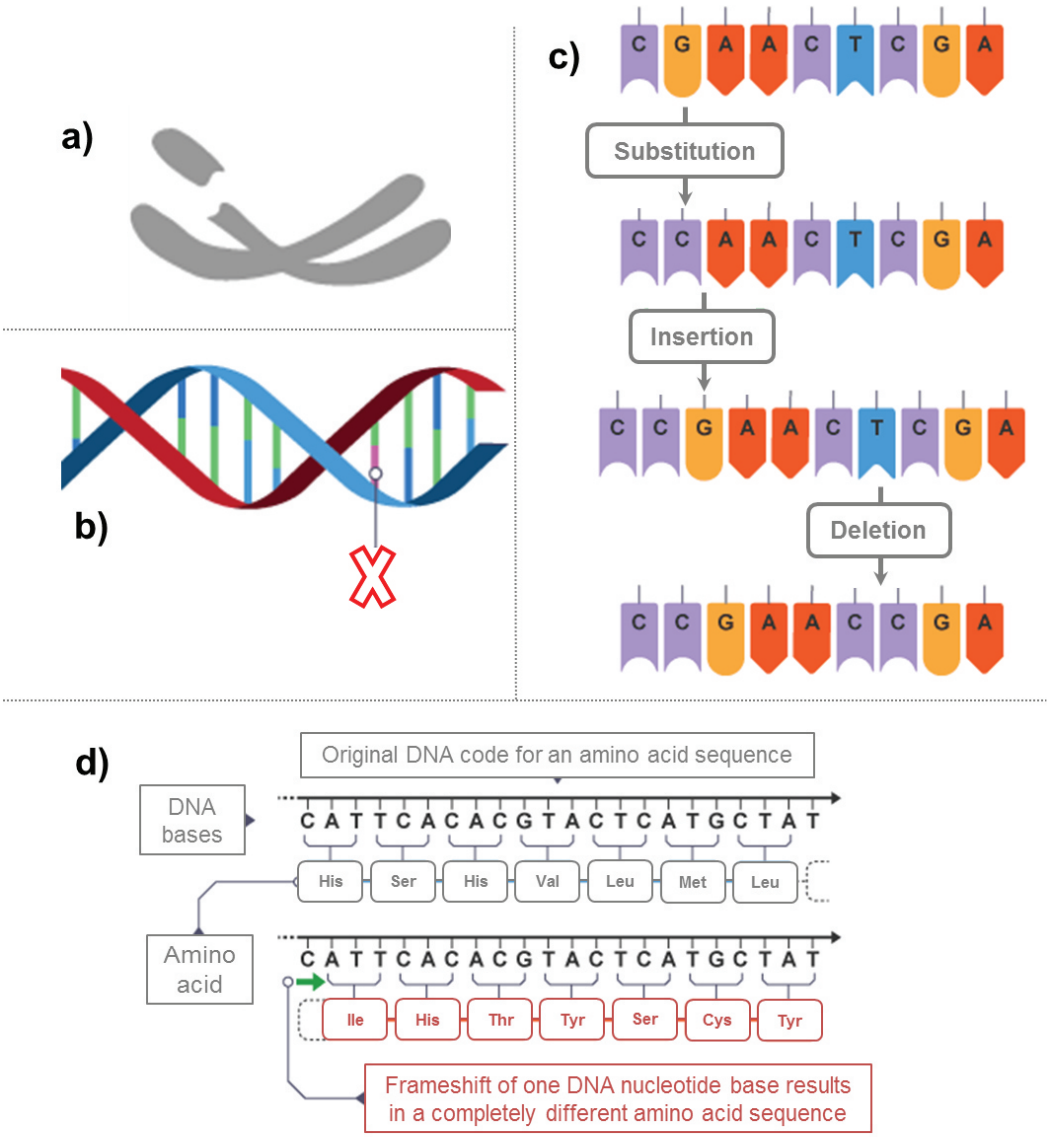

Figure 3: *Figure 3: Mutations: During cell division, the DNA replication process is stringently controlled in order to preserve the genetic code held within the sequence of nucleotides. Despite this, encoding errors do evade this mechanism and exist in the copied genome as mutations, from which no protein or an altered protein can be expressed. Structure mutations affect the structure of one or more chromosomes (a) while single gene mutations affect only a small number of bases (b). Point mutations refer to the substitution of one codon alone which can result in missense, nonsense or a splice-site mutation (c). Frame shift mutations occur when insertions or deletions are not corrected (d).This implies that when nucleotides are grouped in threes to form codons the reading frame is shifted by one so that completely unrelated amino acids are outputted resulting in a most commonly junk protein (adapted from http://www.bbc.co.uk/education/guides/zc499j6/revision/2).*

Gross alterations involve chromosomal number, chromosomal translocation, and partial deletion of chromosomes. These types of genomic alterations can be detected by rather simple techniques, such as microscopy and fragment analysis of implicated chromosomal regions.[20] Mutation detection of **subtle sequence alterations**, however, requires more sensitive techniques, is time-consuming and is more expensive. This perhaps explains why a wide range of techniques have been developed for this purpose. The growing number of methods indicates that a perfect technique which fulfills the required criteria and is able to detect all possible mutations/variations has yet not been described.[21]

The techniques for detecting subtle sequence changes can be divided into three groups. The first is known as scanning methods and is used to search for unknown mutations in pre-defined sequences.[22] The second group is known as diagnostic methods and is used to search for analysis of mutations and variations at defined positions, such as hot-spot sequences and single nucleotide polymorphisms (SNPs)[23]. Since SNPs are much more frequent than hot-spot mutations and because most recent efforts have been focused on detecting single nucleotide variations, the diagnostic techniques will hereafter be referred to as methods for analysis of SNPs[24]. The third group of method is sequencing technologies that are used to reveal the exact nature of a mutation, regardless of being unknown or pre-defined[25].

Some of these techniques and their application fields will briefly be reviewed here. However, irrespective of the mutation status (known or unknown), all the techniques have advantages and disadvantages. Some are simple but do not detect all mutations while others are more complex and detect almost all mutations. Often, factors such as laboratory and personnel experience, required accuracy, required throughput, cost and project type have to be taken into account prior to selection of a method.[26-27]

1.2.2 Single nucleotide polymorphisms (SNPs)

The DNA content of one individual is 99.9 percent identical to any other person's DNA. Differences in the sequence of DNA among individuals are called genetic variation. Genetic variation accounts for some of the differences between individuals, such as eye color, length, and blood group. However, genetic variation may also predispose some people to disease and explain why some respond better to certain drugs than to others. Therefore, detecting genetic differences between individuals and determining their impact on human health are fundamental in genomic research. The most common genetic variations are called single-nucleotide polymorphisms (SNPs). SNPs are single base-pair positions in genomic DNA at which different sequence alternatives, alleles, exist in normal individuals in a population (**Figure 4**). By definition, a position is referred to as a SNP when it exists in at least two variants for which the least abundant allele is present at or above a frequency of 1% in the tested population. Variations that occur at lower frequencies are not considered useful for genetic studies simply because they are not likely to occur in enough individuals. They are referred to as rare variants of the locus instead of SNPs. SNPs occur on 3 per 1000 base pairs in the human genome on average [28].

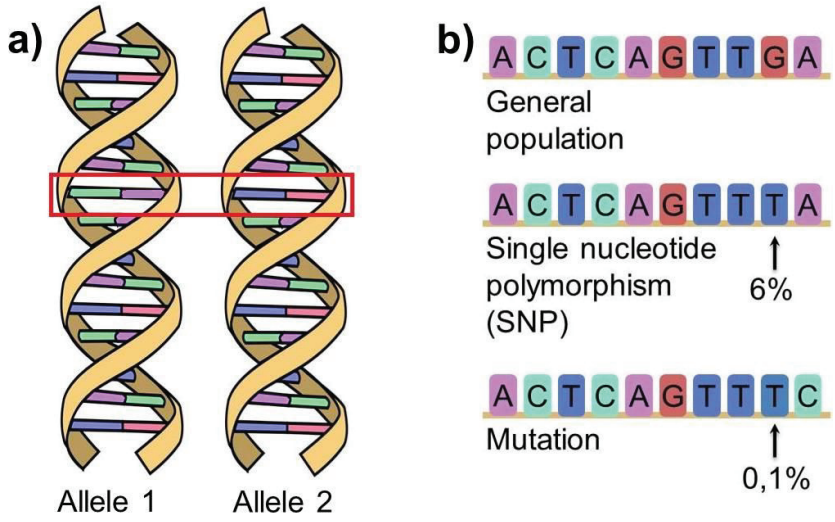

Figure 4. *a) SNP position with two alternative DNA sequences (alleles); b) SNP incidence vs mutation incidence. The percentages shown (6% for SNPs and 0,1% for mutation refer to occurrence in a given population).*

There has been a large academic and industrial effort to discover and catalogue SNPs. To date, nearly 10 million SNPs have been catalogued and entered into public databases, such as the SNP Consortium (TSC) and the Human Genome Variation database (HGVbase). Recently, the haplotype mapping (HapMap) project was initiated in a joint effort by leading academic and commercial teams. A haplotype is defined as a series of closely linked alleles in a unit on the same chromosome. The haplotypes can contain a large number of SNPs, but a few SNPs are enough to uniquely identify the haplotypes in a block. The aim is to characterize the structure of sequence variation throughout the genome. SNP maps promise to increase significantly our ability to understand and treat complex diseases such as cancer, diabetes, asthma, vascular disease, and psychiatric disorders. Furthermore, their high prevalence of distributions across the genome [29-30] makes SNPs suitable for serving as genetic markers in linkage studies. Because DNA segments that lie near each other on a chromosome tend to be inherited together, SNPs can be used as an indirect way of tracking the inheritance pattern of a gene that has not yet been identified but whose approximate location is known. Therefore, pharmaceutical companies may also use SNPs as markers to discover new and better genes for identifying new drug targets for a number of common and complex diseases.

As the number of identified SNPs increases, the demand will increase for efficient methods to score them to fully explore their impact on human health. Several methods that have been developed to meet the demand are reviewed in the subchapter **1.4 SNP genotyping technologies**.

1.3 DNA sequencing techniques

Despite the wide range of techniques available for mutation detection, DNA sequencing is the most accurate method to determine the exact nature of a mutation or a variable position. DNA sequencing is considered to be the golden standard for mutation and SNPs detection, and for this reason, mutations and SNPs determined by scanning methods (described in subchapter **1.4**) must be confirmed by DNA sequencing. Among DNA sequencing methods,

conventional Sanger DNA sequencing has been used extensively, but techniques, such as sequencing by hybridization, mass spectrometry and pyrosequencing, have recently gained attention.

In this subchapter, the focus will be aimed at [31] sequencing methods and technical parameters, such as sequencing speed, read length, and base-call precision.

1.3.1 Polymerase chain reaction (PCR)

Despite not being a sequencing technique, many of such techniques are strongly based or dependent on polymerase chain reaction.

The polymerase chain reaction (PCR) is an in vitro molecular biology technique used to amplify nucleic acids (DNA). It was originally developed by Kary Mullis (Nobel Prize, Chemistry 1993) during his time working at the Cetus Corporation in the 1980s. This technique is now standard in the majority of biology laboratories throughout the world and has been incrementally improved from its introduction in 1983 [32].

The reaction embodied in the PCR technique is a primer extension with serves to augment nucleic acid sequences in vitro. Its application in the field of molecular diagnostics has grown to the degree that its adoption as a tool for nucleic acid detection is nigh on universal and has made the technique a key tool in research, development and clinical diagnostics.

Thermostable polymerase (most commonly derived from the thermophilic bacterium *Thermus aquaticus* and called Taq) has facilitated the isolation of freshly synthesized complimentary DNA with negligible reduction in enzymatic function. As the PCR amplication process is a power function, the increase can be as high as a billion fold in only a short number of runs which allows for the rapid determination of qualative and quantitative information about the sequence of interest. Since its advent, substantial improvements and modificaitons have been reported, including multiplex PCR[33], asymmetric PCR[34], hot-start PCR[35], nested PCR[36], RT-PCR[37], touchdown PCR[38], real-time PCR[39-41], and miniaturization[42-43].

The reaction entails the hybridization of the strands of a DNA molecule of interest to two synthetic oligonucleotides or primer sequences. The hybridized synthetic sections can then act as a substrate for a DNA polymerase to build a complimentary strand through sequential incorporation of the appropriate nucleotide. The whole process can be simplified to three steps (**Figure 5**) which are (i) the separation of dsDNA into its two complimentary strands at a temperature of =/>90ºC, (ii) annealing of the primer occurs at 50-75ºC and (iii) the extension optimally occurs between 72 and 78ºC [44]. The rate at which the changes in temperature occur, referred to as the ramp rate, and the duration at which the reaction remains static at each temperature and the number of times these cycle runs are repeated are controlled by the thermocycler. The progression of technological capacity throughout the intervening years have led to a considerable reduction in the ramp times via the use of electronically mediated heating blocks or forced convection heat exchangers for rapid temperature change.

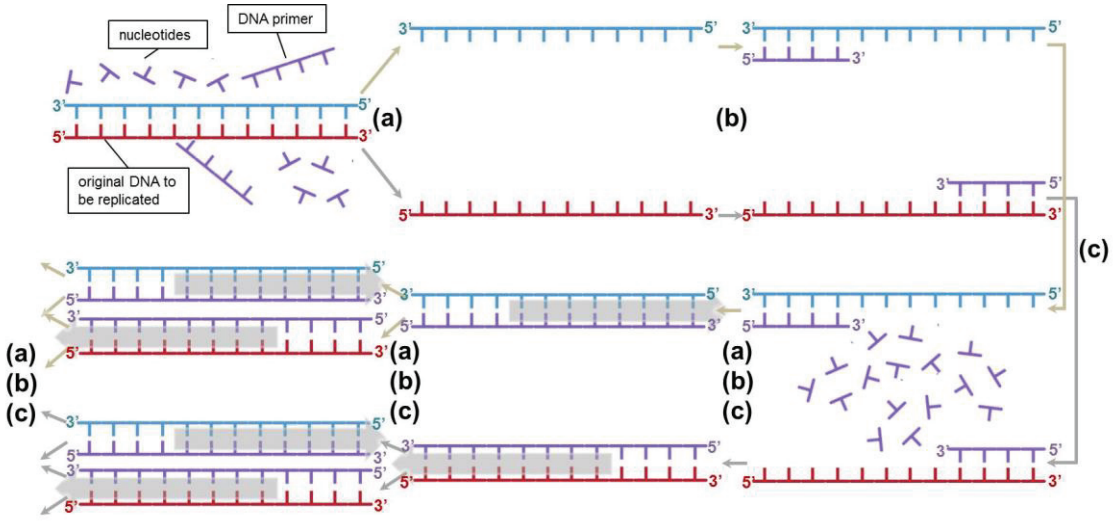

Figure 5: *Schematic drawing of the PCR cycle* ***(a)*** *denaturation: DNA strands separate at temperature of 95ºC;* ***(b)*** *annealing takes places at circa 60ºC when the primer binds to the complementary bases at the end of the sequence of each strand;* ***(c)*** *elongation: at 72ºC a heat resistant DNA polymerase forms the complimentary sequence to the template strand thus forming a new double stranded DNA molecule. This process can be repeated for 25 – 30 cycles to amplify the sequence of interest*

1.3.2. Dideoxy DNA sequencing by chain termination (Sanger DNA sequencing)

The advent of the Sanger nucleic acid sequencing technique [45] has cause nothing short of a revolution within the biological sciences. A testament to the worth of this facile protocol, as already stated above, is the fact that it is still in use to this day, more than a quarter century after its inception, having amassed numerous improvements and advancements over this time. The modulus operandi of this procedure is the termination of enzymatically synthesized DNA. It is not possible for the dideoxynuleotide (ddNTP) to form a proceeding bond in a DNA sequence and thus, the synthetic process is disabled when a ddNTP is inserted into the forming chain. Four separate reactions are executed, one for each base after which each reaction can then be separated by molecular weight using electrophoresis. The sequence can be determined with the combination of the four electrophoretograms with gaps in one being filled with complimentary bands from the other three reactions. This principal is shown in **Figure 6**.

Even with its labor intensive, low throughput tedium, Sanger sequencing remains in use to this day. One factor which can be attributed to its notable resilience within the modern laboratory is the technique's ability to detect virtually any and all mutations as well as describe the specific nature of the alteration form the original. Additionally, it has an average read length of 500 bases and is thus applicable to the genome sequencing and re-sequencing.

The demand for long read-length, or the number of bases read per run, a key necessity for a DNA sequencing technique along with short analysis duration, low cost and high accuracy has obliged several modifications to the original technique. Automation in particular has been a key enhancer to the original method by increasing throughput and freeing up resources to facilitate the sequencing of extended lengths of DNA.

Within the modern automated sequencing protocol, the electrophoretic separation of the strand lengths is combined with a fluorescent detection process via incorporation of a fluorescing moiety into the ddNTP markers and thus can be observed in real time through excitation of the strands by a laser beam (Figure 6). The sequencing techniques applied to this setup can

incorporate either one dye only or four-dye labeling system. The former employs one single dye moiety functionalized with one of the four bases creating, ddA, ddC, ddG and ddT; as each of these molecules have identical emission spectra, they must be separated in to four lanes for electrophoretic identification of their locations [46-47] (e.g. the Amersham Pharmacia Biotech's A.L.F. DNA sequencer). The latter four-dye labeling system avails of the use of fluorescent moieties with dissimilar emission wavelengths thus enabling the simultaneous detection of the location of each base in one lane only [48] (e.g. Perkin Elmaer's ABI DNA sequencer) which makes high-through put screening feasible. It is indeed the development of such a high throughput system that has facilitated the creation of software tools for the rapid quantification of polymorphisms and mutations within a sequence. However, the simultaneous detection of four partially overlapping emission peaks obliges the use of a computer algorithm to interpret and resolve the raw signal to its associated base with the accuracy of this sometimes hampering and delaying the identification of mutations and differences between sequences (**Figure 7**).

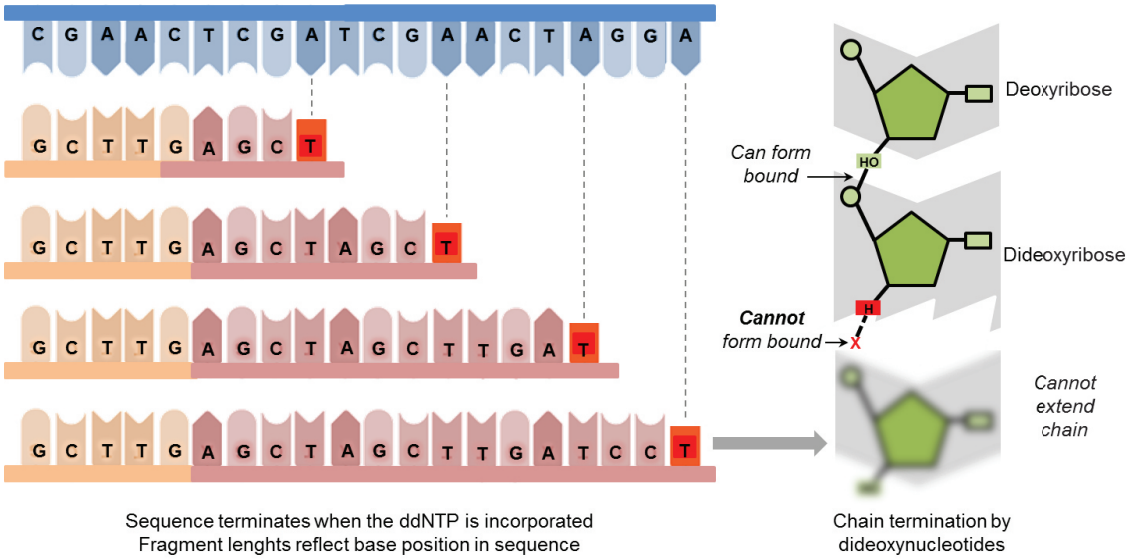

Figure 6: *<u>Dideoxynucleotide:</u> Dideoxynucleotides (ddNTPs) lack the 3'-hydroxyl group necessary for forming a phosphodiester bond. Consequently, ddNTPs prevent further elongation of a nucleotide chain and effectively terminate replication. The resulting length of a DNA sequence will reflect the specific nucleotide position at which the ddNTP was incorporated. For example, if a ddGTP terminates a sequence after 8 nucleotides, then the 8th nucleotide in the sequence is a cytosine*

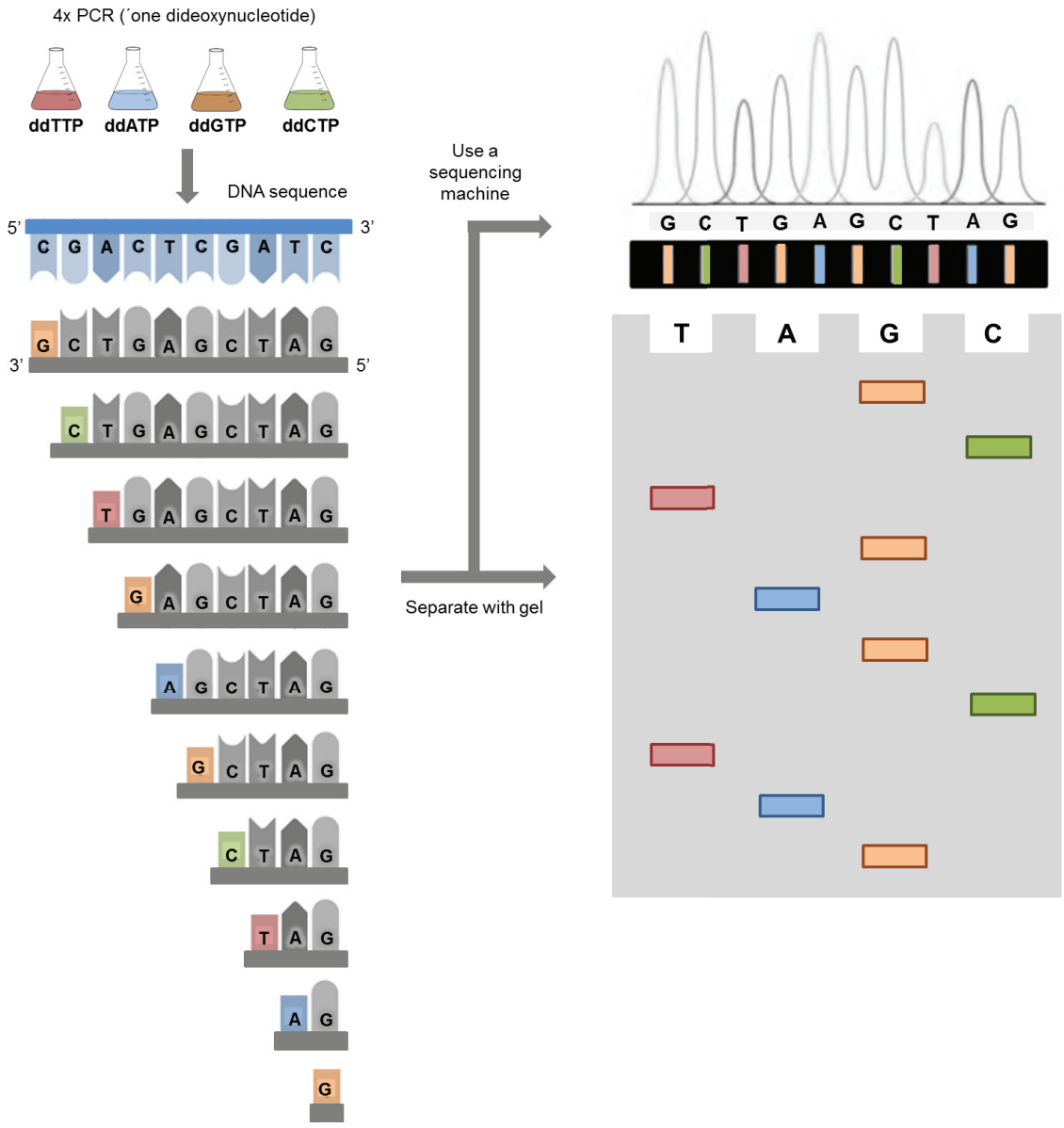

Figure 7: *<u>Sequencing:</u> Dideoxynucleotides can be used to determine DNA sequence using the Sanger method. Four PCR mixes are set up, each containing stocks of normal nucleotides plus one dideoxynucleotide (ddA, ddT, ddC or ddG). As a typical PCR will generate over 1 billion DNA molecules, each PCR mix should generate all the possible terminating fragments for that particular base. When the fragments are separated using gel electrophoresis, the base sequence can be determined by ordering fragments according to length. If a distinct radioactive or fluorescently labelled primer is included in each mix, the fragments can be detected by automated sequencing machines. If the Sanger method is conducted on the coding strand (non-template strand), the resulting sequence elucidated will be identical to the template strand.*

There are three different approaches for dye labeling of the sequencing fragments. The first approach is the use of a 5'-end dye labeled sequencing primer [46, 48]. The second approach is to label the 3'-ends of the sequencing fragment by using dye-labeled dideoxy nucleotides (dye-terminators) [47]. Alternatively, fluorescently labeled nucleotides in an extension-labeling step can internally label the fragments [49].

Acrylamide slab gel electrophoresis has been the most widely adopted format for Sanger sequencing. Relying merely on slab gel technology was not sufficient to accomplish the challenges set by the Human Genome Project. The continual and unrelenting drawbacks of slab gel electrophoresis and the demand for more rapid sequencing and higher throughput led to the development of capillary electrophoresis (CE) [50]. The completion of the human genome was only possible due to several technological advances offered by CE.

Electrophoresis is performed basically in an approach similar to slab gels with the advantage that each capillary contains a single DNA sample and therefore tracking problems are eliminated.

1.3.3. Non-electrophoretic DNA sequencing methods

A few DNA sequencing methods which are not electrophoretic based have been conceived in the last decades. These techniques have advantages and disadvantages compared to electrophoretic separation methods, depending on the type of applications performed and have promising applicability into miniaturized systems.

Sequencing-by-hybridization

The sequencing-by-hybridization (SBH) technique is in fact based on the same principle as that of Southern blotting [51] and was simultaneously described by two independent research groups in 1988 [52]. It key premise was its ability to facilitate *de novo* sequencing with the development of hybridization arrays[53-54]. The technique entails the labeling and subsequent annealing of an unknown strand of DNA to an array of short length oligonucleotides (e.g. all

65,536 combinations of 8-mers) which is followed by the analysis of the sequence by the pattern formed from its hybridization with the array. For this a computer assisted assembly program is essential for the ultimate reconstruction of the correct order and sequence of the original strand (**Figure 8**).

Because of the sheer scale of the data set from which the sequence is determined, the SBH technique has been prone to produce ambiguous results due to repetitive regions within the unknown sequence. Additionally, the formation of secondary structures within the target also reduces the accuracy of this technique. False positives are also caused by single base mismatches resulting from variations within the stability of the duplex of a complete match; this mostly occurs at the 3'-terminus. The effect of these issues can be minimized with the use of expression analysis or comparative sequencing between SBH microarrays though these issues have still not been solved in *de novo* sequencing.

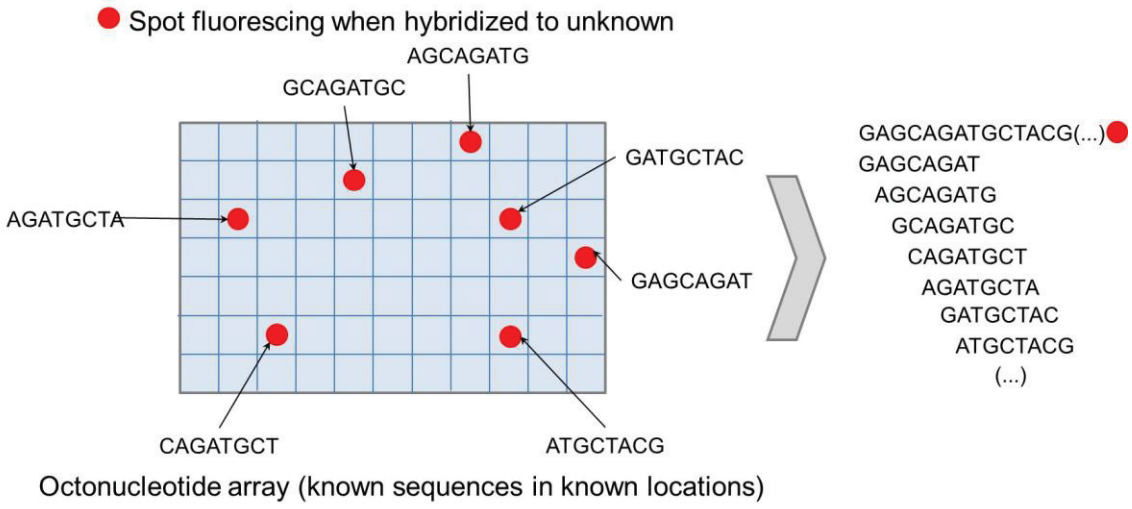

Figure 8 *Sequencing-by-hybridization (SBH) (i.e. the reverse dot-blot format). An unknown target is labeled and hybridized with an array of known octamer oligonucleotides, with the formed hybridization pattern being interpreted to determine the sequence of the targeted DNA sequence.*

Sequencing-by-synthesis

The approach referred to as sequencing-by-synthesis (SBS) was first described in 1985 by Robert Melamede [55]. This technique consists of the

sequential addition and incorporation of nucleotides in an extension reaction directed by a polymerase primer in such a manner that a strand complementary to the original forms through interactive addition of the four dNTPs. **Figure 9** shows the principle of SBH.

The detection of incorporation of nucleotides in the primed DNA strand can be done either directly or indirectly. In the direct method, fluorescent labels are attached to the dNTPs to allow their detection with an appropriate detection method [56-57]. A draw back to this technique is the low number of bases that can be added due to the high failure rate of nucleotide incorporation which can in turn lead to desynchronization of the sequence being copied [57]. The post-synthesis removal of the fluorophore acts as one further step in the process during which errors can be introduced.

The indirect approach to detection employs natural nucleotides for the incorporation process. The pyrophosphate (PPi) released during the condensation polymerization reaction of the growing chain is then detected as an indirect indication of successful nucleotide incorporation [58-59]. The principal advantage of this approach is the ability to use unadulterated, naturally occurring nucleotides which in turn exhibits superior incorporation efficiency in the assay. The enzymatic process laid out in the scheme below details is based on the luminometric detection of ATP through the conversion of PPi molecules through an enzymatic cascade.

$$(\mathrm{DNA})_n + \mathrm{dNTP} \xrightarrow{\text{DNA polymerase}} (\mathrm{DNA})_{n+1} + \mathrm{PPi} \quad (1)$$

$$\mathrm{PPi} + \mathrm{APS} \xrightarrow{\text{ATP sulphurylase}} \mathrm{ATP} + \mathrm{SO_4^{-2}} \quad (2)$$

$$\mathrm{ATP} + \text{luciferin} + \mathrm{O_2} \xrightarrow{\text{luciferase}} \mathrm{AMP} + \mathrm{PPi} + \text{oxyluciferin} + \mathrm{CO_2} + \mathrm{hv} \quad (3)$$

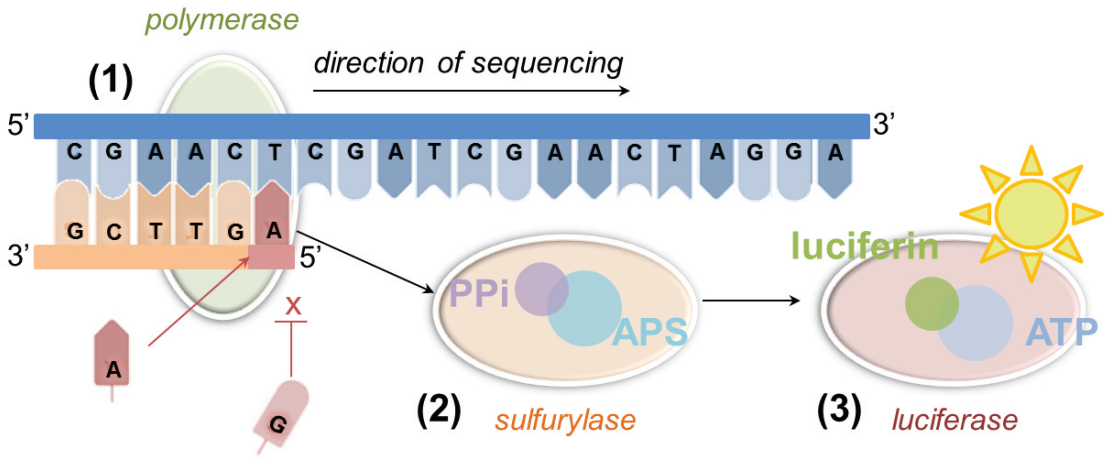

Figure 9. *An illustration of the underlying principal of sequencing by synthesis consisting on the primed DNA template being subjected to iterative additions of nucleotides while in the vicinity of a DNA polymerase molecule, represented in the schematic as an oval shape. If a complimentary nucleotide is added, incorporation of it into the sequence can be conducted through a condensation reaction, releasing a PPi molecule and polymerizing the nucleotide to the chain.*

With the addition of dNTP to the reaction mixture, the DNA polymerase incorporates a complimentary nucleotide onto the 3'terminus of the strand which releases a PPi molecule into the solution. The free PPi molecule can then be observed via a coupled enzymatic reaction consisting of the ATP sulfurylase-mediated conversion of PPi to ATP which is in turn consumed by the firefly luciferase enzyme to produce detectable fluorescence [58, 60]. Detection of the signal is done with a photon multiplier or a charge coupled device (CCD) camera. This method does not, however, lend itself to the robust sequencing of DNA and thus no further progression of the technique is reported in the literature.

In progressive stages over the course of time, the sequencing-by-synthesis method has been developed into a robust, easy-to-use sequencing method for DNA through improvements in the removal efficiency of nucleotides and additional modification of the sequencing-by-synthesis principal. The innovation of the Pyrosequencing technology developed and described by Nyrén and colleagues is a direct result of this [61-63].

1.3.4 Pyrosequencing technology

The negation of unincorporated or excess dNTPs through total removal or degradation has been a key factor in the application of the sequencing-by-synthesis technique to DNA sequencing. In the Pyrosequencing method, the removal of nucleotides is executed in one of two ways (i) the **solid-phase approach** uses a three-coupled enzyme-mediated reaction with interspersed washing steps and (ii) the **liquid-phase approach** which uses a combination of four enzymes in a cascade reaction which requires no additional washing step.

Pyrosequencing by the solid-phase approach

The solid-phase approach localizes the sequencing-be-synthesis method to the surface of a solid-phase. All four nucleotides are added and then removed in dispensing and washing steps with one additional nucleotide being added to the sequence each time. There are several solid-phases currently in use; magnetic beads are on more recent approach [64] where a DNA template and annealed primer is labeled with biotin and immobilized on a magnetic bead which is coated with streptavidin. The primed strand of DNA is incubated with the three enzymes, DNA polymerase, ATP sulfurase and luciferase. Following the addition of each nucleotide, the DNA template is immobilized through the application of a magnetic field to the magnetic particles, holding them stationary while the washing cycle is completed.

There are several drawbacks to this method including the stripping of the DNA templates during the washing step, repetitive addition of enzymes and difficulties achieving a steady baseline; in addition, by its technical nature, this method does not lend itself to facile automation. A more promising approach is the use of a flow system to detect PPi and ATP on streptavidin coated substrates on which are biotin-mediated immobilization of ATP sulfurylase and luciferase. The use of a dynamic fluid flow should result in a more stable base line and in turn improve the detection of the sequence signal. This modified method is also more economical as the enzyme mixture does not need to be replenished after each addition of dNTP; additionally the constant fluid flow

serves to remove all inhibitory products in real time, thus rendering the reaction un-attenuated as well as making the system applicable to a microfluidic format.

The solid phase Pyrosequencing method was successfully applied to the microfluidic paradigm by 454 Lifesciences (since acquired by Roche) [65].

Pyrosequencing by the liquid-phase approach

The introduction of a nucleotide-degrading enzyme, called apyrase, was responsible for the breakthrough of liquid-phase Pyrosequencing [60-61, 63]. The introduction of this enzyme into the Pyrosequencing system negated the use of solid-phase separation and thus rendered obsolete the additional washing and enzyme addition steps synonymous with the latter. Apyrase exhibits high catalytic activity with low amounts of it efficiently degrading unincorporated nucleoside triphosphates in the reaction system first to nucleoside diphosphates and then to nucleoside monophosphate. Apyrase also serves to stabilize the base line with no fluctuations in the procedure as the enzyme catalysis reaction proceeds.

This liquid-phase Pyrosequencing method utilizes a combination of four enzymes in a cascade reaction while the sequencing of the DNA strand is observed in real time. The reaction is begun with the annealing of a primer onto a single DNA strand serving as the template. **Figure 10** presents a schematic description of the sequencing of a partially amplified DNA strand of the human papillomavirus (HPV) with Pyrosequencing devices. The four enzyme-catalyzed cascade reaction is shown whereby APS indicates adenosine 5'-phosphosulphate and *hv* is the light photons emitted by the bioluminescent enzymatic reaction.

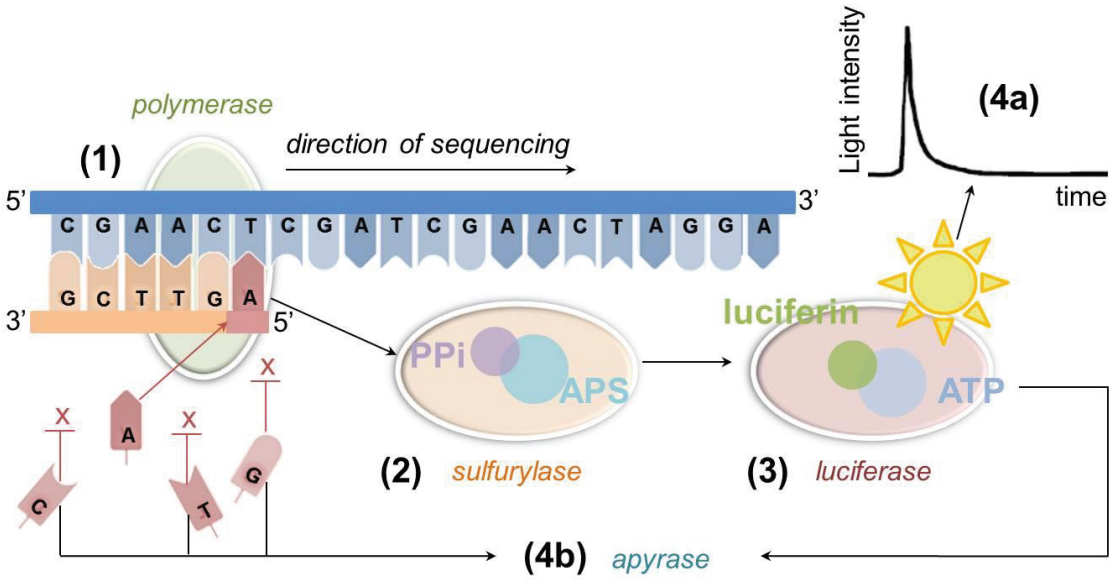

Figure 10. *The liquid-phase Pyrosequencing method is a non-electrophoretic real-time DNA sequencing method which relies employs the release of light from the luciferase-luciferin reaction as a detection signal to indicate the incorporation of a nucleotide onto the target strand of DNA. All four nucleotides are added in iteration to a mixture of four enzymes (1). The pyrophosphate (PPi) which is released in the DNA polymerase-catalyzed reaction is converted quantitatively to ATP by ATP sulfurylase (2); this provides the required energy to facilitate the oxidation of liciferin by firefly luciferase to generate a light (hu) (3). This light can be then detected by a photon detection device and observed in real time through the use of an appropriate piece of computer software (4a). Apryase then catalyzes the degradation of the unincorporated nucleotides at which point the cycle is complete and the system is ready for the addition of the next nucleotide (4b)*

In the liquid-phase Pyrosequencing method, the primer is hybridized with the template strand of DNA and the combined with the reaction enzymes, DNA polymerase, ATP sulfurylasem luciferase and apyrase, along with the substrates APS and luciferin. The four dNTPs are then sequentially added to the reaction. When the appropriate, complimentary, nucleotide is incorporated by DNA polymerase onto the 3'-end of the DNA template, PPi can then be released in an equimolar quantity to the incorporated nucleotide.

The conversion of PPi to ATP is done quantitatively in the presence of APS by ATP sulfurylase. The ATP produced in this reaction the drives the luciferase-mediated production of oxyluciferin through conversion from luciferin

which in turn produces visible light proportionally to the original quantity of ATP. This light can then be detected by a photon multiplier tube or CCD camera and displayed as a peak in a pyrogram. Each signal of light is directly proporational to the number of nucleotides incorporated by the preceding reaction. Apyrase constantly degrades ATP and the remaining excess of dNTPs. Once the degradation process is completed, the systematic addition process is begun again. As this proceeds, a DNA strand complimentary to the template is formed with the sequence being interpreted through the displayed pyrogram peaks.

The Pyrogram, produced by the Pyrosequencing process is analogous to the electropherogram in the Sanger sequencing method. A pyrogram can be read and observed in real-time as the reaction is ongoing and is the de facto display of all the sequence signal peaks, displaying all nucleotide additions, the dispensation order of nucleotides and the incorporated and unincorporated dNTPs which produce the base line.

The modulus operandi of pyrosequencing relies upon the cooperation of several enzymes to allow the monitoring of the synthesis of DNA. Stability, fidelity, specificity, sensitivity, KM, and kcat are all critical parameters to the optimal performance of reaction. The enzyme kinetics can be studied in real-time and are given in **Figure 6**. The ascending pyrogram curve displays a slope indicative of the activity of DNA polymerase and ATP sulfurylase while the height of the signal is indicative of luciferase activity. The slope at which the final curve decends indicates the of nucleotide degradation

As described above, apyrase is the catalyst for the degradation of ATP with unincorporated or excess nucleotides being reduced to form nucleotide monophosphates and inorganic phosphate; this results in a steady and uniform decrease in the luminescence of the light signal to an intensity below that of the baseline of the pyrogram. When this point is reached, there is an additional internal lasted less than a minute to allow the degradation of the nucleotides to be completed so that the next dNTP can be added. The addition of the nucleotides can be repeated several times without any necessity to interrupt the process with a washing step.

The enzymes employed in the Pyrosequencing technique are naturally expressed by various organisms. The chemistry standard to Pyrosequencing employs a modified 3’-5’exonuclease deficient Klenow fragment of E- coli DNA

polymerase [66]. The ATP sulfurylase which is used in the technique is a recombinant version originating from the yeast cell *Saccharomyces cerevisiae* [67] while the luciferase enzyme is taken from the American firefly Photinus pyralis. The apyrase is taken from *Solanum tuberosum* (Pimpernel variety) [68-69]. The global time scale for the event from polymerization to light detection is between 3 and 4 seconds at room temperature.

The conversion of PPi to ATP by ATP sulfurylase occurs in approximately 1.5 seconds while the generation of light from the production of luciferase is executed in less than 0.2 seconds [70]. The light generated exhibits a maximum wavelength of 560 nanometers which can be readily detected by a photodiode, photon multiplier tube, or a CCD-camera.

There are many unique advantages to the Pyrosequencing technique amongst contemporary DNA sequencing technologies. One of these advantages is that mutations, deletions and insertions can be directly observed in the pyrgram (discussed in the next chapter) and that the order of dispensation of the nucleotides can be facilely programed. The ability to perform the sequencing process directly downstream of the primer, beginning with the first base after the annealed primer makes the design of the primer more flexible and thus makes this technique highly advantageous. The real-time production of the pyrogram as the pryosequencing process progresses, allows nucleotide incorporations and base callings to be immediately and continuously observed for each sample sequence. The Pyrosequencing method is finally and most importantly for scalable methods, easily automated for high throughput screening events.

1.4 SNP genotyping technologies

The first DNA sequencing method was described in 1977 by Sanger and co-workers [45]. This method, which came to be called Sanger DNA sequencing, is based on enzymatic chain termination, a set of single-stranded DNA molecules is generated, that is size-separated by gel electrophoresis. This method is by far the most common sequencing approach and has been further developed and optimized. Sanger DNA sequencing was the workhorse in the genome project and has been widely used in SNP discovery. However, its use

in SNP genotyping is limited by its low throughput and relatively high cost per sample. Pyrosequencing, an alternative to Sanger DNA sequencing, was developed in 1998 [61]. It is a real-time DNA sequencing method based on a four-enzyme mixture reaction that uses luciferase-luciferin light release to detect nucleotide incorporation by DNA polymerase into a target DNA This method will be described in detail in Chapter 5.

Over the last ten years, significant efforts have been made to improve SNP analysis with alternative techniques, so a growing number of new technologies have been introduced. The alleles are distinguished on the basis of different reaction principles, and the methods are then combined with general detection methods to reveal the sequence information. With some few exceptions, the methods require a pre-amplification step by polymerase chain reaction (PCR) to produce enough DNA for testing. A number of high quality reviews have been published on the ever increasing number of SNP scoring technologies [23, 71-72]. Most of the methods can be divided between hybridization-based-methods [39, 73-76] (**Figure 11**), ligation-based methods [77-84], primer extension by DNA polymerase[29, 85-93] and invasive cleavage-based method [94-95].

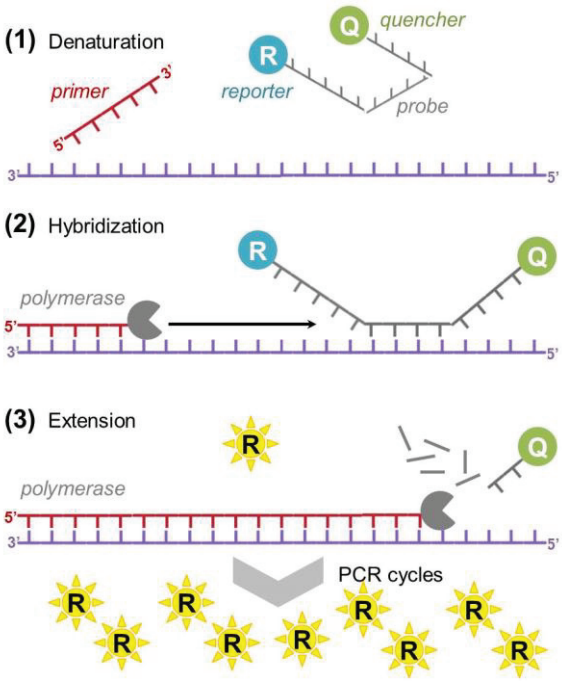

***Figure 11**. The principle of TaqMan assay. Two fluorescent dyes, a reporter (R) and a quencher (Q), are attached to the probes used to allele-specific hybridize with the target DNA. When both dyes are attached to the probe, reporter dye emission is quenched due to FRET (fluorescence energy transfer) from the reporter dye to the quencher dye. During the PCR reaction cycle, the exonuclease activity of the polymerase fragments the probe, and the reporter molecule (R) is released. The PCR is followed in real time and an increase in fluorescence indicates the presence of the matching allele.*

1.5. Detection

A variety of techniques is used to generate signals and determine the allelic status of SNPs and are combined with general detection methods to obtain sequence information. The multiplicity of methods currently available is due in part to the combination of reaction principles with different detection systems. **Figure 12** shows the different combinations used to analyze various reaction principles.

Most of the common detection methods are based on the detection of light emission (fluorescence or chemiluminescence) with, in some cases, separation by gelelectrophoresis or on mass spectrometry. Fluorescence detection methods have greatly increased the sensitivity and ease of analyzing DNA. The availability of different fluorescent dyes and the diversity of their application have made them the most widely applied detection methods today. Fluorescence resonance energy transfer (FRET), in which energy is transferred from one molecule to another, is becoming useful in applications such as the DASH and TaqMan assay. Notable alternatives to fluorescence include chemiluminescence in the pyrosequencing system and mass spectrometric detection.

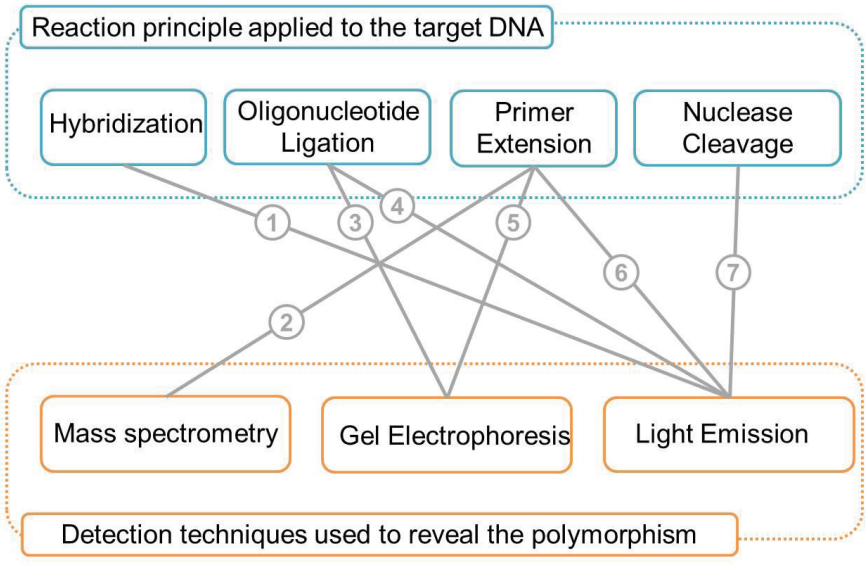

Methods: 1 – DSH & TaqMan; 2 – Good assay; 3, 4 – OLA; 5 – Snapshot; 6 – Pyrosequencing; 7 - Invader

***Figure 12**. SNP genotyping methods categorized by reaction principles and detection.*

1.6 Next stage for DNA sequencing platforms

DNA sequencing is considered the gold standard method for discovering new SNPs, but many alternative methods have been developed for known SNPs. Each method has unique ways of distinguishing a particular SNP position and is coupled with a detection method. There are at least 20 different SNP genotyping methods currently available [96]. A list of some of these SNP genotyping technologies is given in **Table 1**. The list does not cover all the methods but does give a representative picture of what is offered on the market. Many of these methods have been commercialized with a 384-well format and automated, such as the single-base extension based SNPstream, MALDI-TOF MS based Massarray System and Pyrosequencing's high-throughput system [96].

Each SNP genotyping method has advantages and disadvantages and is suitable for a different range of applications [72]. Ultimately, choosing which method to use is based on the type of data to be generated, the number of samples to be processed, and the cost. That there is no single universal method for all situations promises further development of revolutionary methods. There is clearly a need for DNA analysis methods that are more specific, sensitive, fast, simple, automatable, and cost effective than those presently available.

These demands are driving the rapid evolution of a diverse range of new technologies. Some of these technologies have been developed on miniaturized platforms, which in themselves offer numerous advantages. Some of these platforms will be described in the following **Chapter 3**.

Table 1. *Selected SNP genotyping methods.*

Method	**Main advantage**	**Company**
Hydridization		
DASH	Inexpensive labelling	Dynametrix, Ltd
TaqMan	No post-PCR treatment	Applied Biosystems
Oligonucleotide Ligation		
SNPlex	Multiplexing capacity	Applied Biosystems
Primer extension		
SNPs stream	Simple, versatile	Orchid Bioscience
SNaPshot	Sensitive, no labeling	Applied Biosystems
MassArray	Sensitive, no labeling	Sequenom
Pyrosequencing	Informative, *denovo* sequencing	Biotage
Nuclease cleavage		
Invader assay	Does not require PCR	Third wave technologies

Chapter 2

Introduction: Microfluidics and micro total systems (TAS)

Microfluidics involve the manipulation, transport, and analysis of fluids in micrometer volumes. The field has bloomed and branched off into many different areas, for which a number of excellent general reviews are available (e.g. biological and chemical analysis [97-99], point-of-care testing [100], clinical and forensic analysis [101], molecular diagnostics [102] and medical diagnostics [103]). LOC systems are compact, often stand-alone systems featuring full process integration and automation to perform complex tasks.

This subchapter **2.1** briefly describes relevant information over the microfluidics field, emphasizing the inter-relation between the chapters **1** and **2**.

2.1 Microfluidics

Microfluidics involve the manipulation, transport, and analysis of fluids in micrometer sized volumes (**Figure 13**). Microfabrication technology is used to build microfluidic devices that exploit the inherent properties of liquids and gases in the microscale domain. These devices can accurately control minute volumes of fluid on a scale of nanoliters or picoliters. Making explicit use of the unique microfluidic effects, the microfluidic concept has today evolved towards the development of promising tools for analyzing biological samples in a way commonly referred as ”Lab-on-a-chip” (LOC). The concept of LOC or miniaturized total analysis systems (μTAS) as it is known today was proposed in early 1990s by Manz et al. [104]. Since that time the field has bloomed and branched off into many different areas, for which a number of excellent general reviews are available (e.g. biological and chemical analysis [97-99], point-of-care testing [100], clinical and forensic analysis [101], molecular diagnostics [102] and medical diagnostics [103]). LOC systems are compact, often stand-alone systems featuring full process integration and automation to perform complex tasks.

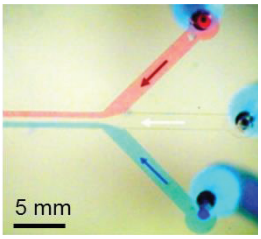

Figure 13 *An example of laminar flow in a junction of microfluidic channels containing flows of blue, yellow and colorless dyes. The design of the shown chip consists of 500 µm by 100 µm channels with the direction of flow being from left to right as indicated by the red and blue arrows.*

The main advantages of microfluidic systems over conventional systems include: minimized consumption of reagents, rapid response times (**Table 2**), well-controlled reaction conditions, parallel processing, speed of separation, excellent mass and heat transfer, low dead volumes, small power consumption, reduced manufacturing costs, portability, and disposability. The concept is still in its infancy, and significant technical challenges have to be overcome before the full potential of this technology is realized in biomedical research. Some of the challenges include fluid transport and the interfaces between the macroscopic and the microscopic environment, which include sample introduction and extraction as well as interrogation.

Table 2: *Comparison of time and costs for the complete screen using traditional methods and in microfluidic emulsions.*

	Robot	**Microfluidic drops**
Total reactions	5×10^7	5×10^7
Reaction volume	100 µL	6 pL
Total volume	5,000 L	150 µL
Reactions/day	73,000	1×10^3
Total time	~2 years	~7 h
Number of plates/devices	260,000	2
Cost of plates/devices	$520,000	$1.00
Cost of tips	$10 million	$0.30
Amortized cost of instruments	$280,000	$1.70
Substrate	$4.75 million	$0.25
Total cost	$15.81 million	$2.50

Adapted from Agresti J. J. et al, Ultrahigh-throughput screening in drop-based microfluidics for directed evolution, PNAS 2010, 107:4004-4009.

With these numerous advantages it is clear why microfluidic devices have received such interest in recent times, having great potential for revolutionizing chemical and biological processes.

2.2 Microfabrication

Microfluidic platforms can be fabricated involving different materials, with the function and ideal properties of the device playing the center role concerning the choice of substrate. Glass and silicon are usually processed using a photolithography and wet etching. [105-106] Glass offers advantages in terms of its optical transparency and stability with strong chemicals. Silicon is used less commonly than glass due to its lack of transparency but tend to be easier to mass produce.

Hard polymers have gained attention as substrates, being examples poly(carbonate) (PC), [107] poly(methyl methacrylate) (PMMA), [108] and cyclic olefin copolymer (COC). [109-110] Their disadvantages is that they are usually not as stable to harsh chemicals and reaction conditions as glass, hence their use in chemical processes is more limited than with glass. [111-112] A big advantage though is that replication technologies can be applied to polymers enabling cuts in cost and time of production of disposable systems, important for example for point-of-care applications. Methods in use for fabrication for polymers comprehend injection moulding, [110, 113] imprinting, [108] hot embossing, [108, 114], and laser ablation. [115]

Poly(dimethylsiloxane) (PDMS) [116] is definitely the most used material for chip fabrication in research environment because of its rapid and simple fabrication that enables fast prototyping, though it is not so useful for mass fabrication. PDMS devices can be prepared via soft lithography. [116-117] Shortly, a “master” is prepared with characteristics from the chip design as positive relief achieved with a photocurable epoxy. Next, the elastomer precursor and curing agent are mixed and placed over the master. The device is then left to cure, then peeled off the master and secured to a cover plate such as glass or PDMS. If the sealing is well performed, the channel network is then ready to be used.

2.3 Diffusion

In the closed channels and chambers networks of microfluidic systems, the diffusion of molecules needed for certain reactions can be estimated using the Einstein-Smoluchowski equation (**Equation 1**). [118]

$$x = \sqrt{2Dt}$$

Equation 1

where x = distance (m), D = diffusion coefficient ($m^2.s^{-1}$), and t = time (s). This equation enables the enhancement or reduction of mixing in the microchannels while designing the chips, depending on the purpose of the system.

Microfluidic systems have been proven to have many advantages over so called conventional systems and they have been particularly very successfully in areas such as separations and chemical or biological assays. In the case of biological assays, the big surface-to-volume ratio of a microchannel enables surface-based assays, in which for example, antibodies attached to the channel surface are used to capture antigens, which is overall carried out efficiently due to the reduced diffusion distances of antigens to the surface. In addition to these advantages, the surface-to-volume ratio can be even more increased by using functionalized microparticles, allowing further increases in reaction efficiency. [119] Subchapter **1.2.4 Microparticles** explains how such particles are incorporated into these devices and the mechanisms by which they can be manipulated for performing a number of procedures, including bioassays and separations.

2.4 Microparticles

Polymers, glass, silica, gold, and inorganic crystals, are a few examples of materials particles can be fabricated from. depending on the, and their purpose and are available in a wide range of sizes (1 to 100000 nm). [120-121] Particles with diameters of 1 nm to 1 μm suspended in solution are known as colloidal suspensions, while particles between 1 μm and 100 μm are commonly referred to as microparticles, and when in suspension form coarse suspensions.

Polymer microparticles, are widely used for many processes because of they versatility, including bioanalysis and chemical procedures. Kawaguchi et al. wrote a review describing the fabrication methods of such particles and their possible applications. [120] Besides their wide range of possible sizes, they have a broad range of functionalization options from chemical (e.g. amine, carboxylic acid, epoxy) to biological (e.g. antibodies, antigens, single-stranded DNA) groups, which allows specificity for binding or reacting (**Figure 14**). Their small dimensions and volume causes them to have a large surface-to-volume ratio, providing a big surface area for reacting and binding on. In addition, the particles can respond rapidly to different parameters as temperature, pH, electric fields, and are highly mobile in solution since the viscous drag forces influencing them are low. Furthermore, some particles that possess soft layers enable water penetration which reduces the fluid resistance on their mobility.

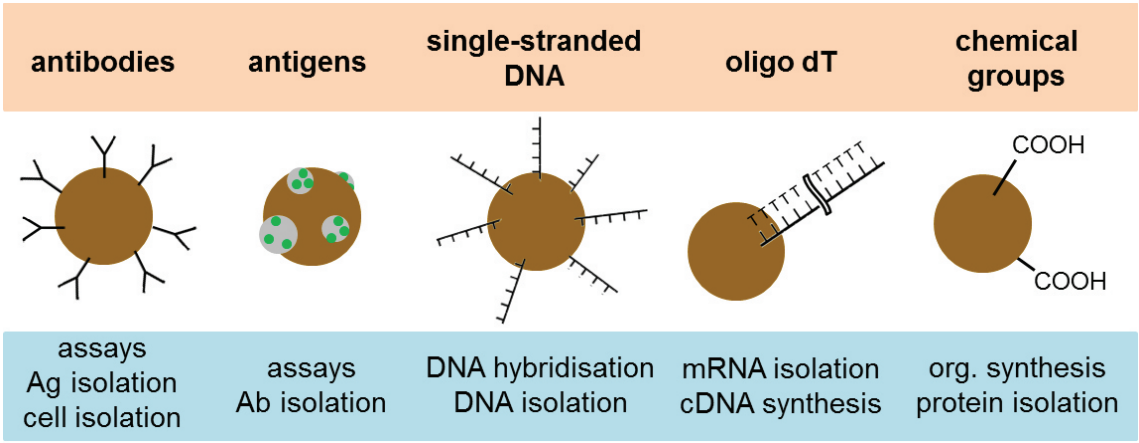

Figure 14. *Microparticles functionalized with different surface groups (orange header) for different bio- and/or chemical procedures (blue footer).*

Given the many possible surface and physical properties of microparticles, they are widely used as solid supports for several bio and chemical procedures which include separations, immunoassays, and chemical reactions. [119-120, 122] Commonly, such procedures are carried out by suspending the particles into a solution or matrix containing target species or reagents that can then bind or react to their surface before removing the particles from the solution or matrix by sedimentation, decantation, centrifugation, or filtration. Despite of all the benefits of employing microparticles for assays and so on, the methods of separating them from the solution are quite time-consuming,

laborious, and inefficient, especially when the process involves several repetitions for washing purposes. In the last years, microparticle separation and assay techniques have been successfully integrated into microfluidic platforms, decreasing overall diffusion distances while maximizing binding efficiency and enabling more control over the fluid flow and particle mobility. In the next chapters, the theory of particle stability will be explained, and the literature related to the use of microparticles in microfluidic systems will be briefly mentioned, giving more attention to continuous flow procedures.

2.4.1 Particle handling on-chip

The strategies and advantages of using microparticles in microfluidics have been reviewed by Verpoorte [119] and Peterson. [123] Further applications for immunoassays have also been reviewed by Lim and Zhang. [124] In summary, there are two main methods for particle manipulation in microchannels: (i) trapping, and (ii) continuous flow.

2.5 Miniaturized platforms for DNA analysis

More traditional sequencing technologies have still disadvantages in terms of cost, speed, throughput, and sensitivity which results in lack of capacity to properly address the always increasing demand for more sequencing information. Therefore, there is a need to combine sequence information acquisition with faster, cheaper, and better technologies for DNA analysis. These technologies will most probably involve smaller reaction scales, evolving into nanotechnology direction. The processes are wished to be robust enough for general applicability while being simple enough for automation. Cost is a very important aspect for developing new and high-throughput technologies. There are two principal strategies behind designing new miniaturized assays while reducing costs: parallel assays in solid-phase microarray formats and homogeneous assays carried out in distinct channels of microfluidic devices [125]. There are many terms present in the literature describing miniaturized platforms, such as microarrays, microfluidic devices, bio- , DNA- and gene-chips, and biosensors. A distinction must be made between microfluidic chips,

which typically involve fluids in channels, and chip-based microarrays, where DNA molecules are bound and arrayed on a solid support to investigate target DNA-probe interactions in parallel. In the following sections, an overview of miniaturized platforms based on different concepts for DNA analysis is presented.

2.5.1 Microarray technologies

A microarray is device designed for analysis consisting of an array of molecules as oligonucleotides, cDNA, PCR products, and others, which are immobilized at discrete, ordered or non-ordered, in the mM to mM scale solid substrate, enabling a great number of parallel analyses. In general, there are four steps involved in a microarray process: DNA immobilization on solid support, hybridization with a probe, detection, and data analysis. Several methods for the immobilization of DNA were developed by different research groups. In the beginning, two types of arrays were reported: synthesized *in situ* and pre-synthesized and spotted. Affymetrix Inc. (Santa Clara, CA, USA) and prepared synthesized oligonucleotide probes on a silicon support by using photolithography. [126] With suitable masking strategies, oligonucleotide arrays of known sequence and known location can be fabricated with very high densities (hundreds two thousands per cM^2). The arrays can be created by two main methods: by pin-based fluid transfer [127], and piezo-based inkjet dispensers [128]. Several materials can be used as solid support for arrays, being glass slides the most commonly but other have been reported as well, as nylon membranes [129], beads [130], polyacrylamide gel pads [131], and activated dextran. [132]

Once fabricated, these probe arrays are ready for hybridization. The nucleic acids to be analyzed, i.e., the target, are labeled with a fluorescent dye. The labeled target DNA is then incubated with the array. The formation of stable duplexes between the complementary probes and the sample DNA is facilitated by passive diffusion. The temperature and buffers determine the stringency of the hybridization condition. When the hybridization reaction is completed, the slide is inserted into a fluorescent scanner where patterns of hybridization are detected. The hybridization data are collected as light emitted from the

fluorescent-labeled target, which is hybridized to the probes on the array. Probes that perfectly match the target produce stronger signals than those with mismatches. Since the sequence and position of each probe on the array are known, the identity of the target nucleic acid applied to the array can be interpreted by a computer program.

When the DNA microarray technology was introduced, it promised to be a massive parallel genotyping method using simple, allele-specific hybridization detection [133]. However, while DNA microarrays completely revolutionized the field of RNA expression analysis, microarray-based allele-specific genotyping has thus far found few applications. In gene analysis, the oligonucleotide (or cDNA) arrays target sequences with different compositions and hybridization-based analysis can clearly distinguish between the different sequences involved. However, unlike gene-expression analysis, it is very difficult to design a high-density oligonucleotide array in which single-base mismatches can be resolved using standard hybridization conditions [134]. Thus, additional treatments and optimizations have been used to increase the specificity.

One of the first strategies used to analyze SNPs in a microarray format was sequencing by hybridization (SBH) as described by Southern *et al*. in 1992 [135]. A set of short oligonucleotides covering a large DNA fragment is arrayed onto a DNA chip. The precise sequence of the oligonucleotide at each location on the chip is known, and the pattern of hybridization of the fluorescently-labeled DNA probes can be interpreted using an algorithm to give a sequence. However, while the method has high throughput capacity, it is not very accurate due to extremely small differences in the duplex stability between a perfect match and a mismatch at one base [136]. Alternative approaches involve hybridization followed by an enzymatic discrimination with DNA polymerases or DNA ligases, as described in Chapter 3 above. The combination of single-base extension with solid-phase bound oligonucleotides [137] has been successfully applied to microarray formats for parallel SNP analysis [137-139]. In this approach, each oligonucleotide printed on the array is designed complementary to the sequence immediately next to the 5'end of the target SNP. One version of the primer extension method involves placing the primer's 3'end at the allelic variation instead of immediately 5'end of it and allowing the polymerase to fully extend the primer. DNA polymerase will only extend those primers that match

perfectly at their 3'ends. In this way, only one labelled nucleotide per reaction is required and higher detection signals can be obtained than with single-base extension since more fluorophores are incorporated during the primer elongation process [140]. However, this approach is not as specific as single-base extension since it gives false positive signals that are twice as high as single-base extension [140]. The false positive signals are caused by the ability of DNA polymerase to extend certain mismatches if given sufficient time. In AMASE (apyrase-mediated allele-specific extension), the nucleotide degrading enzyme apyrase is used to remove the nucleotides continuously, which minimizes the risk of mis-incorporation during the extension reaction [141]. Ligation-assisted genotyping on microarrays is performed by ligating the single-stranded target DNA to a probe hybridized to an immobilized oligonucleotide [142]. Ligation-based chemistry offers an advantage for multiplexing on microarray platforms because the interference is less between primers than is the case with base extension assays.

Microarray technology is being proposed as the future platform for high throughput genotyping, and an increasing number of companies are active in this field, either with a whole new microarray platform or with conventional technology. Affymetrix remains the best known DNA chip-maker and continues to dominate the market. The Affymetrix GeneChipTM (**Figure 15**) is a highly dense array of oligonucleotide probes on a silicon support arrayed by photolithography. These chips have been used in a number of studies [143]. In the GeneChip system, each SNP position is composed of a series of oligonucleotides and complex computer algorithms are used to evaluate the numerous signals for each SNP. The need for large amounts of oligonucleotides for each SNP position is due to the difficulties in achieving hybridization stringency that is capable of differentiating a match and a mismatch configuration at one base.

***Figure 15**. The Affymetrix GeneChip (http://www.affymetrix.com).*

Nanogen Inc. (San Diego, CA) developed a completely different type of microarray chip that uses an electric fields in a microfabricated semiconductor device [144], as shown in **Figure 16**. Through the use of microelectronics, movement of charged molecules to and from designated test sites is achieved to obtain concentration at those sites. This allows rapid hybridization, and unhybridized molecules are removed by reversing the electrical potential. The active hybridization approach removes many of the limitations of the passive hybridization processes and can significantly improve the performance of DNA array analysis for a variety of diagnostic purposes. The incorporation of microelectronics limits the array density to 400 spots. However, the chip offers flexibility of design since reactions occur only at individually controlled charged test sites. Nanogen's technology is an excellent demonstration of the applicability of electronics and may ultimately lead to complete automation to achieve integrated lab-on-a-chip systems.

Figure 16. The NanoChip from Nanogen (http://www.nanogen.com).

2.5.2 Microfluidics-based technologies

The main driving force within microfluidic-based genomic research has been the need for a quick and easy way to perform DNA analysis. In the following Section, microfluidic chip-based systems for DNA analysis are described.

Microchip-based CE for SNP analysis

Electrophoresis is a separation technique used to fractionate and analyze both DNA and proteins. Traditionally, 1- to 5-mm thick gel slabs of usually

cross-linked acrylamide have been the most common format for electrophoretic separation. Over the past 10 to 15 years, significant efforts have been made to improve on this separation method and have resulted in the development of automated, high-throughput DNA sequencing and genotyping technologies. These efforts have led to the transformation of the platform system from thick slab gel to thin slab gel to capillaries and currently to a microfabricated chip format.

In the early 1990s, miniaturized formats for analytical chemistry and biology in microfabricated chips were critically evaluated by Manz and co-workers [104]. The first papers demonstrating the potential of microfluidic chip-based analysis involved the fast separation of fluorescent dyes [145-146] and fluorescently-labeled amino acids [147] by capillary electrophoresis. Other groups then used microfabrication technology to further develop such systems. The advantages of microchip based capillary electrophoresis (CE) over conventional capillary are reported by a number of reviews in the literature [101-103, 146-149]. In general, almost all references report an enormous reduction in separation time when switching to microchip CE. The increase in speed is generally on the order of 10- to 100-fold relative to capillaries and slab-gel formats, respectively [101]. Increased dissipation of heat generated by joule heating and the ability to inject very small and well-defined sample plugs are some of the most important features of the microchip based systems. In addition, there is the possibility of integration with sample preparation. **Figure 17** is a schematic drawing of a basic photolithography-defined microchip device for electrophoretic separations. The channel defined by Points 1 and 2 provides the separation, and the one defined by 3 and 4 is the sample-introduction channel. At the end of each channel, there is reservoir. These reservoirs also provide access for the electrodes. With the introduction of the cross-channel and double-T injector setup, well-defined sample quantities can be analyzed on electrophoresis microchips. Samples are typically loaded electrokinetically into the injector region by applying voltage between Points 3 and 4 and then separated by applying the electrical field between point 1 and 2. The detector is placed close to Reservoir 2 and is usually laser-induced fluorescence (LIF), but other methods such as mass spectroscopy [150] and electrochemical detection [151-152] have also been described.

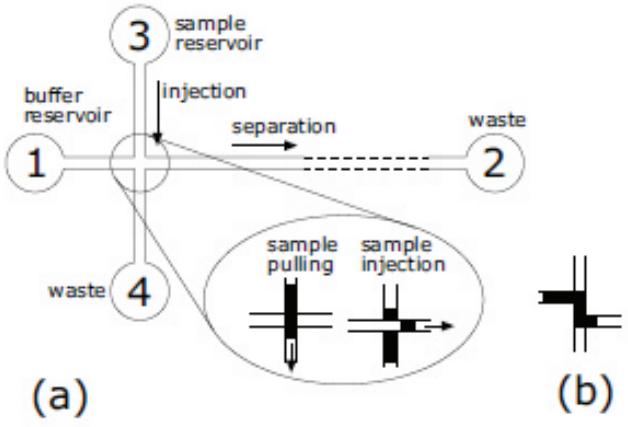

Figure 17. *Illustration of the main sections of a chip-based electrophoresis system with either a (a) cross injection or (b) double-T injection system. The vertical channel 3-4 is used for sample addition and the horizontal channel 1-2 as the separation/reaction portion. The detector is typically located on the far right, near Reservoir 2. Reproduced with permission of ACS Publications as seen in Anal Chem. 2002 Aug 15; 74(16): 4054–4059.* [153]

To increase the throughput even further, arrays of microfluidic devices have been developed [154-157] to provide parallel analyses. One way to achieve the necessary separation distance and high-speed analysis without sacrificing throughput is to fabricate a dense array of long separation channels on a single device. Systems of 16, 96, and 384 channels have been fabricated on 20-cm diameter glass wafers [156-158]. In these devices, geometrically optimized turns [159] were used to provide the necessary separation length. The radial chips in combination with the innovative high-speed rotary LIF scanner [160-161] and a high-pressure sieving matrix loader have increased the throughput capability of these devices.

Chip-based CE for SNP analysis is becoming well-established. For example, fast analysis of the candidate gene for hereditary hemochromatosis [156-157], alleles of the D1S80 locus [162], and PCR products of Hepatitis C virus [163] have been demonstrated. A comprehensive summary table of articles describing chip-based genotyping using CE is given in the review by Verpoorte [101]. A number of companies are beginning to commercialize microfluidic DNA chips for electrophoretic separations. Caliper Life Science was one of the first companies established in the field of microfluidics and is presently developing lab-on-a-chip systems for various applications. Caliper's LabChip system offers automated SNP interrogation using very small volumes in microchannel networks. A combination of pneumatic and electrokinetic forces are used to move fluids and perform separations on chip and to integrate sample

pretreatment procedures. The first commercial instrument for microchip-based DNA analysis was the Agilent 2100 Bioanalyzer, by Agilent Technologies. Since then, a number of genotyping studies have appeared in the literature based on the use of this technology [101].

In conclusion, microchip-based CE has recently evolved as a promising method for genotyping. The more recent development of sequencing technologies in microfabricated channels may deliver significantly reduced reagent costs and increase throughput by decreasing reaction volumes and reducing run times. However, it is important to bear in mind that molecular diagnostic analysis is a multi-step process of which separation is only one part. The pre-electrophoresis steps including DNA extraction and PCR amplification have to be integrated with the separation.

Polymerase chain reaction

DNA amplification by PCR has become a key tool in modern molecular biology, but PCR is also the rate-limiting step in many genotyping applications. Therefore, this step needs to be speeded up. Conventionally, PCR is performed in benchtop instruments, whose large thermal mass limits the speed at which thermal cycling can be carried out, so the reaction times are on the order of a couple of hours or more. The benefits of miniaturization come from improved thermal-energy transfer, which reduces the typical cycling times from several minutes to 30 seconds or less. A number of groups have investigated microchip-based PCR systems in both disposable microchambers and microfluidic formats. Two different concepts have been reported for chip-based PCR. In the first configuration, the reaction mixture is stationary and entrapped in a thermocycling chamber that is typically micromachined in silicon or glass. The first papers dealing with this configuration were presented by Northrup and co-workers [164] in 1993 and Wilding and co-workers [165] in 1994. The devices consisted of a reaction chamber with the inlet and the outlet in silicon and sealed with Pyrex glass. The chamber was then placed on a conventional thermocycling instrument for heating and cooling. Later on, heaters and temperature sensors were integrated into the device [166]. The integration of optical windows in the silicon chamber permitted real-time monitoring of the

PCR reaction. The second configuration, which was introduced by Kopp et al. [43], involved a continuous-flow amplification system. The reaction mixture is pumped continuously through the chip and flows repeatedly through three different copper blocks side by side, providing three distinct constant temperature zones to ensure denaturation, annealing, and extension.

Integrated systems for DNA analysis

The vision of a lab-on-a-chip requires integration of all the steps onto one chip, in particular the integration of PCR and product analysis. Initially, only individual steps were performed in the microfluidic chips and only a handful of integrated genotyping devices have been developed until now. DNA sample preparation and integrated analysis were first published in 1996 [167-169]. In these systems, the PCR step was coupled with microchip CE to produce integrated DNA analysis systems.

An integrated silicon chip that extracted DNA from a sample, separated fragments, and detected samples with an integrated photodiode [170] has been described. This impressive chip is capable of moving samples in microchannels with heaters, temperature sensors, and a fluorescence photodiode detector. Amplified DNA are mixed with intercalating dye, separated in a cross-linked polyacrylamide gel, and detected with the photodiode - all on board the microchip. Quake and co-workers have developed microfluidic systems using components fabricated with flexible polymer (polydimethylsiloxane) parts with a variety of microchannels and membrane valves for nanolitre-scale biological sample processing and analysis [171]. They have managed to integrate a variety of different biological processing techniques, such as amplification of nucleic acids and cell sorting in the same system, which allows parallelization [171-174].

2.5.3 Particle-based methods

Nano- to micrometer-size particles are used routinely in molecular biology. The surface of these microspheres can supply active groups, such as carboxylic or amino groups, for covalent coupling of biomolecules. The high degree of flexibility in surface coatings allows them to be used in a wide variety

of applications. These applications include immunoassay, affinity assay, DNA hybridization assay, and protein-protein interactions. Microspheres have many advantages including a high surface-to-volume ratio, which enables reactions to be performed in lower volumes, increased diffusion - thereby decreased analysis time, and easy separation from the bulk of the reaction mixtures. Beads are mostly used in suspension mixtures and are interrogated individually by flow cytometry. In microfluidic devices that are not based on suspension mixtures and cytometric analysis, the beads must be controlled inside the chip. A number of different methods have been described to control the beads in confined areas. In this thesis, two different strategies have been used to capture beads: 1) a flow-through filter-chamber device consisting of grids of pillars and 2) microcontact printing-based immobilization of beads without the use of a physical barrier.

Bead-based systems have emerged as a promising tool for genomic applications. Some of the platforms for DNA analysis will be briefly reviewed below.

Particle-based platforms for SNP analysis

An alternative to DNA microarrays is an approach whereby the solid phase is composed of beads. Bead-based systems can be combined with most of the allele-discrimination chemistries used in the microarray format described earlier. One advantage of beads is that reactants can be added to them before or after they are immobilized. This opens up many ways to use reaction multiplexing, since mixtures of different beads and reagents can be integrated across various time and spatial coordinates. For example, samples from different individuals could be combined and simultaneously examined on one micro-surface. Doing this would require prior bead coding by chemical [175], spectrometric [176], electronic, or physical means [177] so that the results could be decoded and assigned to appropriate samples or assays.

Luminex Corporation (Austin, TX, USA) has developed a genotyping platform based on microspheres that are internally dye-labeled with two spectrally distinct fluorochromes (red and orange) [176]. When the colors are combined in different ratios, codes of up to approximately 100-color resolution

with specific spectral addresses can be achieved. Hence, it is possible to perform a hundredplex detection reaction in a single tube. A third fluorochrome (green) is coupled to the DNA immobilized on the microspheres for the genotyping signal. The microspheres are interrogated individually by flow cytometry simply by rapidly flowing through two separate lasers, one laser to excite the two dyes contained within the microsphere and the other to excite the reporter dye on the immobilized DNA. This combination of encoded microspheres and flow cytometry is known as suspension array technology (SAT) and is a very fast detection method. The Luminex bead-based platform has been shown to work with several assay chemistries for SNP genotyping. Allele-specific hybridization [178] and the use of enzymatic allele discrimination by means of single-base extension [179-180] and oligonucleotide ligation assay [181] have been described. Recently, a microsphere based invasive cleavage assay has been described for genotyping SNPs directly from human genomic DNA samples without prior PCR amplification [182]. This assay uses a cleavage reaction that generates a fluorescent signal on the microsphere surfaces followed by flow cytometry analysis of the microspheres.

In a different bead-based platform, commercialized by Illumina Inc. (San Diego, CA), microspheres are randomly assembled on the end of an optical-fiber substrate [183-184]. The fiber-optic arrays are prepared by fusing together densely packed fibers into a bundle of about 50 000 individual fibers packed into a hexagonal matrix. Wells at the ends of each fiber are created by dipping the fiber-optic bundle into various chemical-etching reagents. Each well is dimensioned to accommodate a single microsphere and is typically about 3 to 7 μm in diameter. A particular oligonucleotide probe is conjugated to each bead, which is followed by quantitative pooling of the bead types in a stock solution. This library of beads is then exposed to the fiber optic bundle and each bead is captured in a well of the fiber-array surface.

Once the beads are attached to the wells, the concept is very similar to that of DNA microarray assays. However, oligonucleotides attached to the microspheres are spectrally registered in function of a random distribution in the wells rather than fixed surface positions predetermined during array fabrication. Since the beads are attached randomly, a decoding process is needed to identify the captured beads. This is accomplished by a series of hybridizations

with fluorescently-labeled oligonucleotides that are complementary to the capture probes on the beads. The combinations of different fluorescent dyes (with different excitation and emission wavelengths and intensities) allow each bead to be independently identified. The optical properties of the fiber are used to detect the fluorescent signal from the beads and the genotyping signal from the oligonucleotides of interest. The fiber-optic bundle is regenerated after the reaction by removing the beads. This highly miniaturized platform has enormous potential in multiplexing capabilities.

Illumina introduced bead-chip arrays in a slide-shaped substrate. Each region can interrogate separate bead assays and can be configured in different sizes and densities depending on the application. Today, Illumina uses a library of 1500 bead types, each with a unique oligonucleotide capture probe ready to hybridize to a complementary sequence in a multiplexed SNP assay. The Illumina platform is compatible with most of the SNP assays described earlier. The platform produces accurate genotyping results with single-base extension [180, 185], ligation assay [181, 186], and allele-specific extension. Extremely high throughput is obtained by arranging the fiber-optic bundles to match the layout of the 96-, 384-, and 1536-well microplates.

The DNA bead arrays described above have smaller feature sizes and higher packing densities than DNA microarrays. The advantages of this high-density randomly distributed micrometer-sized bead-based DNA array include cost effective production of the bead arrays in seconds, high-throughput analysis, easy replacement with different or additional beads when different testing is desired, and facile regeneration of the sensor and substrate.

454 Life Sciences developed an innovative approach to sequencing an entire genome that uses a microfluidic format with beads integrated in all the steps from the sample preparation, to amplification, and sequence analysis. They developed a novel platform, PicoTiterPlate, consisting of 44 μm in diameter microwells which are 50 μm deep for simultaneous amplification and analysis of over 300 000 beads in parallel [187]. Genomic DNA is fragmented and single-stranded DNA is captured at one copy per bead with complementary capture primers. Solid-phase PCR is performed to amplify the entire genome at one time in a water-in-oil emulsion. The beads are loaded into the PicoTiterPlate wells, each of which permits only one bead. Solid-phase PCR

can also be performed directly in the PicoTiterPlate [187]. Massively parallel sequencing is performed using bioluminometric sequencing-by-synthesis method. The reagents flow through the PicoTiterPlate wells and can diffuse uniformly into and out of the wells. The light generated by the nucleotide incorporation into the system is detected by a light detector.

In this chapter, I described various miniaturized platforms for DNA analysis. The best-known example of a miniaturized tool today in this field is the DNA microarray, which has become increasingly important as a clinical diagnostic tool and is playing a central role in genomic research. Microarray-based testing is faster and more convenient than serial testing and has largely revolutionized gene-expression analysis. In recent years, bead-based platforms have entered the arena. They are a more cost-effective than the traditional planar microarray, and beads can be integrated into the sample preparation steps. Microfluidic systems are more versatile than surface-based microarrays, and their importance in genomics is growing steadily. These systems promise to reduce cost and improve performance by integrating several processes that otherwise require a suite of bulky instruments and manual handling.

These platforms all have both advantages and disadvantages, which makes it difficult to select a single platform as ideal for all applications. The meaningful exploration of genome variation for the purposes of bioscience/biotechnology will require meeting the ultimate goal of defining all genome variation in an individual at manageable cost and throughput. A combination of these techniques in conjunction with other innovative technological development will be necessary.

Chapter 3

Open surface microfluidics

Over the last 10 years, a pursuit of an increase in throughput, reduction in material consumption and function integration to improve the analytical performance, led to downscaling molecular and cellular analysis by using the microfluidic format.[188-193] The early development of miniaturized assays greatly expanded from a limited simple fluidic operations to assays required complex and more sophisticated fluid handling.

Microfluidics have been widely employed both in chemical and biological analysis for decades. Microfluidics are based in a variety of micro-manufacturing techniques, allowing the use of little amount of reagents, giving access to accelerated reaction rates, process integration and multiplexicity. A clear disadvantage of such closed systems however includes the flow confinement which requires complex multilayer structure manufacturing. [194-199] Further, any gas in a closed microchannel liquid interface (e.g., enclosed air bubbles) in the operating fluid can lead to unexpected failure, which is another problem in miniaturization. Surface microfluidics is a new alternative to conventional microfluidics that solve the obstacles mentioned above, and will receive more and more attention in the microfluidic community.[200-202]

Automatic microfluidic manipulation is one of the most relevant chores to be carried out by a lab-on-a-chip device aiming to compact and to integrate several chemical and biological functions into a microchip. Early microfluidic platforms, commonly utilizing single-phase fluids in microchannels, have made tremendous advances in the direction of fully operational instruments for miniaturized biochemical assays with increasing complexity. [203-207] Nevertheless, such continuous-fluid systems often require complex micropumps and microvalves as well as external appliances in order to carry on with liquid manipulation through the channel network interfering with the miniaturization development and future commercialization. Recently, droplet-microfluidics have gathered great interest. micro-droplet-based microfluidic system considerable attention.[208-209] In comparison to the continuous-flow platforms, the handling of

droplets offers more flexibility of operation, reduction of sample and reagents usage, as well as reduction of fabrication costs, particularly in the case of droplet-manipulation on an open surface.

3.1 Droplets as reaction and transport units

Many approaches have been adopted for droplet actuation on a surface, as electrowetting, [210-211], dielectrophoresis, [212] and magnetism. [213-215] Even though “digital-microfluidics” which mainly involves electrowetting has gathered popularity, the choice of magnetic actuation for droplet manipulation through particles present in suspension in the droplets to actuate offers relevant advantages. The range of magnetic particles ready for use, considering already the different particles possible to functionalize with many sorts of biomolecules, provides a strategy for both biomolecular separation and/or reaction. In addition, magnetic particles and droplets are simple to manipulate which cuts in terms of cost and size of the equipment involved. Magnetic particles have been already utilized for small-volumes transportation on miniaturized platforms. Garcia *et al.* [216-217] investigated the movement of viscous droplets caused by magnetic gradients on top of a superhydrophobic surface. Ohashi *et al.* [218] created a PCR instrument using droplets and magnetic transport. Nguyen *et al*. [219-220] described their work on the effect of planar magnetic coils on ferrofluid-droplets and respective kinematics, as well as developed a circular closed-loop device using ferrofluid for fast PCR. [221-222] Magnetic particles actuation on planar surfaces were also used in combination for bio-separations and -reactions. Shikida *et al.* [223-225] developed a system able to handle magnetic particles-clusters by conducting these from well to well through an interconnect. Lehmann *et al.* [213, 226-227] showed an adaptable platform by fabricating an array of coils placed on a PCB plate to create a magnetic gradient, thus manipulating magnetic particles in an oil well with a hydrophobic base for extraction and fusion reactions. Pipper *et al.* [214] reported a micro-droplet platform for cell lysis, RNA extraction and purification, and real time RT-PCR, having all steps integrated in one device by actuating magnetic particles with an external magnet through an array of micro-droplets. In addition, these researchers broadened the platform for purification of certain cells with extraction of the

respective DNA. [215] In this platform, the particles are not only the support for biomolecular adsorption but also work as carriers, meaning that droplets are not only reaction vessels, but also transport units. The potential given by the flexibility of designing arrays of stationary- and moving- droplets according to demand and for different applications is enormous.

Generally speaking, the flexibility involving droplet-volumes, obtainable particle mass in the droplets, speed of the particle motion, settings for droplet splitting or merging, among other variables, under magnetic actuation is enormous on an open surface. It is necessary though, that all these conditions are influenced by particle type, droplet size, surface tension, viscosity and effect of oil coating on droplet kinetics.

3.2 Droplet actuation platform

A conventional magnetic droplet-actuation platform is depicted in **Figure 18**. Water-based droplets covered with a layer of mineral oil are placed on an hydrophobically coated glass substrate (glass slide). Hydrophilic magnetic particles are suspended in the droplets. An external magnet is placed beneath the slide holder and is used for droplet manipulation.

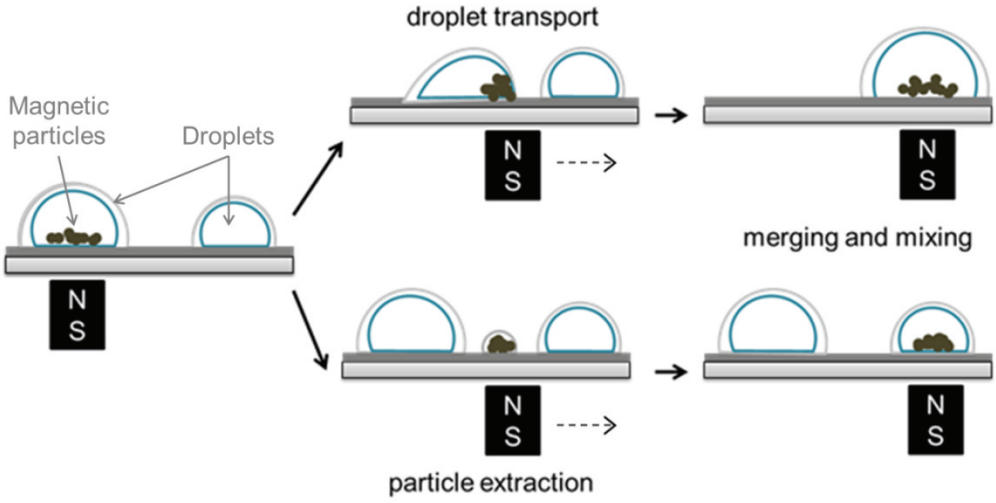

Figure 18 *Illustrative set-up and basic operations in a magnetically actuated droplet-system.*

3.3 Droplet manipulation

Figure 18 shows the fundamental response of droplets and droplet-contained particles in magnet-actuated droplet handling. It starts with the attraction of the magnetic particles present in the droplet to the base of this same droplet by the magnetic force (cause by the approximation of an external magnet). The particles can be moved by moving the magnet horizontally underneath the glass slide. The particles will form a cluster by being forced towards the wall of the droplet (contact line). The magnetic force will move the magnetic-cluster to the water/oil interface which results in droplet deformation. From this stage on, two different operations can be carried out. On one hand, droplet movement can be done if the droplet is fully "dragged" by the magnetic-cluster. On the other hand, magnetic-cluster extraction can be done by splitting of a daughter droplet containing the magnetic cluster from the reaction mother droplet. [228] These two operations correspond to the fundamental ones in magnetically actuated droplet manipulation platforms.

In preceding bio-separations and -reactions with droplets containing magnetic particles, the contained magnetic particles were used either as a droplet driver [216, 218] or as an extractable solid support.[213-214, 229] It is important to emphasize, that integration of operations in these cases wasn't easy which makes crucial taking measures to reduce the conflict betweendroplet motion and particle extraction. In order to facilitate the bead extraction from the mother droplet, Shikida *et al* .[223-225] used a channel that worked simultaneously as a gate to stop the droplet from being dragged along by the magnet motion while the magnetic force pulled the magnetic-cluster daughter droplet from it. As another alternative, Lehmann *et al*.[213, 226-227] developed hydrophilic and hydrophobic patterns onto the glass substrate to restrain the droplets on the base surface. Superhydrophobic surfaces and smaller droplets size are also commonly used for droplet transport. By designing asnd preparing such surfaces with special topographies for droplet manipulation increases the complexity of device fabrication. The work of Pipper *et al*., is an exception to this. This was achieved by combining solid phase extraction (droplet splitting) with clockwork PCR, using droplet transport to cycle the droplet though zones with the different PCR required temperatures. [215] (**Figure 19**) They observed

that, with a magnet moving at a steady speed, exclusively droplets with volumes below 10 µL could be stably transported without splitting into daughter droplets.

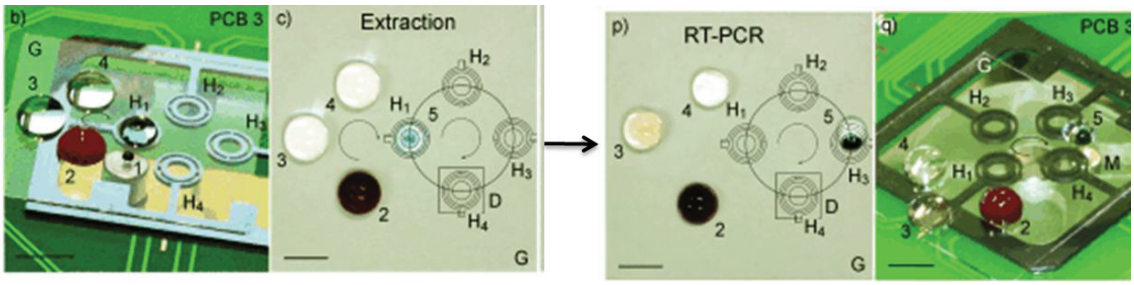

Figure 19: *Device integrating sample preparation and RT-PCR by using magnetically actuated droplet manipulation on an open surface (Pipper et al. 2008). Reproduced with permission of Wiley-VCH as in* [215].

Overall, one can say that in such system, the droplet kinetics and resulting operations are determined by the balnce between the horizontal parts of mainly three forces: the **magnetic force (*Fm*)** acting on the particle clusters, the **capillary force (*Fc*)** induced by the droplet deformation and the **frictional force (*Ff*)** between the oil-coated droplet and the substrate surface.

Magnetic force, Fm

$$F_m = \left(\frac{M}{\rho}\right) x \frac{B_m}{\mu_0} \nabla B_m$$

Equation 2

where M is the mass of the magnetic particles cluster, $\mathbf{r}$ is the mass density of the magnetic particle material, **c** is the magnetic susceptibility of the particles, $\mathbf{Bm}$ is the magnetic field applied and μ_0 is the permittivity of free space.[230-231] From **Equation 2** the maximum magnetic force that can be applied to the droplet along the magnet motion axis can be estimated:

$$F_{m,max} = K_{m,max} x \left(\frac{M}{\rho}\right)$$

Equation 3

where $K_{m,max}$ is the maximum value of $\frac{B_m}{\mu_0}\nabla B_m$ that can be achieved for a specific magnet and device setup.

Frictional force, Ff

$$F_f \cong K_f R_b \mu_{oil} U$$

Equation 4

where K_f is the friction constant, R_b is the radius of the base contact area between the oil-coated droplet and the substrate, m is the viscosity of the oil and U is the velocity of the drop.[220, 232] It is important to emphasize that the dynamic friction is proportional to the base radius of the oil-coated droplet, and not its contact area with the substrate, because the viscous drag in the proximity of the contact line dominates the sliding friction for small drops, whose radius is of the order of the capillary length, $k^{-1} = \left(\frac{\gamma_{oil}}{pg}\right)^{\frac{1}{2}}$, or smaller.[232] γ_{oil} is the surface tension of the neighboring oil phase, r is the fluid density, and γ is the acceleration caused by gravity.

Capillary force, F_c

When a magnet is moved horizontally away from a droplet, magnetic particles suspended in the droplet will be pressed against the side of the droplet, deforming it. This deformation generates a capillary force, which keeps the particles in the droplet. Over a sustainable capillary force, the particle cluster will detach and a smaller daughter droplet containing the particles will be extracted from the mother droplet. The capillary force at which this happens was given by [224] and can be defined by the following **Equation 5**.

$$F_{c,max} = 6^{\frac{1}{3}} \pi^{\frac{2}{3}} \gamma_{0-w} \left(\frac{M}{\rho}\right)^{\frac{1}{3}}$$

Equation 5

The analysis of the combination of the three forces described above can be illustrated with the three distinct regions in the operating diagram shown in **Figure 20**- The 3 described regions can be defined as follows:

- **Region 1 –** steady transport of the droplet takes place in this region, which means the magnetic force, *Fm*, is balanced by the frictional force, *Ff,* resulting in both the droplet and the magnet moving at the same speed.
- **Region 2.** –magnet detachment happens in this region. Both the frictional force, *Ff*, and the maximum capillary force are greater than *Fm, max.*
- **Region 3**. - *Fm, max* is greater than *Fc, max* in this region but *Fc, max* is smaller than the friction force which means that the magnetic pulling force acting on the particle cluster conquers the interfacial force and a particle daughter droplet splits off the mother droplet.

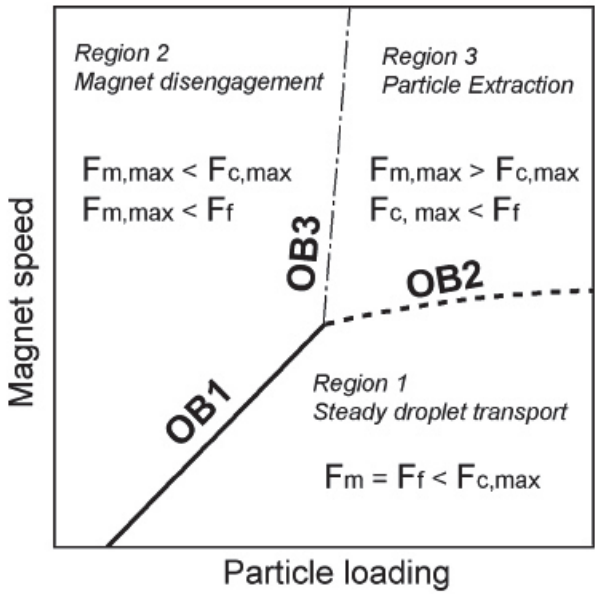

Figure 20 *Diagram illustrating the analysis of the combination of the main forces involved in droplet transport/merging. OB1, OB2 and OB3 represent the operating boundaries between three distinct operation regions. Reproduced with the permission from Royal Society of Chemistry as seen in* [228].

3.4 Important parameters

Magnetic properties

Equation 2 demonstrates that the magnetic force required for a droplet operation, motion or split, is influenced by both the magnetic field's strength and gradient together with the amount of used magnetic particles and their magnetic

properties. Despite existing other ways of creating a magnetic gradient as for example arrayed coils [213, 219, 227], these do not remove the necessity of having a strong and homogeneous magnetic field which can be achieved with the use of a permanent magnet, and overall require a more complex fabrication procedure. Using this reasoning, a Nd-Fe-B permanent magnet placed on a translation stage that can be motorized vertically aligned and close to the substrate used for droplet manipulation can be used. Such setup generates strong magnetic fields and enables a considerably easy control of the magnet's movement.

Many types of magnetic particles are commercially available with different degrees of magnetic susceptibility and sources to answer the demand for several applications in bioseparation and bioreaction. These particles can be superparamagnetic, with a wider range of purposes in biosciences because of their resuspension properties, their greater surface area and slower sedimentation in solution, when compared to the ferromagnetic particles. The ferromagnetic particles possess in contrast very strong magnetic properties and are therefore quite simple to manipulate even in case viscous solutions are involved.

Droplet size

In summary, the frictional force rises with the increase of droplet volume and velocity, the maximum magnetic force and the maximum capillary force do not depend on the droplet volume but exclusively on quantity of magnetic particles loaded into the droplet. Due to this, the maximum velocities that can be achieved by a droplet will decrease as the droplet size increases. This tendency is illustrated in **Figure 20**, with the operating boundaries OB1 and OB2.

This means, magnetically manipulated droplet systems are capable of droplet motion with volumes up to hundreds of microliters, while the so called digital-microfluidics typically involved droplet motion with volumes of few microliters by using electrowetting. [210-211]

On **Figure 20** also illustrates that a large droplet volume enables splitting, and therefore extraction, while achieving the same with smaller droplets is difficult. Such challenge can be conquered by readjusting the smoothness and roughness of the substrate used. These are aspects to

consider while designing devices using this strategy for bioassays, since the volume of the droplet dictates the quantity of reagents and material that can be analyzed and handled in one droplet.

Surrounding oil layer

So far, the presence of an oil medium has been needed to perform droplet manipulations. The oil aids the droplet manipulation by firstly, lowering the interfacial tension existing between the aqueous part of the droplet and the surrounding medium which makes splitting and extraction considerably easier.

In addition, the oil also averts evaporation of the aqueous droplet and reduces the risk of contamination. Earlier studies reported that the magnetic-bead-containing droplets were usually suspended or immersed in a container of oil,[213, 218, 226-227] which not only involves more complex fabrication process but causes as well handling and imaging issues. In alternative, as Pipper *et al.* [214-215] suggested, the aqueous droplets can be sealed by a layer of silicone oil.

Surface tension and viscosity of the aqueous phase.

The interfacial tension of a droplet depends on the surface tension of both the aqueous and oil phases which can be altered by using different buffer solutions. This can influence the magnetic actuation in ways such as, for example, when the magnet in the proximity of the droplet is moved, not all the magnetic particles move onto the contact line of the droplet during transport which means that not all the magnetic particles loaded into the droplet contribute to the magnetic force. Consequently, the actual magnetic force acting on the droplet is reduced and the magnet disengagement might occur at a lower velocity than predicted. Therefore, droplets with higher viscosity should involve a lower manipulation speeds.

Merging and mixing

The covering oil layer should be thin, since droplet merging always takes place as soon as the two droplets are brought into contact. However, for

droplets covered by a thick oil layer there is a higher challenge to merge both aqueous droplets, particularly when smaller volume droplets are involved. In such cases, a double-core emulsion comprehending both aqueous droplets is formed when the manipulated droplets merge. Because the two aqueous droplets are covered separated by a thick oil layer, the two droplets are actually separated and do not merge spontaneously. In some cases the passive droplet (recipient droplet) moves further away from the active droplet (manipulated droplet) which prevents merging from happening at all.

3.5 OSM for DNA analysis

Magnetic Manipulation of Droplets via Surface Energy Traps

Zhang *et al*. [233] reported a surface energy traps (SETs)-based magnetic droplet manipulation platform for a wide range of fluidic operations. A SET is an etched area of high surface energy (hydrophilic) on a glass substrate coated with a low surface energy (hydrophobic) film to make droplet manipulation easier (**Figure 21**). Similar designs can also be used to functionalize superhydrophobically coated surfaces for bio-adhesion in electrowetting-based microfluidic systems.[234-236] The proposed design enabled a wide range of possible droplet manipulations, including droplet transport, fusion, particle extraction, and liquid dispensing.

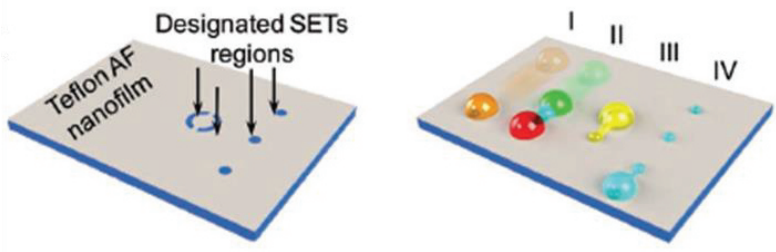

Figure 21. *Droplet handling with SETs. A pattern with SETs is done on a Teflon-coated glass substrate using lithography. The SETs are patterned selectively with the aid of a SU8 mask by etching the Teflon film with 02 plasma. The Teflon film provides a low energy surface (superhidrophobic) for (I) droplet transport and (II) droplet fusion. These SETs can be used to (III) reference the contact line for extraction of magnetic particles from a droplet and (IV) to hold*

volumes of solution to create new daughter droplets. Reproduced with permission of Wiley-VCH as in [233].

SET-Assisted Magnetic Droplet Manipulation for serial dilution.

Droplet microfluidics can be used for applications as biochemical assays without the need for complex fluidic networks of pumps and valvut not only. By using EWOD, an aliquot droplet can be easily created, but the resulting volume an be difficult to predict and to control, as it is influenced not only by the handling parameters as driving voltage and signal duration and also other aspects as surface roughness, surface coating and environmental humidity [237]. In comparison to EWOD, the biggest advantage of magnetic actuation is its capability to simultaneously manipulate both liquid and magnetic particles (MPs) at the same time for performing heterogeneous assay that need solid phase extraction [214-215, 238]. The magnetically manipulated droplets systems have been studied under various conditions and applied to different demands. [228, 233, 238-239] To address the lack of applications on operations such fluid metering and dispensing this issue, further research was carried out with SET-assisted magnetic droplet manipulation technique [233] (**Figure 22**). SETs provide an additional mechanism for droplet control. Zhang *et al*. reported a magnetic droplet microfluidic platform for facile and rapid generation of serial dilutions using these SETs that meter and dispense fluid at defined volumes. They did this by demonstrating an antibiotic susceptibility test (AST) using the developed platform by preparing droplet-based serial dilutions of antibiotics using the SET method. [240]

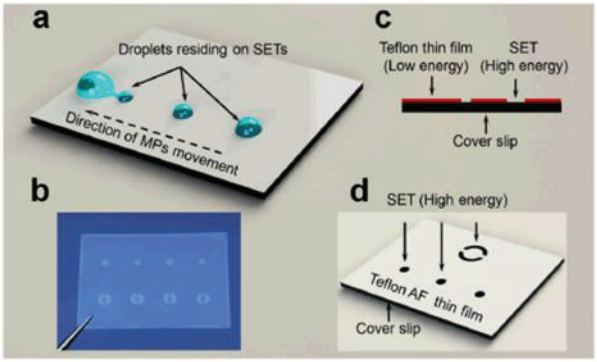

Figure 22. *Scheme of SET-enabled magnetic droplet manipulation. (a) Illustration of droplet operations on the platform where SETs control the size of*

the resulting daughter droplets. (b) Picture of an actual SET-based platform. (c) and (d) Side and top views of a SETs device. Reproduced with permission from Royal Society of Chemistry as in [240].

Biocompatible open-surface droplet manipulation

Since the earlier times of MEMS and microfluidic technologies there was interest in providing applications biomedical analysis. A few microfluidic devices for detection and sequencing of nucleic acids have been already developed. [241] The detection part can be carried out simply in a mere microchannel, which requires not as many pieces of large-scale equipment and simplifies the experimental procedure. [242] In one hand, such systems have been tested and reported with advancements in sensitivity, detection limit and specificity in DNA bio-sensing. [243] On the other hand, microchannel-based systems can be used exclusively to hybridization, since detection continues to require other peripheral instruments as for example a PCR device or a fluorescence reading for SNP identification. In addition, precision on controlling parameters as temperature (e.g. exact melting temperature of the DNA) which adds on the cost of a more complex integrated system. Such systems can be designed to identify SNPs, however they are unable to effectively detect variations with more than one consecutive nucleotide. Elghanian *et al*. reported a colorimetric method for detecting polynucleotides dependent on the optical properties of AuNP [244] however, the precise control of the experimental temperature and the sensitive manual handling was proven to require further improvement. The improvement of a new platform for multinucleotide polymorphism detection, requiring less manual handling, no thermal control and with straightforward detection results readout detection was the next objective to achieve. Therefore a new open-surface droplet manipulation microfluidic platform was designed, integrating a module for pneumatic droplet control and a superhydrophobic surface to detect multinucleotide polymorphisms. This was reported by Huang *et al*. in 2014 while adopting a novel colorimetric approach based on the growth of AuNP probes mediated by DNA hybridization in order to detect DNA present in a sample. [245] The driving energy in this case was pneumatic suction and the multinucleotide polymorphism could be detected directly with the naked eye. The proposed

platform was used for and found suitable for biological and chemical applications. (**Figure 23**)

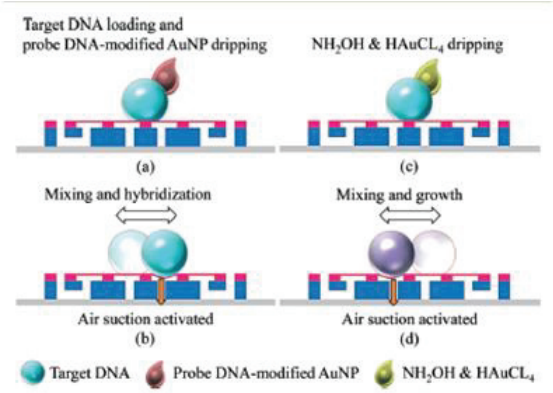

Figure 23 *Illustrated principle of the platform proposed by Huang et al. 2014 [246]. (a) Loading of the droplet containing target DNA and the probe-modified AuNP; (b) mixing and hybridization step; (c) further mixing and growth steps (d) shift in the absorption peak which can be detected with the naked eye. Reproduced with permission of Royal Society of Chemistry.*

Digital microfluidics for sequencing

The successful use of electrowetting-based digital microfluidics in DNA sequencing was demonstrated by Boles *et al.* 2011 [247] with pyrosequencing chemistry. (**Figure 24**). The earlier success of using digital microfluidic pyrosequencing to picoliter scale was demonstrated by Welch *et al*. [248] The premise was that scaling down the amounts and volumes in the processes would enable not only higher density of reactions, but also faster operation rates, and simpler fabrication involving lower costs per device.

Most next-generation sequencing technologies available reach high levels of throughput with the parallelization of large number of solid-phase reactions within one transport or solution compartments. This results in a plateau of the cost and time generated by these systems after a few hundred bp of sequence. Barcoding strategies do in fact reduce the sequencing costs per sample, however, the initial cost considering the required sample preparation and library construction is substantial. The use of droplets as single and distinct transport units for small amounts of reagents in a precised control manner gives great flexibility to modulate the throughput, cost, or run time according to the requirements of a specific application. Some clinical applications require just a

small sequence, however ideally at a low cost per run and with a rapid turnaround time. Borman *et al*. [249] showed that sequencing 35 base pairs located within the ITS2 region was enough for the correct identification of more than 40 different pathogenic yeasts. Implementing pyrosequencing as described above has advantages considering instrument size, complexity, cost, disposable cost, and obtainable degrees of functional integration. The fluid control was obtained with electrical switches and the instrument was built quite compact and inexpensive for portability potential. The disposable cartridge consisted of a PCB top. With this device, the flexible potential of digital microfluidics opened possibilities of combining DNA sequencing with upstream processes such as PCR, sample preparation, or cell-based manipulations within an integrated device.

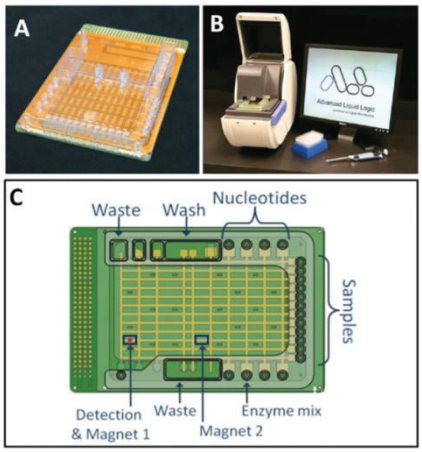

Figure 24. *(A) Photograph of the multiwell-plate-sized PCB cartridge, (B) photograph of the full device and (C) illustration of the cartridge with the mapping and highlighting of different regions and spots.* [247] *Reproduced with the permission from American Chemistry Society.*

Miniaturization research and development, together with system integration, is strongly directed by the quest of further costs reduction while reducing consumables, increasing throughput and promoting further automation.

Chapter 4

Motivation

4.1 DNA, genome and microfluidics

Deoxyribonucleic acid or DNA is a double-stranded molecule inside the nucleus of a cell and carries the genetic instructions for making living organisms. The information is carried in the form of a genetic code and is determined by the sequence of the four bases: adenine (A), thymine (T), guanine (G), and cytosine (C). The structure of DNA was first described by James Watson and Francis Crick in 1953 [250] for which they were awarded the Nobel Prize. In April 2003, 50 years later, one of the most important scientific achievements in history was announced - the sequence of the human's 3.2-gigabase genome [251]. This accomplishment was the work of thousands of scientists from around the world in the public Human Genome Project [251] and the private Celera genome project [252]. Although it took about 20 years from conception to completion, the sequence of the genome itself was produced over a relatively short period with coverage rising from about 10% to more than 90% over roughly fifteen months [251]. Crucial factors in achieving the exponential efficiency of sequence throughput were the automation in the form of commercial sequencing machines, the process miniaturization, and the optimization of biochemistry and algorithms for sequence assembly [25] (**Figure 25**).

With the completion of the draft of the human genome, the challenge now is to understand how the genes interact with proteins, drugs, metabolites, and other molecules in the cell to control its functions. Identifying genetic variations between individuals will increase our understanding of genetically related diseases and disorders and lead to molecular-level treatment specific to each individual. Consequently, a great deal of effort is being put into the development of robust, cost-effective, and high-throughput technologies for genetic-variation analysis. At the same time, in the past decade, there has been a growing trend towards downscaling molecular and cellular assays into a microfluidic format to

improve assay performance for enhanced throughput, reduced material consumption, and functional integration (**Figure 26** and **Figure 27**)**.** Thus, the work described in this thesis focused on developing methods for genetic variation analysis primarily by system miniaturization based on microfluidic technologies towards low-cost and accessibility. To put this work in context, the most common types of genetic variation are described briefly, and the current technologies involved in genetic-variation analysis are reviewed. An overview of current miniaturized formats for high throughput analysis is presented. Finally, my work in this thesis

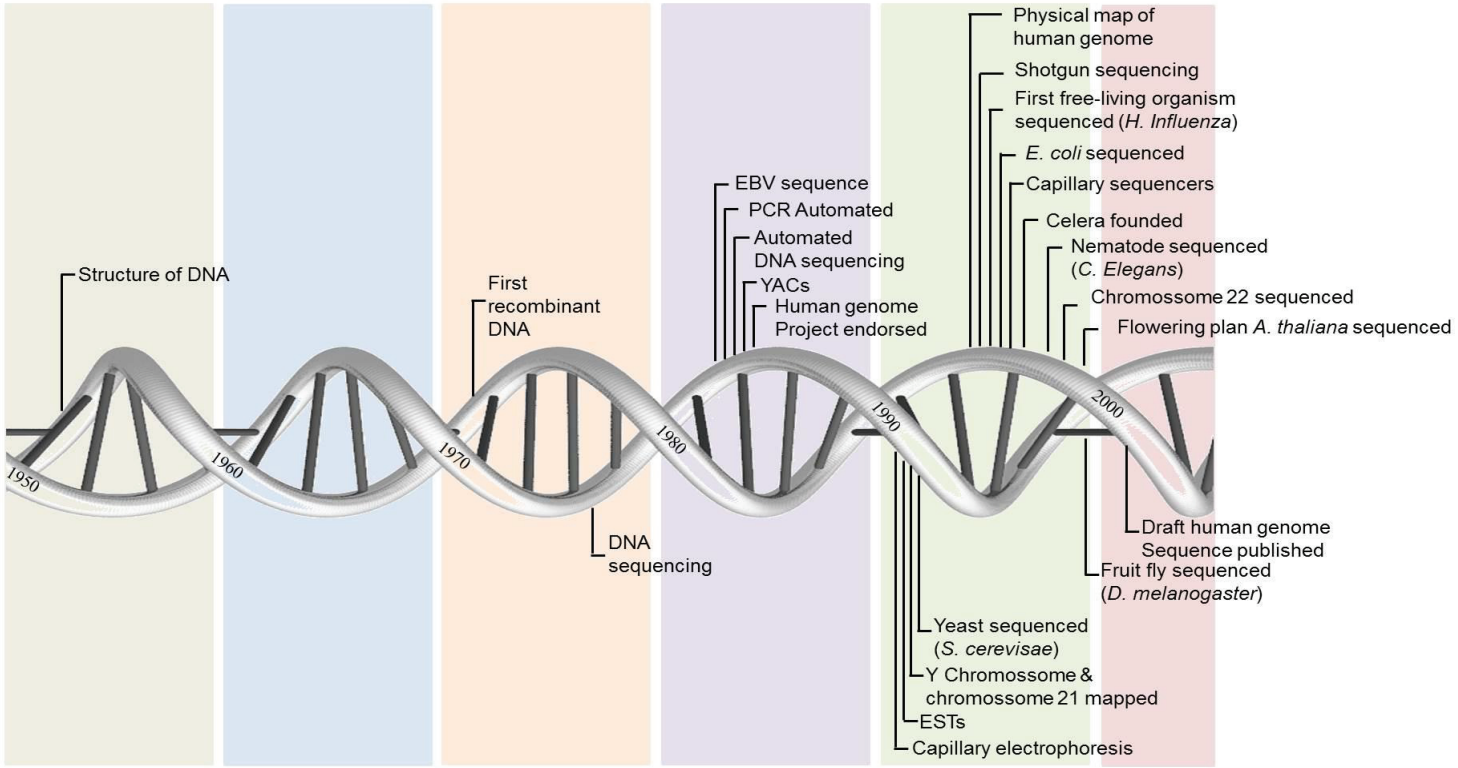

Figure 25: *A Timeline of a few advances resulting in genome-scale engineering. Everything started in 1953 with Watson and Crick and the discovery of the DNA double helix structure. In 1977, Frederick Sanger developed one of the first DNA sequencing methods and since then the technology has advanced rapidly, becoming extremely popular and developing. Afterwards, in 1990 a 13 year-long internationally funded effort was created to decode the entire human genome. Next generation sequencing technology started to be developed, and the technology advanced and still advances at a rapid pace. The most recent methods are take nanotechnology to create further faster and more effective readings*

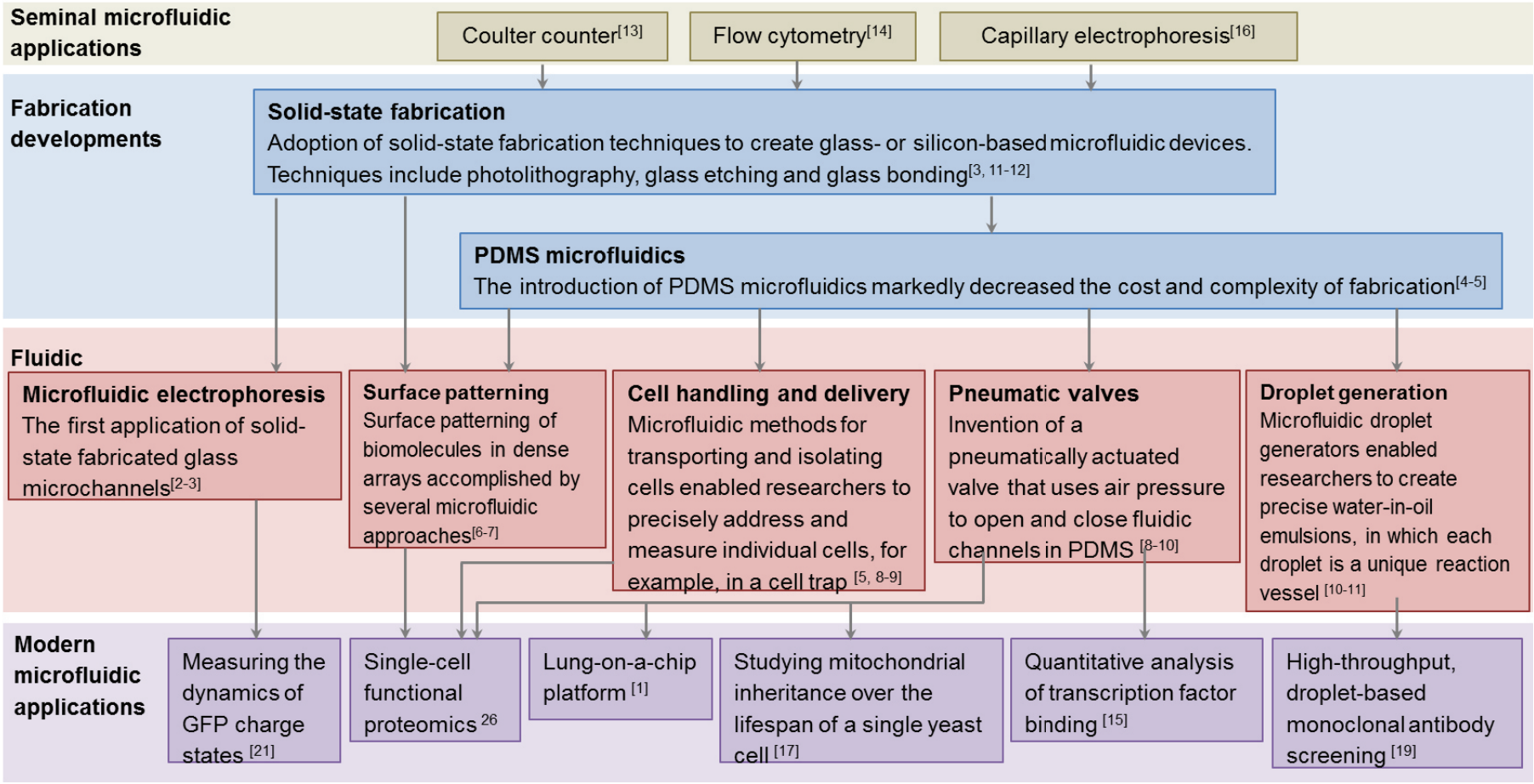

Figure 26: *A flow diagram marking key developments in the microfluidic field from fabrication approaches and functional developments to a few applications. [1] In the 1960s, technologies using microfluidics were improving both bioanalytical speed and resolution for a few analytical tools. [2-4] Starting in the 90s, major improvement in fabrication enabled researchers to quite using pulled glass capillaries and start using micro-fabricated glass or polymer microchannels. [5-7] Functionalization of portions of increasingly complex microfluidic devices is achieved [8-9]. The increasing availability of fluidic components and number of experts in different areas of the microfluidics field have opened possibilities of new biological applications including new single cell measurements[10-12], high-throughput monoclonal antibody screening[13], analysis of dynamic phenomena[12, 14-15] and organ-on-a-chip platforms[16].*

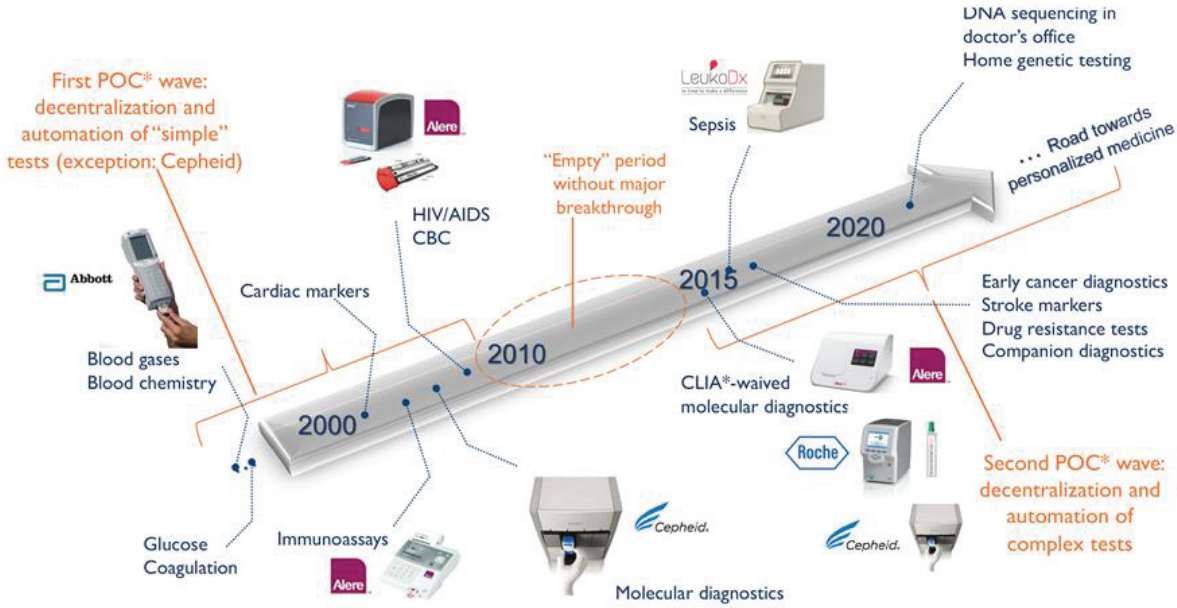

Figure 27: *Microfluidics for point of need testing – roadmap. (Source: Saphire Applications and Market 2016: LED and Consumer Electronics report, September 2016, Yole Développement)*

4.2 Objectives

Summarizing the overall motivation given in the previous chapter, the objectives of this thesis are:

1. To study the potential of droplets as virtual reaction chambers for nucleic acids handling.

2. To investigate virtual reaction chambers as a platform for DNA sequencing.

3. To devise and test the platform for single nucleotide polymorphism analysis.

4. Provide scope and perspective for the research trajectory towards more efficient and stable low cost and simple sequencing platforms.

Chapter 5

OSM and Virtual Reaction Chambers

The general aim of the research presented in this thesis is to develop a miniaturized platform for sequencing nucleic acids and detecting single-base variations. The study involves the design, microfabrication and application of a microfluidic platform: a microfluidic approach based on surface droplets (refer to subchapter **1.3.1**) and magnetic actuation (refer to subchapter **1.3.2**) is evaluated to handle nucleic acids, more particularly DNA. The feasibility of adapting pyrosequencing to a microfluidic platform was also investigated and a novel approach involving on-chip bead-based DNA analysis was developed for DNA sequencing and SNP detection.

The choice of platform for the research described in this thesis, besides all the arguments given already, is also connected with the research line of my supervisor and colleagues. During the course of my stay in KIST-europe, University of Saarland, under the guidance of Andreas Manz and supervision of Pavel Neuzil, our group pushed the boundaries on the use of surface droplets as reaction units (Virtual Reaction Chambers, VRC).

The stability of these VRCs was tested and reported in several ways by colleagues, mentioned and cited below to contextualize the research carried out for this dissertation.

5.1 Microfluidic superheating for peptide analysis

Microfluidic devices provide optimal conditions for superheating and sample handling without requiring manual labor, being three factors associated with these conditions the absence of: (i) nucleation sites, (ii) temperature gradients, and (iii) mechanical disturbances. An application for this microfluidic superheating was the energy-based fragmentation of polypeptides which drastically shorten analysis times and simplify sequence identification and conformation. This was achieved reported by Altmeyer *et al.* using the VRCs as

the suitable vessel to perform successfully thermal peptide cleavage through superheating. [253]

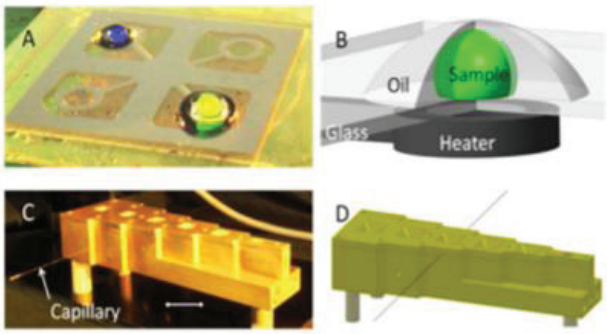

Figure 28. *Two superheating devices: (A) photograph of two VRCs on a glass slide on top a silicon heater. (B) Drawing of the VRC. (C) Fused-silica capillary placed in a brass heater. (D) Drawing of the capillary system.* [253] *Reproduced with the permission of American Society of Chemistry.*

5.2 Superheating for protein thermal stability analyses

A similar approach was applied for a few different proteins, as GFP, BSA and Taq polymerase for protein stability analysis and reported by Ahrberg *et al.*

It was demonstrated that thermostable proteins can be easily analyzed using the capability of VRCs to superheat water to temperatures over 100 degrees Celsius. While in other methods as scanning calorimetry extensive pressurized set-ups are require to measure above 100 degrees, the experimental set-up required for this work is simpler and measurements could be performed within 3 to 5 min. Furthermore, sample consumption is still lower using VRCs with sample volumes between 100 to 300 nL than for other fluorescence methods performed with commercial machines. [254]

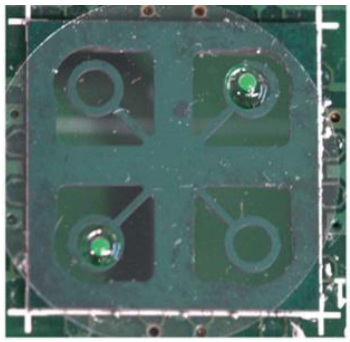

Figure 29. *Photograph of the heating chip with two VRCs on top. It is possible to perform the parallel heating of up to four samples.* [254]*. Reproduced with permission from Royal Society of Chemistry.*

5.3 qPCR with VRCs for different applications.

Many publications, being the first ones from 2006 with a first collaboration between Pavel Neuzil and Juergen Pipper, were achieved by developing platforms for the use of VRCs for PCR and sample preparation [214-215, 255-258].

The latest progress comprehends application of qPCR in the smallest instrument up to date[259], improvement of the throughput[260] and for Ebola detection[261] (**Figure 30**).

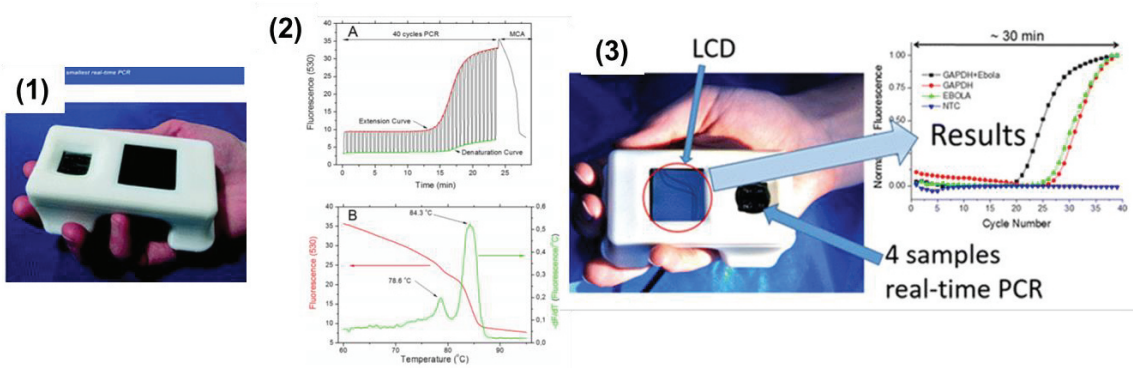

Figure 30. *(1) Photo of the handheld real-time PCR device [262] (2) Representation of the data resulting from the Real-Time PCR [260] (3) Photo of the device for Ebola detection. [261] Reproduced with permission from both Springer Nature and Royal Society of Chemistry.*

5.4 My published research

- Fast spore breaking by superheating[263]
- Pyrosequencing on a glass surface[264]

5.5 Wrap up

Quoting Neuzil:

"Stationary systems are simple, therefore more trustworthy than dynamic ones. In addition, complex systems have a much higher chance of failure than simple ones."

Therefore, "**simplicity**" is the keyword behind the goals of this thesis.

Chapter 6

Materials and Methods

The overall objective of the research presented in this thesis is to develop an accessible miniaturized technology for sequencing nucleic acids and detecting single-base variations. The study involves the design and microfabrication of a microfluidic platform with attention being given to the biological compatibility of the process and the evaluation of the biological assays. A microfluidic approach based on surface droplets (refer to subchapter **1.3.1**) and magnetic actuation (refer to subchapter **1.3.2**) is evaluated to handle nucleic acids. The feasibility of adapting pyrosequencing to a microfluidic platform was also investigated and a novel approach involving on-chip bead-based DNA analysis is was developed for DNA sequencing and SNP detection.

In this chapter more details on the materials and experimental design approached are described.

6.1 Glass substrate

Recently, maneuvering droplets on an open surface offers an alternate way of performing bioassays at the micro level [210, 265-267]. Here, sample droplets are confined by surface tension and function as reaction or transport units (virtual chambers). In order to actuate these droplets, magnetic force[214-215, 228, 233, 238-239, 268] has been employed to enable a wide range of droplet operations including dispensing, moving, splitting and mixing[233, 269-270].

These virtual reaction chambers are prepared on a flat substrate. For this flat substrate it was decided that the material should be easily accessed (for potential in point-of-care applications it must be disposable and easily replaced) and not rise issues with surface modifications. Due to this, and considering previous platforms using a VRC system [213-215, 228, 253, 256, 271], a microscope glass cover slip was selected as the flat substrate.

The microscope glass cover slip was coated with fluorosilane (heptadecafluoro-1,1,2,2-tetrahydrodecyl)trimethoxysilane, (tridecafluoro - 1,1,2,2-tetrahydrooctyl)trichlorosilane (FOTS) or 1H, 1H, 2H, 2H-perfluorodecyl-triethoxysilane (FAS-17), typically by a chemical vapor deposition (CVD) process at temperature of ≈150°C. This was chosen over Polytetrafluoroethylene, PTFE (being best known as the commercial brand Teflon) coating due to materials cost and high similarity of contact angle results between both coatings.

6.2 Droplets

The water contact angle at the FAS-17 surface was as high as ≈115° and mineral oil type Sigma M5904 exhibited an angle of ≈65°. These hydrophobic and oilophobic properties ensured that both liquids did not spread around and stayed where we dispensed them. The water-based sample was pipetted into an oil droplet with typically volume 100× smaller than that of the sample. Surface tension of both liquids with their ratio of 100:1 resulted in self-aligned system with the water sample covered with a layer of oil. The cross section through the water-based sample in a VCR-PCR system is shown in **Figure 31** where the ratio is 1:3 (sample:oil). On **Figure 32** we can see the higher contact angle with the ratio 100:1

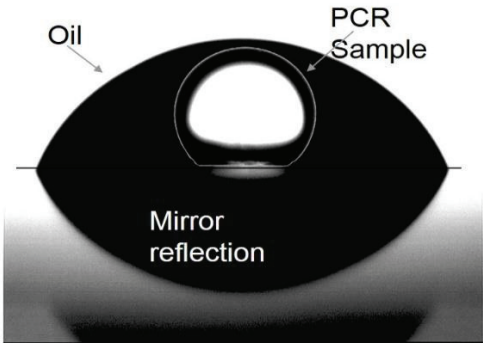

Figure 31: *VCR used for a miniaturized PCR device (Neuzil et al, 2006): 2 droplets, one sample droplet (PCR sample) within a mineral oil droplet on an hydrophobically coated glass surface.*

The stability of VRCs was tested in several contexts, having been used for superheating of spores[263], peptides[253], sample preparation[272] and PCR [256-259, 273-274] among, possibly, others.

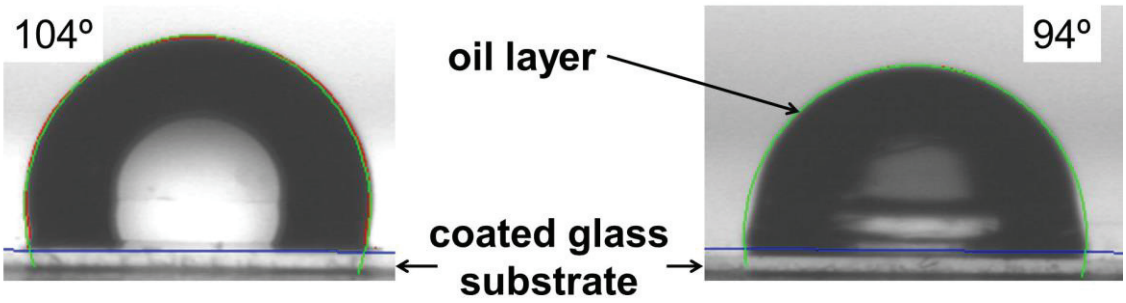

Figure 32: *Profile photo on the left of a water droplet on an hydrophobically coated (FAS-17) glass cover slide.exhibiting a contact angle of 104°, and on the right, of a VRC with ratio of water-sample:oil-layer of 100:1, giving a contact angle of 94° on the same hydrophobically coated (FAS-17) glass cover slide.*

6.3 XYZ stage

Initially, a manual way of magnetically actuating the VRCs was designed. A xy-translation microscope stage was adapted to a holder, together with a z-translation platform. A magnet was fixed to this z-translation platform in order to test the magnetic actuation of the droplets spotted on the glass slide placed in the center and on top of the xy-translation stage. In order to move the xy-translation stage, a ratchet-style system was implemented to move the magnet in increments of 3 mm both on x- and on y-axis. (**Figure 33** and **Figure 34**)

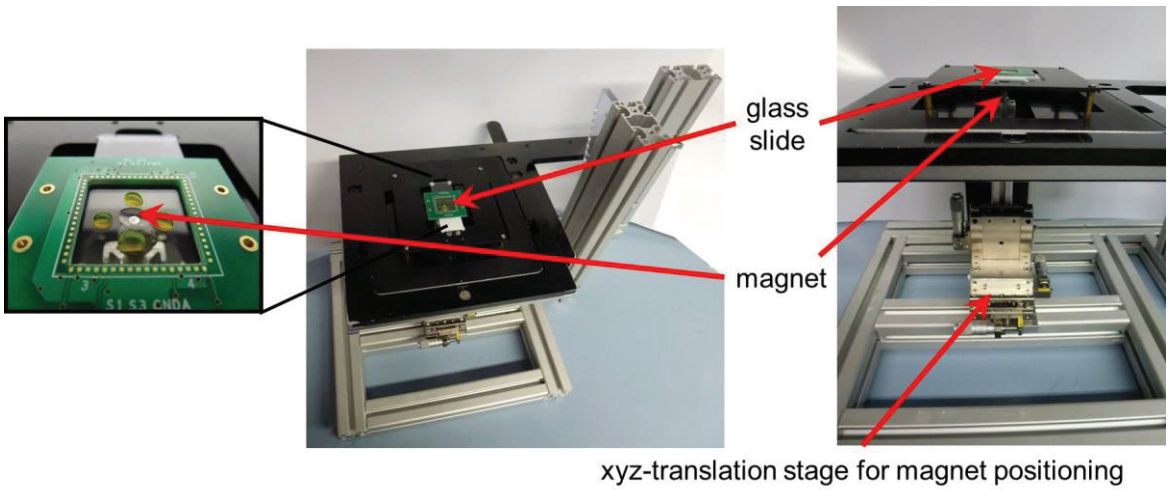

Figure 33*: Microscope translation stage on "homemade" setup. The microscope xy-translation stage is fixed. A precision z-translation platform is coupled underneath and a magnet is attached to its centre. A glass slide is*

placed on top and on the centre of the xy-translation stage, having the magnet placed just beneath.

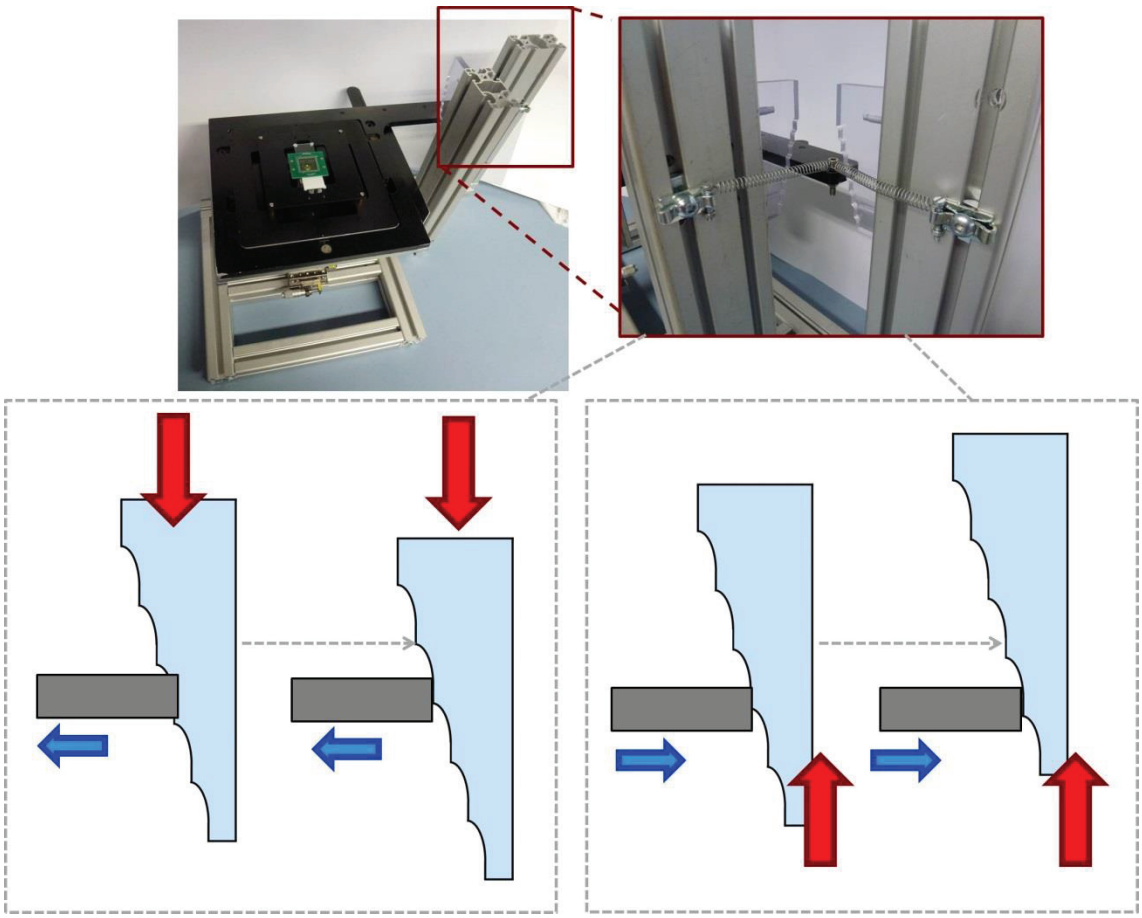

Figure 34: *Manual, incremental steps using ratchet-style system; 3 mm steps for forward/backward, and left/right motions.*

A disc (1/8 in.) neodymium magnet (no. B421, Supermagnetic.de) was placed 0,6 mm beneath the glass slide, with vertical alignment. This model was chosen due to the combination of ability of focusing the particles through the glass slide thickness and availability in the lab.

After the magnetic actuation was concluded and the decision on the magnet to use was done, there was a need to exchange the manual xyz stage for an automatic (the movement and positioning of the magnet must be more flexible, smooth and not done in increments, rather on a continuous movement) (**Figure 35**).

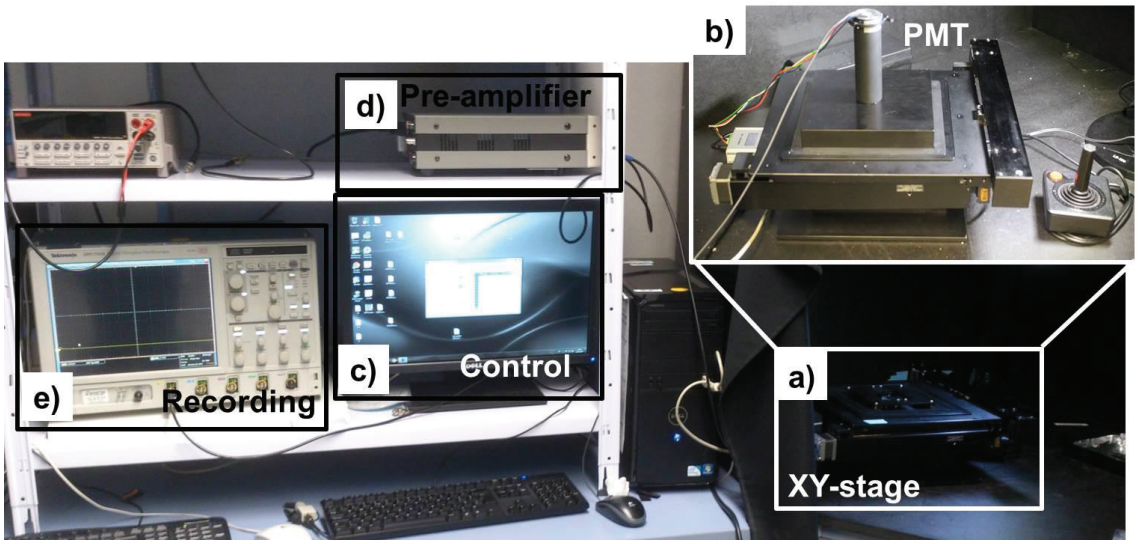

Figure 35: *Photograph of the entire set up, where a) corresponds to the motorized xyz-stage placed in a black box, b) illustrates the PMT placed on top od the xyz-motorized stage for detection, c) the software to program the xyz-motorized stage, d) the pre-amplifier for the secondary photodiode that works as control to the PMT (placed underneath the glass slide.), and e) the recording oscilloscope.*

6.4 Detection system

Luminescent detection was tested and achieved using a 1x1 cm photodiode placed underneath the glass slide, on top of the z-translation stage with the magnet attached to it, and a photon-counting photomultiplier tube (PMT) module (H7155, Hamamatsu, Japan) placed on top of the glass slide holder. Both the photodiode and the PMT were connected to a current amplifier, and the signal was recorded with an oscilloscope. Thus, all reactions were conducted at the sample location with respect to the PMT. With this setup, both the magnet and the PMT were stationary while the glass was movable. The stage with the PMT and magnet was placed in a black box to eliminate ambient light noise. The PMT was equipped with an internal current-to voltage converter, with its gain adjusted to ≈0.7 V using a custom made PMT controller setting the gain value to ≈105 as interpolated from a graph supplied by the manufacturer. The PMT output was directly connected to the input of an oscilloscope model DPO 7054 provided by Tektronix, Inc. (USA) to record optical power as a function of time (**Figure 35**).

6.5 SPP/ssDNA/primer complex preparation

For pyrosequencing, ≈100 µL of superparamagnetic particles M280 Dynabeads functionalized with streptavidin from Life Technologies, GmbH (Germany) was washed three consecutive times and re-suspended in 100 µL of binding buffer (10 mM Tris buffer pH 7.6, 2 M NaCl, 1 mM EDTA solution and 0.1% Tween 20). All products were acquired from by Sigma-Aldrich, GmbH (Germany).

DNA has to be extracted from the sample organism/solution, purified, and amplified by PCR, all prior to pyrosequencing.

An amount of circa 4 µg of biotinylated PCR amplicon suspended in 100 µL of H_2O were added to the superparamagnetic particles and incubated at 65 °C for 15 min with intermittent mixing for allowing the DNA binding. The double-stranded amplicon was denatured by adding the superparamagnetic particles to denaturation buffer (100 µL of 0.5 M NaOH for 1 min). The superparamagnetic particles were then washed with NaOH followed by three additional washing steps in annealing buffer (20 mM Tris acetate, pH 7.6, 5 mM magnesium acetate) to obtain ssDNA. The superparamagnetic particles were re-suspended in 100 µL of annealing buffer before adding 5 µL of 10 µM sequencing primer for hybridization of the primer. The solution was heated to 80°C for 2 min using a heating block and let cool down to room temperature for the primer to hybridize. The SPP/ssDNA/primer complex was washed three times in pyrosequencing wash buffer as described in **section 6.6**. Afterwards, 15 µg of single-stranded binding protein (SSB) by Promega, GmbH (Germany) was added and the mixture incubated at room temperature for 10 min. The SPP/ssDNA/primer complex was washed with pyrosequencing wash buffer and re-suspended in 200 µL of this same buffer to achieve a final particle mass concentration of circa 5 µg μL^{-1}. Considering the manufacturer's given specified binding capacity for the SPPs, it was estimated that the 5 µL aliquot used in each sequencing reaction contained between 100 and 500 pmol of template DNA.

6.6 Buffers and solutions preparation

Distinct stock solutions were prepared for performing pyrosequencing: washing buffer, enzymes, dNTPs, and DNA. Pyrosequencing washing buffer was prepared by adding 100 mM Tris acetate pH 7.6 with 0.5 mM ethylenediaminetetraacetic acid (EDTA) pH 8.0, 5 mM magnesium acetate, and 0.01% Tween 20. Enzymatic aliquots were prepared with pyrosequencing washing buffer by adding 13.5 mU μL^{-1} ATP sulfurylase by New England BioLabs Inc. (Germany), 1.5 µg μL^{-1} luciferase and 1.8 µg μL^{-1} D-luciferin by Sigma-Aldrich, GmbH (Germany), 6.9 U μL^{-1} Klenow (exo-) fragment by ThermoFisher Scientific, GmbH (Germany), and 0.01% Tween 20, 18 µM stock solutions of each dNTP by Thermoscientific, GmbH (Germany) were added to pyrosequencing washing buffer with 15 µM APS by Sigma-Aldrich (Germany), 3 mM dithiothreitol (DTT) by Sigma-Aldrich, GmbH (Germany), 120 ng μL^{-1} single stranded binding protein (SSB), and 4.6 U μL^{-1} Klenow (exo-) fragment.

6.7 Glass spotting

The oil-coated and bead-containing droplets were placed on the hydrophobic surface of the substrate by precision-pipetting. In our experiments, the amount of surrounding oil layer, reaction or washing solutions and the SPPs/ssDNA/primer complex suspension were sequentially added, which spontaneously formed the droplets. Firstly, the suspended SPP/ssDNA/primer complex in the aqueous droplet is attracted to the bottom of the droplet by the magnetic force from the permanent magnet placed below. When the magnet is moved horizontally and parallel to the glass substrate, the SPPs follow the magnet until they reach the edge of the aqueous droplet, where they form a compact cluster. Secondly, the magnetic pulling force acting on the SPP-cluster is transferred to the water/oil interface and deforms the droplet. Thereafter, and as explained previously in **section 3.3** two distinct operations were achieved: droplet transport for mixing reagents that need to be separated until the moment of reaction and SPP extraction for washing steps.

With this in mind, a few different designs for spotting of the VRCs were tested.

6.7.1 X-design

Similarly to the pattern used before in a PCR platform (**Figure 36**) the initial idea for an experiment would be having 4 droplets containing all reagents needed for pyrosequencing and each one of the nucleotides on the chip with one droplet for washing in the center and make the magnetic particles move inwards and outwards to fulfil cycles of reaction and washing (**Figures 37** and **Figure 38**).

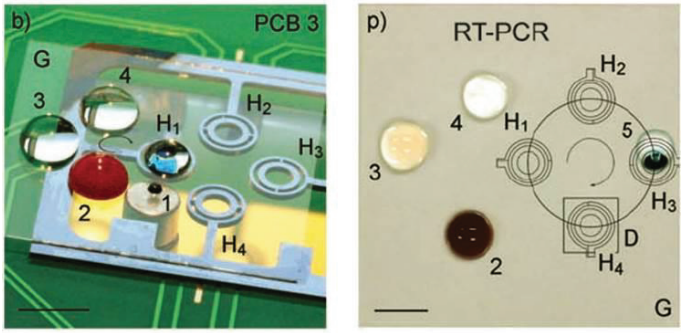

Figure 36: *Sample preparation and PCR platform using VRC (Pipper et al, 2008).*

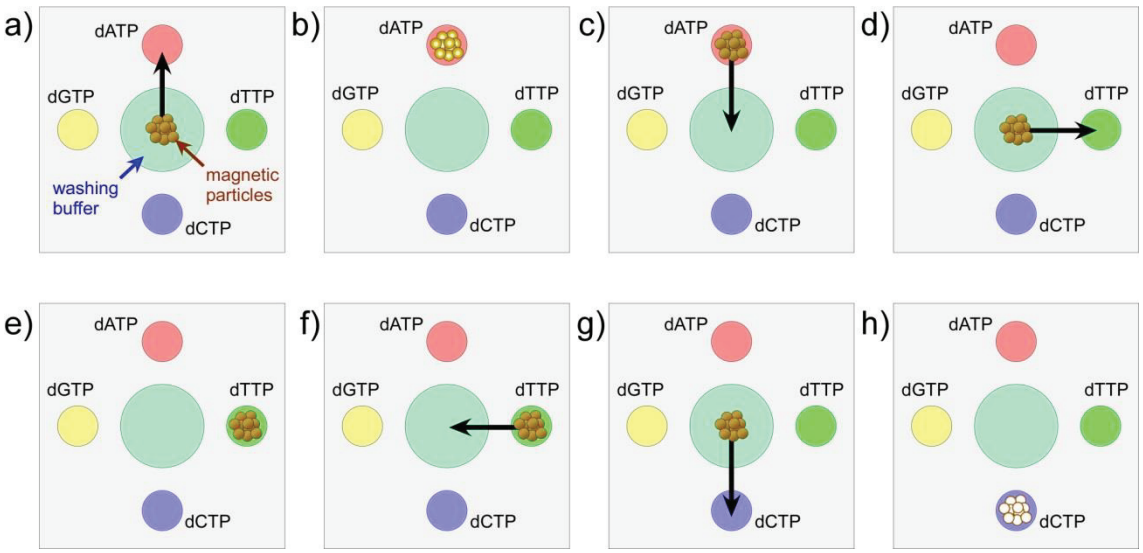

Figure 37: *Droplet-based pyrosequencing. (a) ssDNA bound to magnetic particles is pulled into the first nucleotide droplet (dATP) where (b) dATP is incorporated and light is emitted. The particles are then (c) washed, and (d) dragged into the dTTP droplet, where (e) no light is produced, hence dTTP is*

not incorporated. The procedure continues to the remaining droplets completing one cycle. The cycle is repeated until no more light is detected (end of sequencing or depletion of reagents).

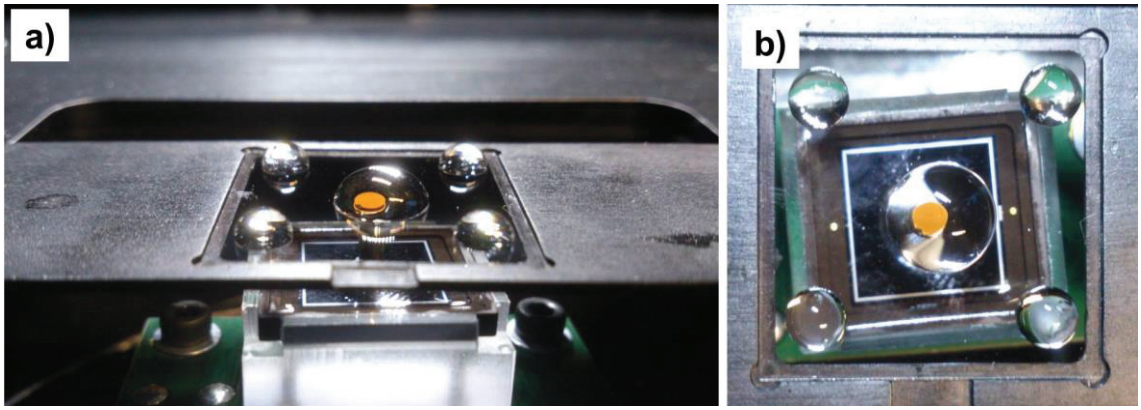

Figure 38: *Photograph of the setup, showing the central wash droplet and the four nucleotide droplets around it a) side view, b) top view. The magnet can be seen underneath the glass slide. The glass slide was moved via a motorized translation stage, while the magnet was fixed in position. A PMT was used for detection and all reactions took place inside a black box. The particles can be seen as a brown pallet on top of the glass actuated by the magnet beneath it.*

6.7.2 Circle/linear design

If contamination would be evident than a washing step before each reaction droplet could be added (**Figure 39**).

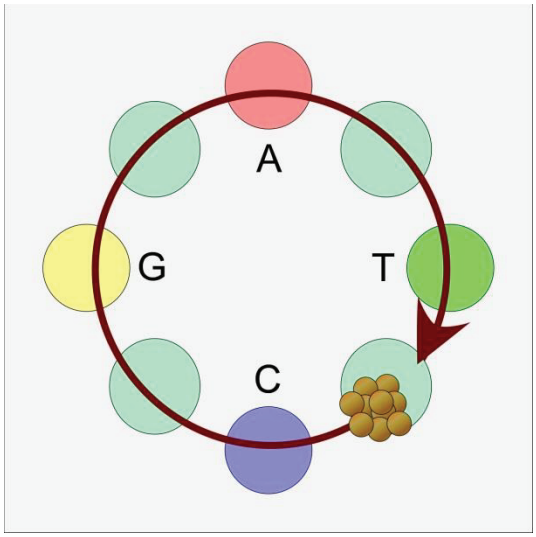

Figure 39: *Droplet-based pyrosequencing. ssDNA bound to magnetic particles is pulled into the first nucleotide droplet (dATP) where dATP is incorporated and light is emitted. The particles are then washed, and dragged into the dTTP*

*droplet, where no light is produced, hence dTTP is not incorporated. The procedure continues to the remaining droplets completing one cycle. The cycle is repeated until no more light is detected (end of sequencing or depletion of reagents) and the motion happens in a circular movement of the magnet. In comparison with the previous design (**Figure 37**) there are more washing stations present in order to reduce contamination issues.*

6.7.3 Enzymes separated from substrate design

For this design, the enzymes needed for pyrosequencing are separated from the substrates in different droplets. These two smaller droplets (3 and 2 µL respectively) are merged only when the SPP/ssDNA/primer complex moves and drags them into the space between them.

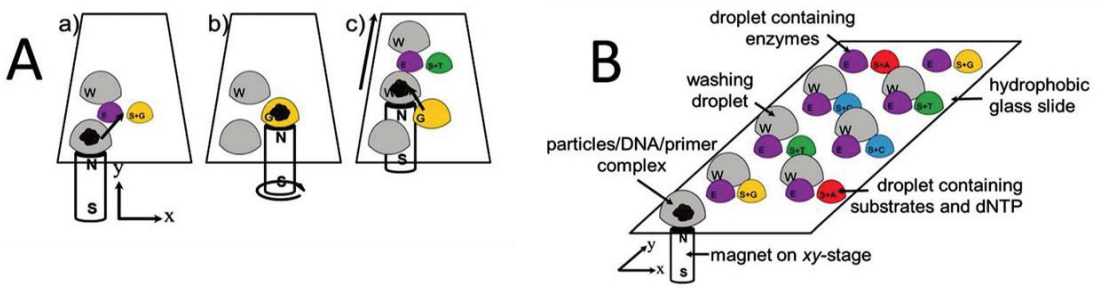

***Figure 40:** (A) Scheme of a nucleotide addition cycle.(a–c) Three phases of the droplet manipulation being a) extraction from SPP from washing droplet and moving to reaction station, b) merging of enzyme and substrate droplets and c) extraction of SPP towards a fresh washing droplet. (B) Overview of the experiment setup; (W) washing droplets; (E) droplets containing all the needed enzymes for the pyrosequencing reaction (S + G − T − C − A).*

6.8 DNA preparation

Preceding the sequencing, DNA has to be extracted from the sample, purified, and amplified by PCR.

The DNA used for *de novo* sequencing was prepared by nested PCR for biotinylation of the amplicon (221 bps long). A section from the pfcrt 271 region from human genomic DNA was picked. (Primers: external forward: 5'-GGC TAT GGT ATC CTT TTT CCA A-3'; external reverse: 5'-CGA CTG TGT TTC TTC CCA AG-3'; internal forward: B-5'-ATC CTT TTT CCA ATT GTT CAC TTC-3'; and internal reverse: 5'-CGA AAC CAT TTT TTA TAT TTG TCC-3'.) Sequencing was carried out with the sequencing primer 5'-TTT CCT AAT TAA

TTC TTA CG-3'. The amplification was carried out in a LightCycler®1.0 System (Roche, Switzerland) and a SYBR Green based kit compatible with the system.

The sequence B-5'-ATG GGG GGG GGG ATG GGG GGG GGA TGG GGG GGA TGG GGG GGA TTG GGG GGT TGG GGG ATG GGG TCT GGT ATG GAT GTA AAC GCC TGG TAT CTT TAT AGT CCA-3' was assessed with the sequencing-primer 5'-GGA CTA TAA AGA TAC CAG GCG TT-3' using the concentrations of DNA 0.315 pmol, 1.25 pmol, 5,pmol, 15 pmol and 20 pmol.

The sequence B-5'-ATG GGG GGG GGG ATG GGG GGG GGA TGG GGG GGG ATG GGG GGG ATT GGG GGG TTG GGG GAT GGG GTC TGG TAT GGA TGT AAA CGC CTG GTA TCT TTA TAG TCC A-3' was assessed with the sequencing-primer 5'-GGA CTA TAA AGA TAC CAG GCG TT-3'.

The resulting PCR product was cleaned with the PureLink® PCR Purification Kit (ThermoFisher Scientific, Germany) and the biotinylation was checked with the Agilent Bioanalyzer 2100 (Agilent, Germany) together with the DNA 12000 Kit following standard protocols.

Chapter 7

Results and discussion

The aim of this thesis, as has been stated in the preceding chapters, is to explore miniaturized technologies for sequencing nucleic acids and detecting single-base variations. The study involves the design and microfabrication of a microfluidic platform with attention being given to the biological compatibility of the process and the evaluation of the biological assays. A microfluidic approach based on virtual chamber reactions (and magnetic actuation is evaluated to handle nucleic acids. The feasibility of adapting pyrosequencing to a microfluidic platform was also investigated and a novel approach involving on-chip bead-based DNA analysis is was developed for DNA sequencing and SNP detection.

This chapter is meant to report and discuss all relevant results obtained on the pursuit of the goals above mentioned.

DISCLAIMER: The results presented on this thesis are published in Open Access format (A. V. Almeida, A. Manz, P. Neuzil, *Lab on a Chip* 2016, *16*, 1063-1071) [264], with the knowledge and permission of co-authors and publisher, Royal Society of Chemistry.

7.1 Experimental design

The basic experimental idea can be represented by the workflow presented in **Figure 41**. The first step (experimental design) comprises the knowledge of the nucleic acid sequence to be analyzed and arranging all resources needed.

Figure 41: *Diagram expressing the workflow from experimental design to sequencing step. Design stands for experimental design and comprehends all thought processes leading to have all the correct PCR and sequencing primers, adjusting of reagents, preparation of the glass slide and programming the motorized stage. The PCR is used for biotinylation of the DNA and to make the sequences more manageable and pure. The check involves the PCR product purification and the confirmation of its purity by Bioanalyzer. The last two stages correspond to the preparation of the VRCs responsible for washing and reaction stations and to perform the magnetic actuation of the system.*

Then, the DNA to be sequenced must be extracted, prepared and checked for biotinylation and purity as mentioned in **subchapter 6.8** (**Figure 42**). This ssDNA must then be bound to streptavidin coated paramagnetic particles via biotin-streptavidin bond. The sequencing primer must as well be annealed after this point as described in **subchapter 6.5** (**Figure 43**).

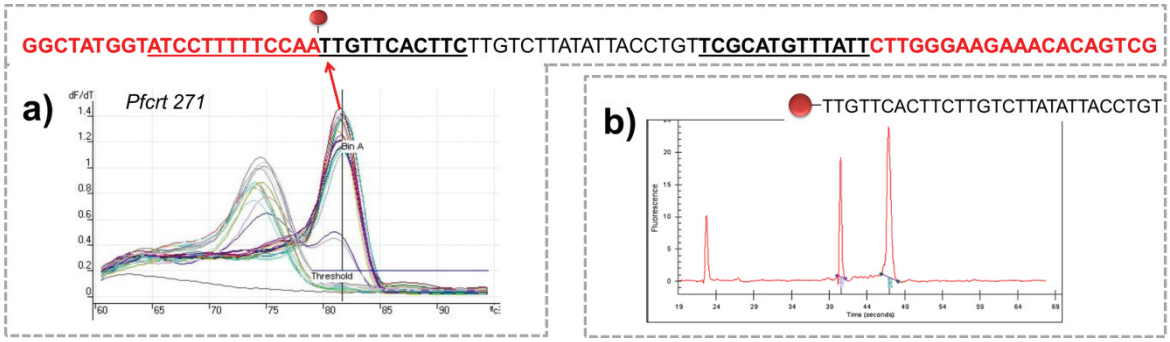

Figure 42: *On top of the figure, the target-sequence is analyzed according to the required primers and where the biotinylation should occur (marked by the red circle). Red nucleotides and underlining show positions of internal and external primers used in the nested. In a) we can see the result on the qPCR, beinfg the highest peak correspondent to the desired product (desired sequenced to test the sequencing on). b) After proceeding to purification of the product(to remove the enzymes, excess of primers and other byproducts, the purified and desired sequence in analyzed for biotinylation success using the Bioanalyzer and the corresponding kit.*

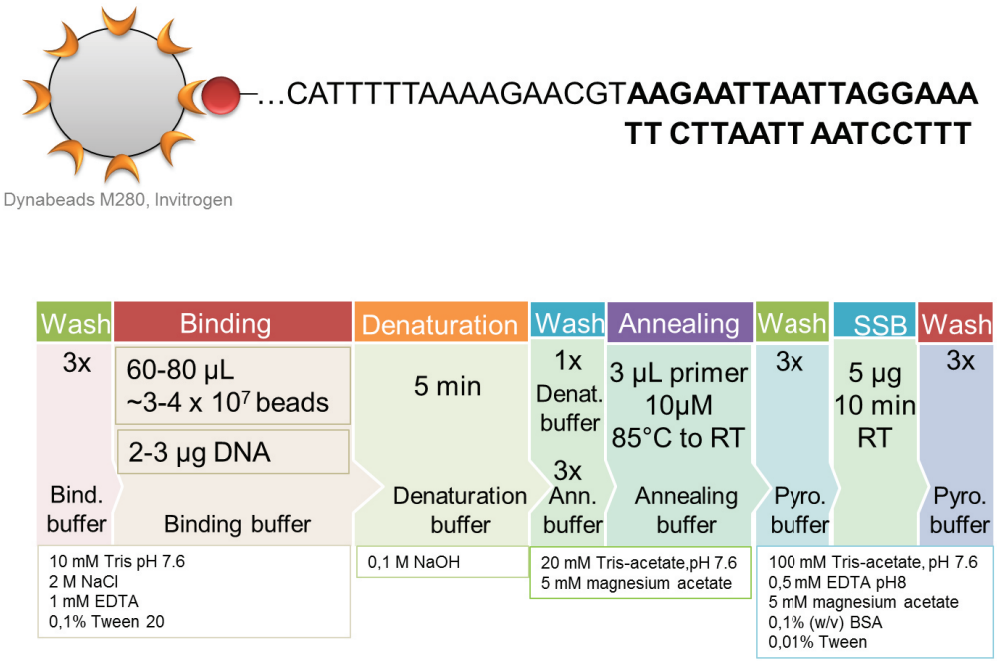

***Figure 43**: Biotinylated DNA from is obtained by PCR and then bound to streptavidine-functionalized superparamagnetic particles. Further washing and incubating steps are perfomed until an amount of 0.25-0.5 pmol of template per µL of paticles is achieved. The exact composition of the buffers and procedures are described in the table.*

7.2 First experiments

Finally, the VRCs must be placed on the flat hydrophobically coated glass substrate in a pre-determined position and the paramagnetic particles can then be actuated using the xyz-translation stage (**Figure 44**).

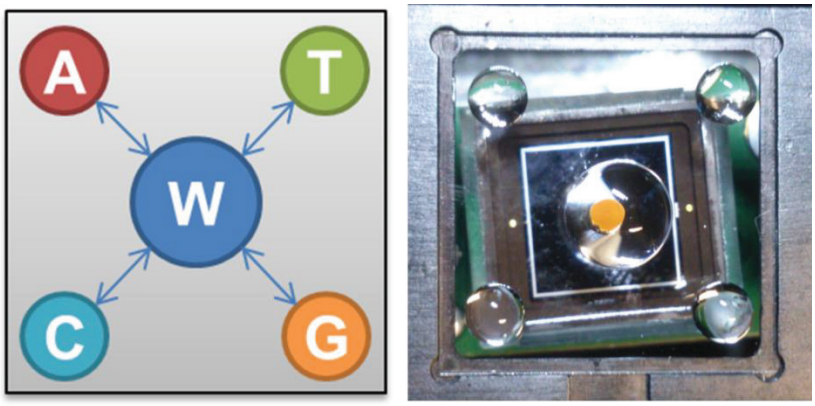

***Figure 44:** Scheme and photograph of the setup, showing the central wash droplet and the four nucleotide droplets around it. The magnet can be seen*

underneath the glass slide. The hydrophobic glass slide is moved via a motorized translation stage, while the magnet is fixed in position. A PMT is used for detection and all reactions took place inside a black box. Five droplets are spotted in a cross pattern onto the cover slip): a large central droplet (60 µL) containing only washing solution, and four droplets (20 µL) arranged around it containing one of the nucleotides together with the necessary pyrosequencing enzymes. The droplets are each sealed in a layer of mineral oil to prevent evaporation. On the photograph, the paramagnetic particles can be seen in the washing droplet forming a brown coloured pellet on top of the magnet.

To test the detection system before performing pyrosequencing and wasting reagents, luciferin and luciferase were mixed with ATP (the needed substrate for the luciferin to be oxidized by the luciferase with release of photons, refer to **subchapter 1.3.4** for more details). An intense and sharp peak was easily detected using the prepared set up (**Figure 45**) meaning the detection system is sensitive enough for the goal of this project.

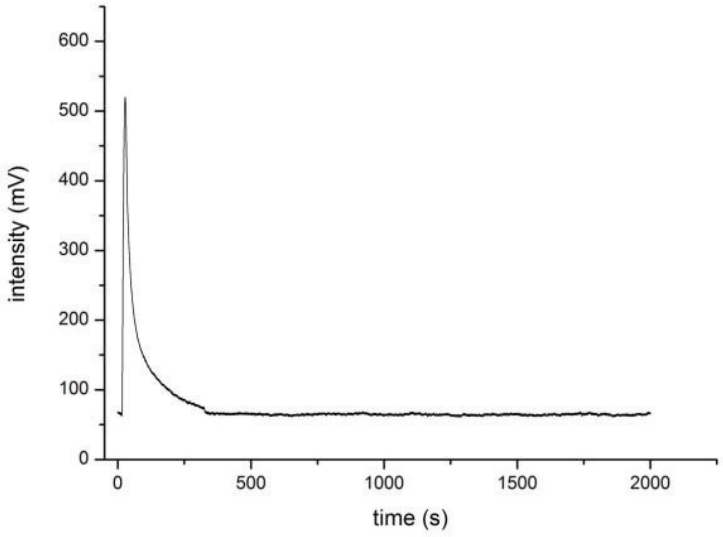

Figure 45: *Plot derived from the detection system. Mixture of ATP, luciferin and luciferase produced photons that could be easily be detected by the photodiode from the set up. The signal was recorded in intensity (mV) over time (seconds).*

In order to see if the motion of the motorized stage for magnetic actuation would interfere with the detection system, a simple program mimicking the magnetic actuation through the reaction and the washing VRCs was programmed. As seen in **Figure 46**, in fact the motion of the stage can be detected and it follows a pattern (as expected since the program selected follows the same movement between 5 different droplets for a number of cycles.

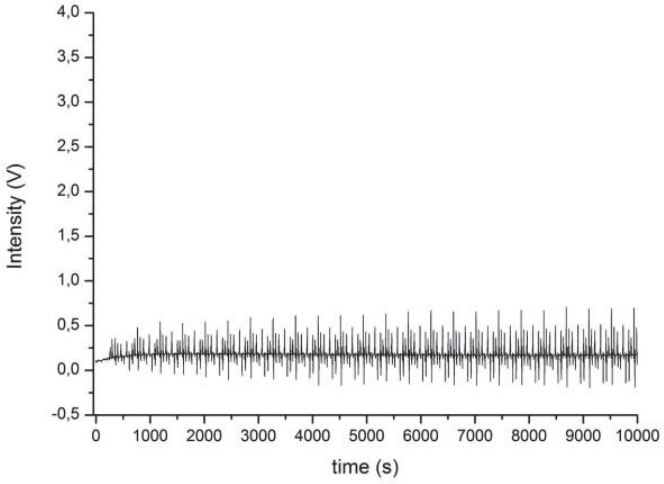

***Figure 46**: Background noise detected with a run of the motorized stage performed without reagents. Here; the pattern of the repeated cycles of the same movements combination can be easily observed.*

After the background noise derived from the inevitable motorized stage motion was determined, the first try for pyrosequencing using the cross design for VRC spotting was performed. **Figure 47** shows the same pattern obtained for the background check. However, a wide, single peak was detected. As the "peak" occurs, the noise becomes more prominent making it difficult for extraction of the background or further interpretation. Nevertheless, more time was given for the particles to be in a droplet (both reaction and washing) in order to evaluate differences to the initial try and the results can be seen in **Figure 48**.

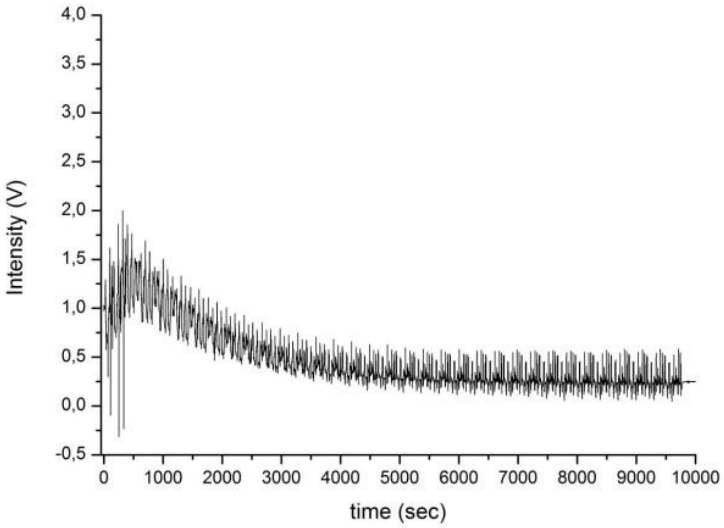

***Figure 47:** Failed pyrogram showing the motion pattern with a wide peak not corresponding to the reaction droplets. Almost like a single reaction event. The motion noise seems to be sharper within this "peak" which makes difficult for background noise removal.*

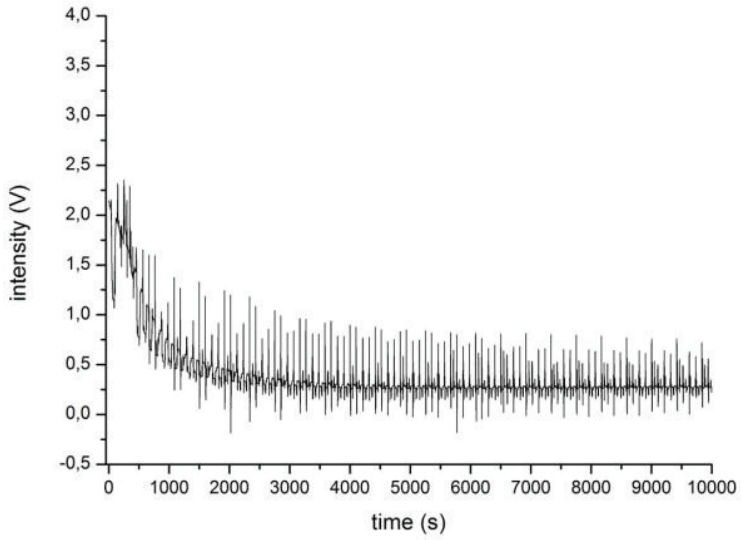

Figure 48: *Failed pyrogram showing the same motion pattern with a wide peak not corresponding to the reaction droplets. With more time in a specific droplet it is more obvious the pattern to be related with the stage motion and not from light detection.*

A longer time for reaction was tested as well and is summarized in **Figure 49.**

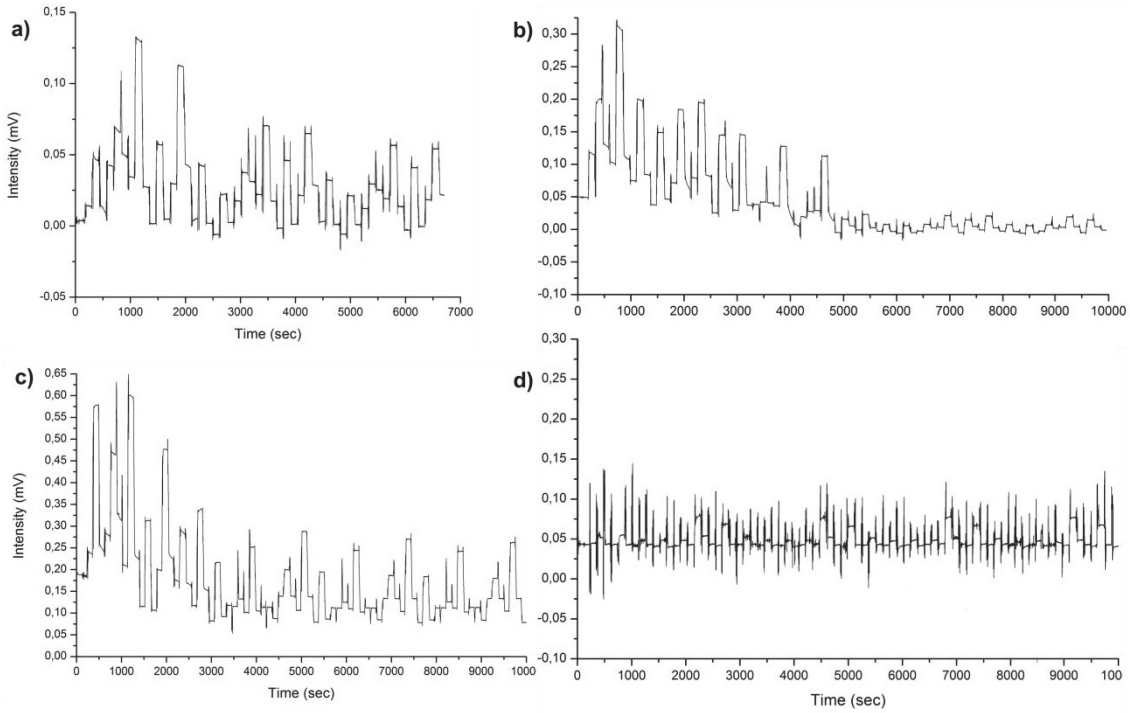

Figure 49: *a) GCTA; b) AGTC and c) ATGC are all tries of sequencing using a longer reaction time. And d) is the corresponding blank.*

At this stage it was obvious that major changes and improvement was needed. and main priorities were established:

- Test different VRC spotting patterns.
- Optimizing the ratio between beads – DNA - droplet size – droplet distance (kinetics evaluation).
- Investigate Z influence on particles dispersion.
- Test washing efficiency.
- Demonstrate the technique feasibility by detecting a known sequence

7.3 VRCs placement

For testing different VRC spotting designs, the 5 droplet system was put aside and in order to have more flexibility of rearrangement the 2x2cm glass slide format was substituted by the 2x6 cm format (**Figure 50**). As well, washing efficiency was tested to see if there was any carry over/contamination by the SPP.

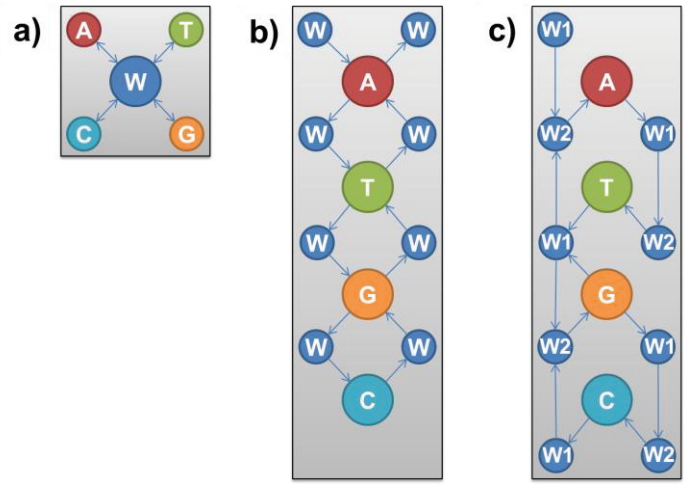

Figure 50: a) *was the one tested, the* ***b)*** *is the same as the circle design but this in linear form which gives more possibilities of cycling more often with fresh washing droplets (refer to circle design on subchapter* ***4.7.2****.* ***c)*** *represents a design for incorporation two washing droplets between two reaction.*

By using single-use VRCs and extending further the time for each reaction to happen, the first expected peaks started to appear. Two different testes, being one having all reagents, with all 4 nucleotides and the complex SPP/ssDNA/primer letting to react until reaching baseline, and the other all

reagents without the complex SPP/ssDNA/primer letting to react until reaching baseline as well, were carried out (**Figure 51**). From this, it was confirmed that whenever substrates and enzymes are together in solution there is always a background reaction. Either the entire sequencing should happen in this window or substartes and enzymes should be kept separated until needed.

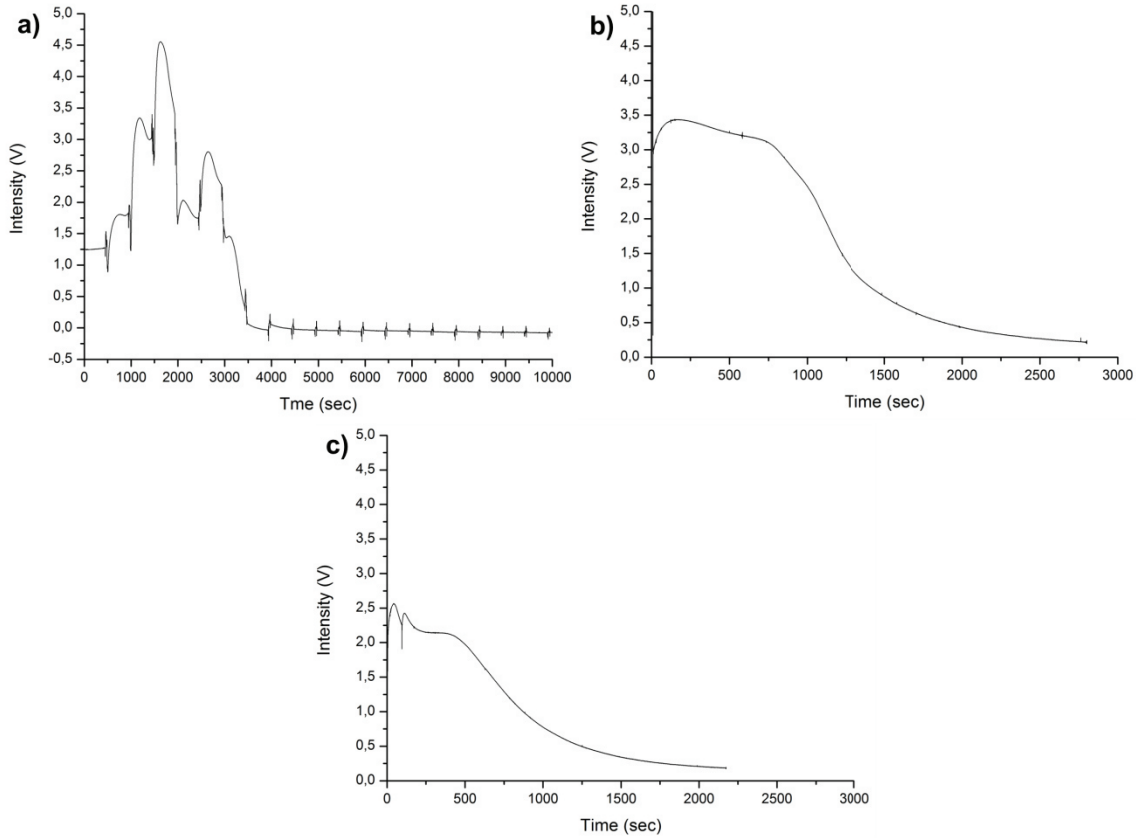

Figure 51: *a) was having both reaction and washing VRCs beingsingle-used having each reaction last for 500 sec. b) was having all reagents with all 4 nucleotides and SPP/DNA/primer complex simulatenously; c) having all reagents without the SPP/DNA/primer complex.*

In case of the first option, some success was achieved (**Figure 52**) but the peaks still didn't show the typical curve.

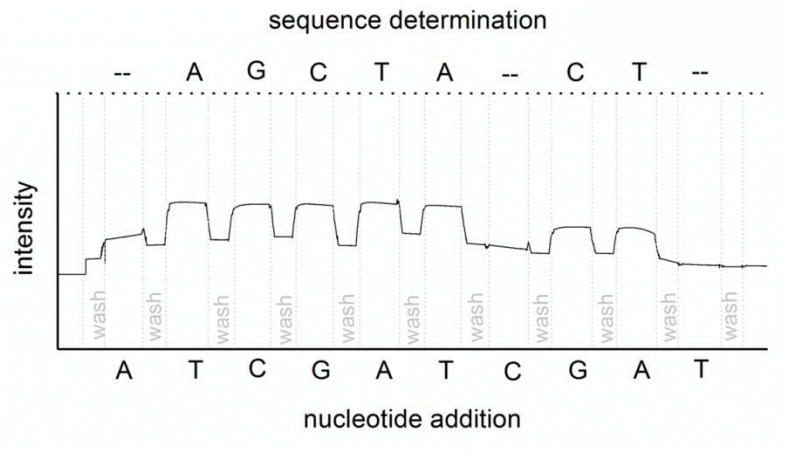

***Figure 52**: Success 1 with incorporation of better washing…still don't see curves and there is still a decrese of signal over time*

7.4 Optimization of reagents and buffers

In order to optimize the reaction, an optimization of the content of the buffers (particularly in regards to oil:sample ratio and Tween in order to improve the surface tension of the VRCs to allow removing of the SPP complex from the droplets without and with dragging as wished) was carried out. (**Figure 53**)

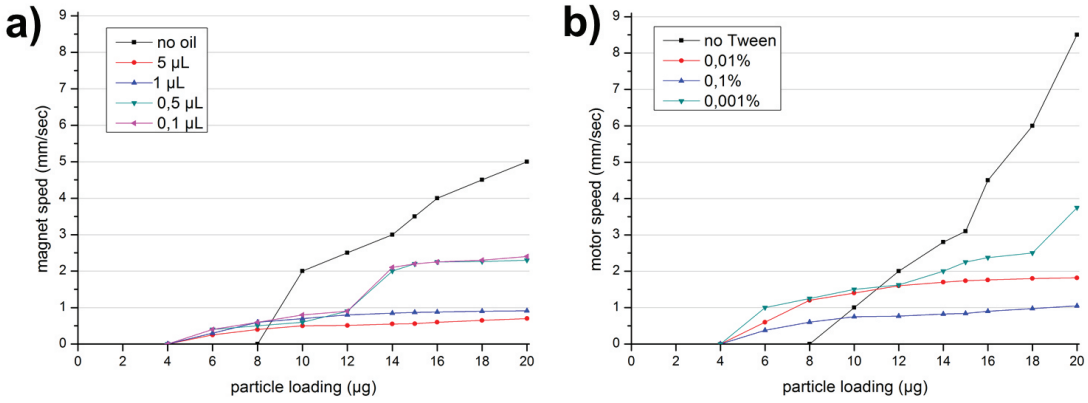

***Figure 53:** Effect of oil loading on dynamic droplet shape (a) and of Tween content (b). The white arrows refer to the transport direction. The volume of the aqueous phase was 5 µL in all cases. A stock suspension (~20 µg/µL) of 0.5 µm diameter SiMAG particles was used for the test.*

Due to this, another spotting design was tested where the reaction VRCs were divided into two VRCs, one containing the substrates and the other one containing the enzymes, both needed for the pyrosequencing chemistry (**Figure 54**). With the movement of the complex SPP/ssDNA/primer these two smaller

VRCs would merge and the background reaction and reagents depletion wouldn't occur before time (**Figure 55**).

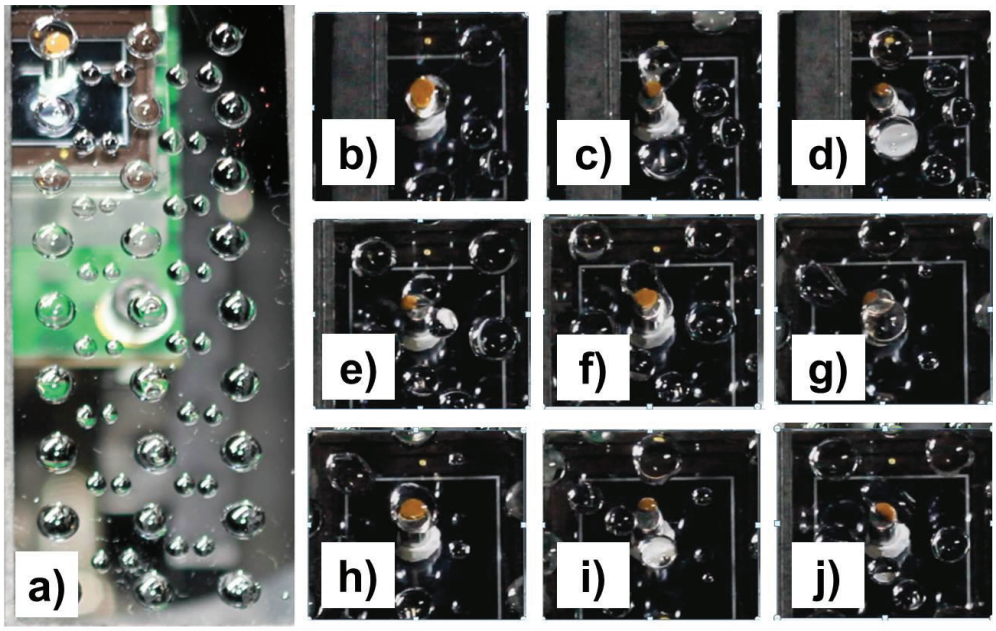

Figure 54: *Photograph of the prepared spotted glass. On a) the overall view with the SPP complex being located on the top left washing droplet. b) the first stage of the motion. c), d) and e) the SPP complex finds its way via magnetic actuation to the first enzyme droplet. In f) the enzyme droplet merges with the substrate droplet. g) The SPP complex will move to the next washing station h). and to merge the next enzyme and substrate VRCs in i) and j).*

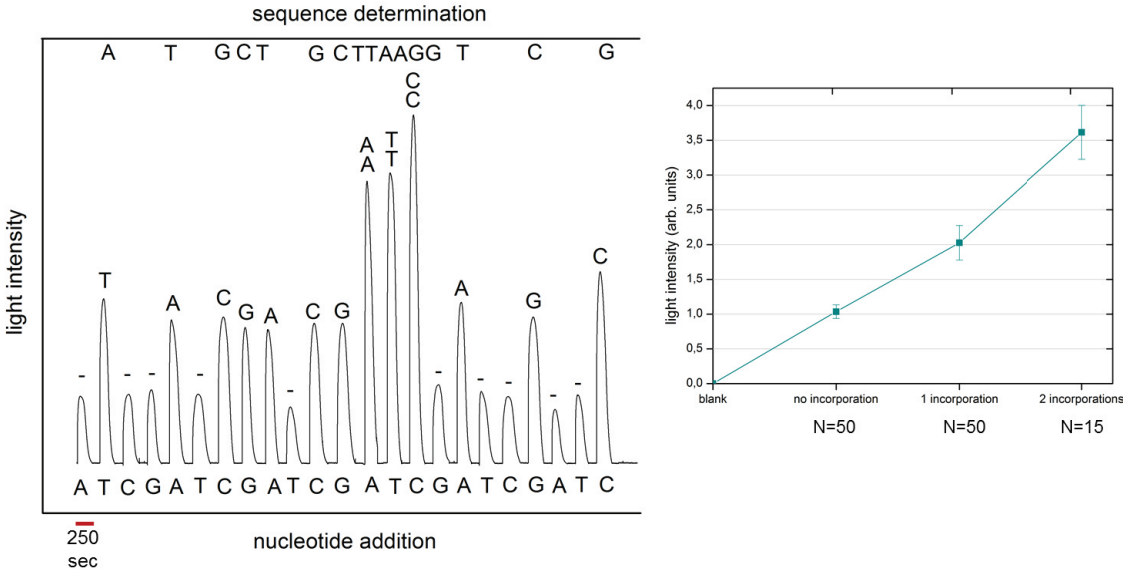

Figure 55: *Pyrogram showing the order of in which the magnetic particles were pulled into each nucleotide droplet (lower axis), and the order in which the nucleotides were successfully incorporated into the DNA chain (upper axis), yielding the final nucleotide sequence. DNA was sequenced with a read-length of 7 bp which corresponds to first success.*

7.5 Washing efficiency

Additionally, an initial series of experiments with the presence and the absence of a washing step was carried out. Conducting the pyrosequencing nucleotide additions without the washing step resulted in a 30% carry-over signal caused by the DNA/primer/SPP complex. Once the washing step was included, the carry-over signal was eliminated (**Figure 56**); therefore, each nucleotide addition reaction was followed with a single washing step. As one can see from **Figure 56**, once the washing step was included into the experiment design, no photons were detected from the sample, which indicates no significant amount of chemicals were carried over.

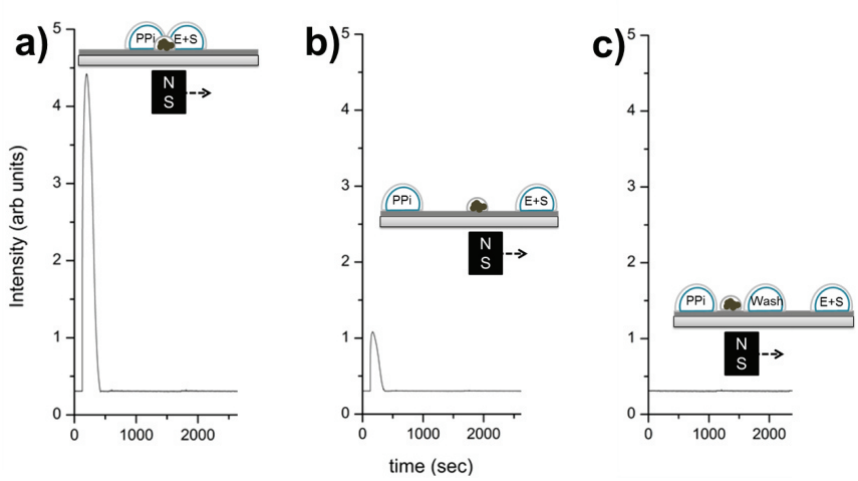

Figure 56*: Washing efficiency. SPP were moved between two droplets, one containing inorganic pyrophosphate (PPi), and the other enzymes and substrates used for pyrosequencing while the luminescence was continuously monitored by PMT and recorded by an oscilloscope.* ***a)*** *We have merged both,* ***b)*** *extracted the SSP from one droplet to the next and* ***c)*** *included a washing step between. Results demonstrated that efficiency of using a washing step successfully canceled the signal coming from cross-contamination. Peak amplitude (minus baseline subtraction) dropped from around 4V to around 1.5V and to practically 0V once the washing step was included.*

7.6 Mixing improvement

For each experiment, fresh superhydrophobic glass cover slips were used to remove possibility of sample-to-sample cross contamination, which is a benefit of disposable and microfabrication-free platform. The diffusion-

dependent rate of the pyrosequencing process was improved upon by moving the SPPs within the droplet during the reaction for active mixing. The stage moved by ±≈2 mm along both X and Y axes at the speed of ≈2 mm s^{-1}, which reduced the reaction time by a factor of almost 2 (**Figure 57**).

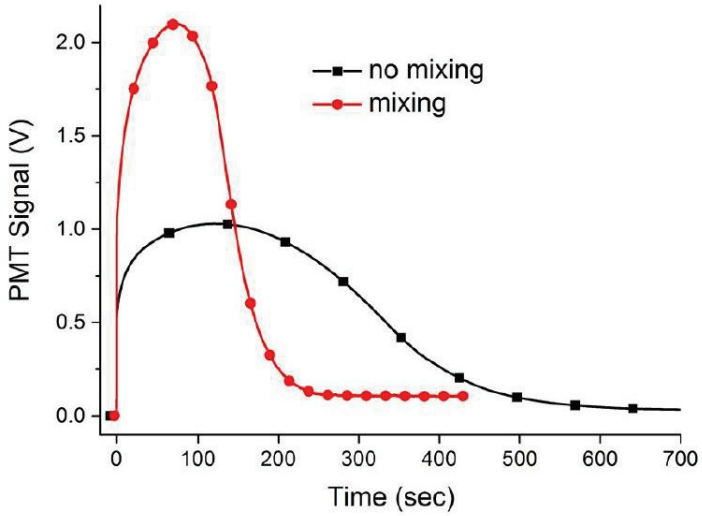

Figure 57 *SPP/primer/DNA complex was moved within droplets with enzymes, substrates and dNTP whilst monitoring with a PMT and recording with an oscilloscope the resulting luminescence. The resulting luminescence was both recorded while having the magnet static in position (black squares) and moving in the reaction droplet with speed of ≈2 mm/s (red circles). This Figure can be found in the supplementary information of Almeida et al. (2015)* [264] *and it was reproduced with permission of Royal Society of Chemistry.*

Initially, the signal peak amplitude was 1.00 V and its area was 0.32 mC. Stimulated by stirring, the peak amplitude increased to 1.99 V and the area dropped to 0.27 mC. The AUC amplitude dropped to 85% of its original value while the signal peak amplitude increased by factor of 2. The signal reached the baseline amplitude at time 275 seconds; thus, we decided that keeping the reaction under the PMT for 300 seconds should be sufficient. Next, we performed a set of experiments to determine optimum DNA quantity.

7.7. Effect of DNA concentration

55 µg of SPPs were used in combination with DNA concentrations from 0.3125 pmol to 20 pmol. The DNA concentration of 1.25 pmol seemed to be

optimal considering the lowest amount possible to use in order to have a detectable difference between.

The sequence B-5‘-ATG GGG GGG GGG ATG GGG GGG GGAT GGG GGG GGA TGG GGG GGA TTG GGG GGT TGG GGG ATG GGG TCT GGT ATG GAT GTA AAC GCC TGG TAT CTT TAT AGT CCA-3‘ was assessed using the sequencing-primer 5‘-GGA CTA TAA AGA TAC CAG GCG TT-3’ with different concentrations of DNA, such as 0.315 pmol (**Figure 58**), 1.25 pmol (**Figure 59a**), 5,pmol (**Figure 59b**), 15 pmol (**Figure 59c**) and 20 pmol. (**Figure 60**).

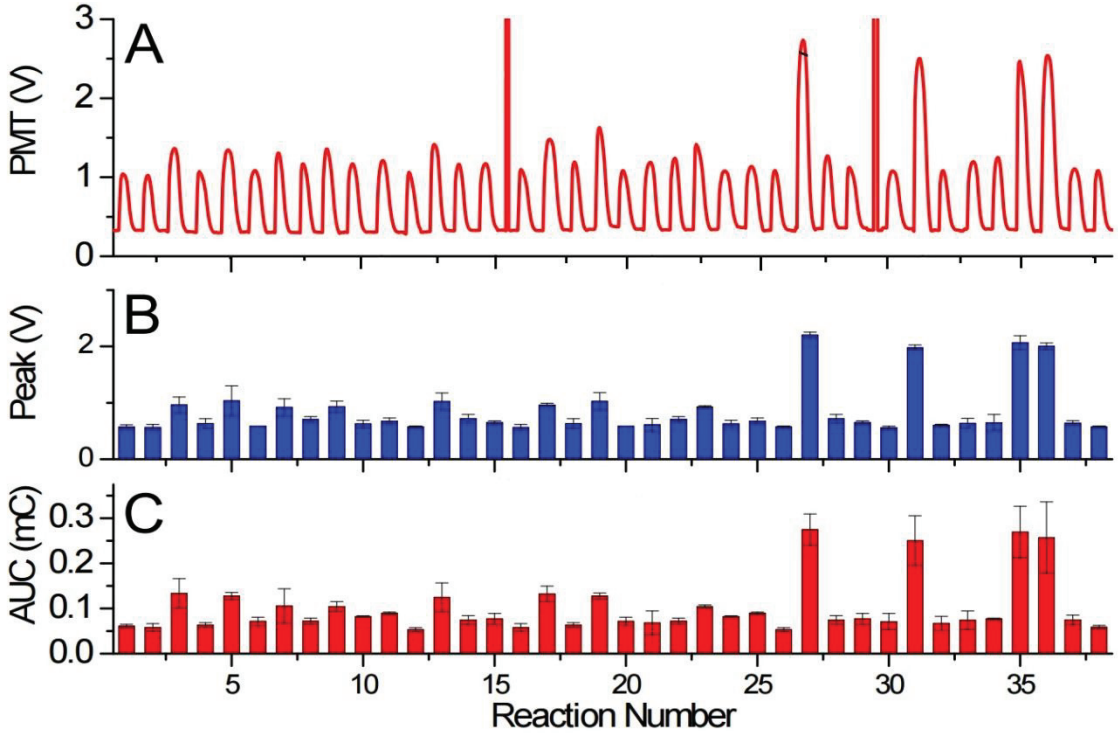

Figure 58. *Effectiveness of using concentration of 0,315 pmol DNA on SPPs for pyrosequencing on OSM. (A) Pyrogram consisting of 38 reactions performed on 3 glasses with two changes marked by peaks around 15th and 30th reactions. (B) Extracted peak voltages (mean value) with standard error as function of reaction number from three measurements to compare with (C) extracted AUC (mean value) with standard error as function of reaction number from three measurements. Figure present in Almeida et al (2015) and reproduced with permission of Royal Society of Chemistry.* [264]

By using 0,315 pmol DNA, there was practically no difference between background reaction noise and the luminescence detected from the incorporation of 1 nucleotide by DNA molecule which makes it unsuitably low.

The same was carried out with the concentrations of 1.25 pmol (**Figure 59a**), 5 pmol (**Figure 59b**), 15 pmol (**Figure 59c**) and 20 pmol (**Figure 60**).

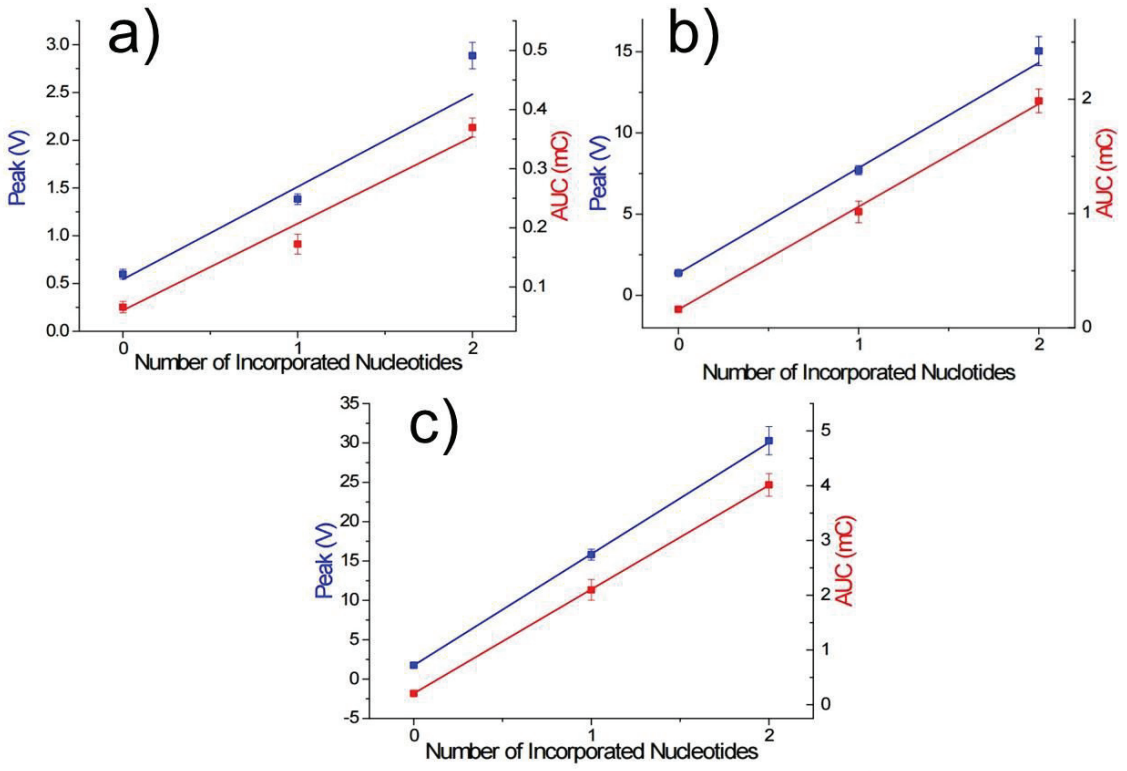

Figure 59. *Effectiveness of using concentrations of 1.25 pmol (a), 5 pmol (b) and 15 pmol (c) with the peak amplitude (blue) and AUC (red) as function of number of incorporated nucleotides: a) with slope of (0.969 ± 0.227) V and (0.147 ± 0.021) mC, both (mean ± standard deviation) for peak voltage and AUC, respectively; the nonlinearity is significantly smaller than the one for 0.315 pmol concentration of DNA with correlation coefficient of 0.959 and 0.896 for peak voltage and AUC, respectively; b) with slope of (6.478 ± 0. 242) V and (0.899 ± 0.025) mC, both (mean ± standard deviation) for peak voltage and AUC, respectively; the nonlinearity is even smaller than the one for 1.25 pmol concentration as the correlation coefficient is near unity, 0.997 and 0.998 for peak voltage and AUC, respectively;. c) with slope of (14.144 ± 0.099) V and (1.900 ± 0.005) mC, both (mean ± standard deviation) for peak voltage and AUC, respectively; the nonlinearity is even smaller than the one for 1.25 pmol concentration as the correlation coefficient is practically unity, 0.999 for both,peak voltage and the AUC. Adapted from figures published by Almeida et al. (2015).* [264]

The concentrations of 1,25 pmol, 5 pmol and 15 pmol (**Figure 59**) resulted in well-distinguished groups for each number of nucleotide incorporation. Even if the linearity increases with the concentration of DNA, the

1,25 pmol concentration results indicated efficient discernment between number of consecutive incorporations of nucleotides.

When the concentration used was 20 pmol such distinction between the different numbers of consecutive nucleotide additions was non-existing for some reactions which makes this concentration unsuitable for the pyrosequencing purpose (**Figure 60**).

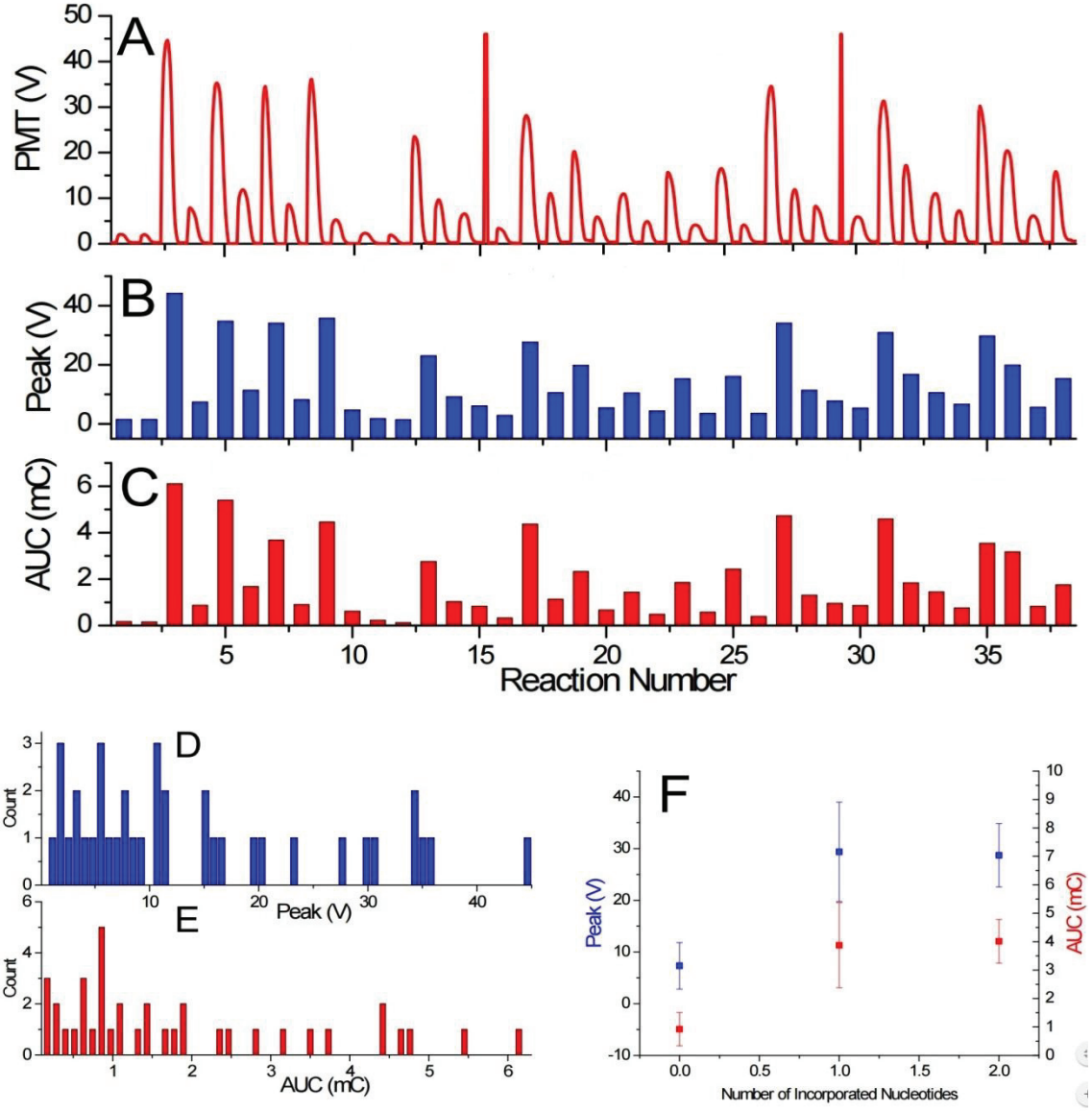

Figure 60 *Effectiveness of using concentration of 20 pmol DNA on SPPs for pyrosequencing on OSM (A) Pyrogram with 38 reactions carried out on 3 glasses with transitions marked by detected luminescence peaks around reactions 15 and 30. (B) Peak voltages (mean value) with standard error as function of reaction number from single measurement. (C) AUCs (mean value) with standard deviation as function of reaction number from single measurement. Both (D) frequency count of mean peak values and (E) AUCs do not distinguish groups by number of incorporated nucleotides as lower*

concentrations. Additionally, (F) peak amplitude (blue) and AUC (red) as function of number of incorporated nucleotides confirms that this DNA concentration is not suitable for pyrosequencing. Reproduced from Almeida et al. (2015) with permission of Royal Society of Chemistry[264]

With the 1,25 pmol concentration, the peak voltage and AUC amplitude were (0.969 ± 0.227) V and (0.147 ± 0.021) mC (mean ± standard deviation) per single nucleotide incorporation, respectively, with correlation coefficient of 0.959 and 0.896 for peak voltage and AUC, respectively. This peak voltage signal was 100 times higher than the background noise while requiring minimum DNA consumption (**Figure 61**).

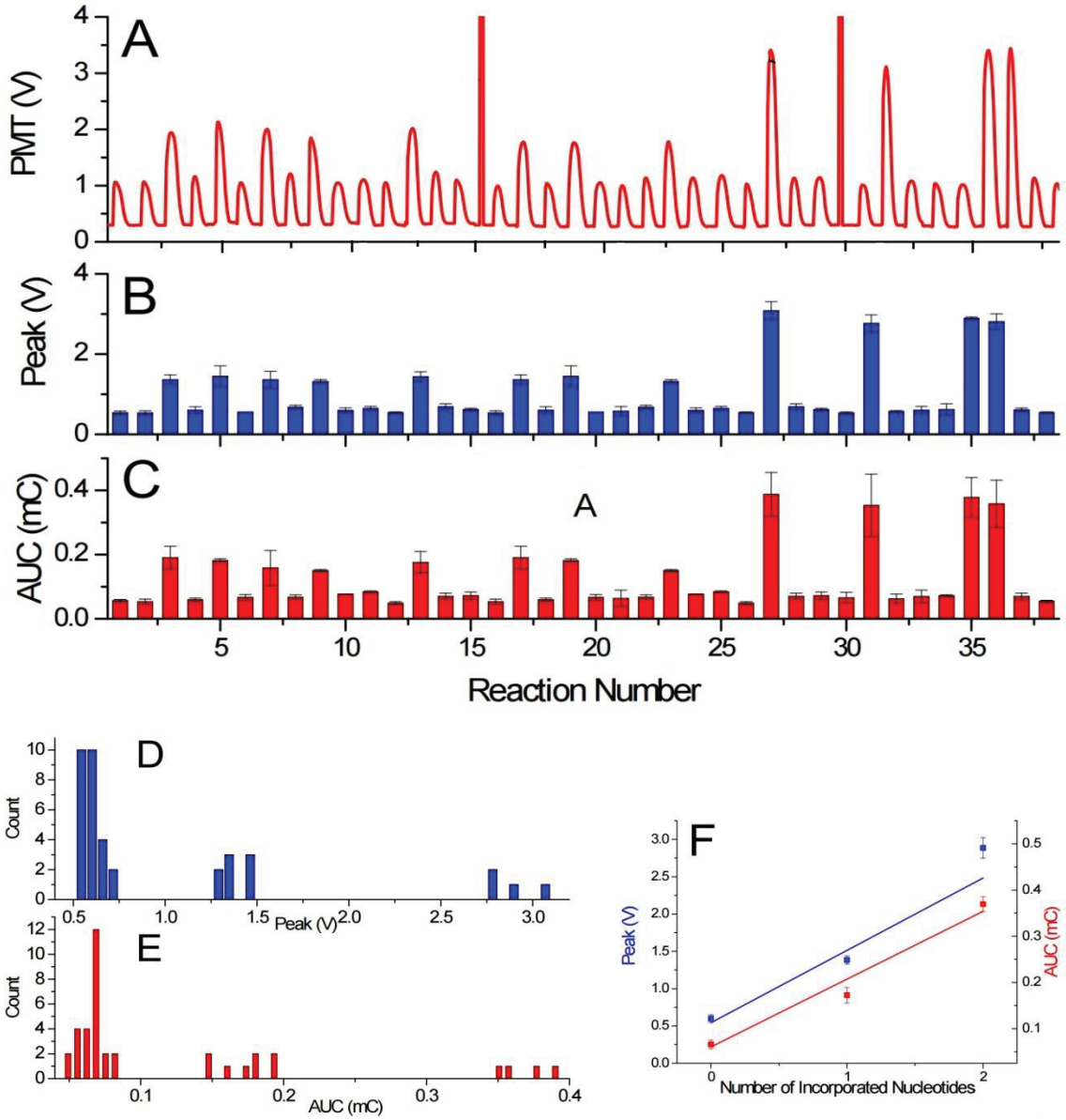

Figure 61. *Effectiveness of using concentration of 1,25 pmol DNA on SPPs for pyrosequencing on OSM (A) Pyrogram with 38 reactions carried out on 3*

glasses with transitions marked by detected luminescence peaks around reactions 15 and 30. (B) Peak voltages (mean value) with standard error as function of reaction number from single measurement. (C) AUCs (mean value) with standard deviation as function of reaction number from single measurement. Both (D) frequency count of mean peak values and (E) AUCs do not distinguish groups by number of incorporated nucleotides as lower concentrations. Additionally, (F) peak amplitude (blue) and AUC (red) as function of number of incorporated nucleotides confirms that this DNA concentration is not suitable for pyrosequencing. Reproduced from Almeida et al. (2015) with permission of Royal Society of Chemistry. [264]

As previously mentioned, each glass cover slip can host up to one-use 16 reaction stations (washing droplets + enzyme and substrate droplets). This means, sequencing more than 16 nucleotides will require many glass cover slips and the sample has to be transferred from one glass to the next glass. These unloading/loading stations were designed not to contain matching nucleotides, but just to be reference points to determine the background signal working as additional washing stations. The unloading was performed via pipetting with a magnet attached to the outside surface of the pippete tip and the loading by detaching this same magnet. After completion of the experiments, both the AUC and peak voltage amplitudes were calculated from 5 transfers in unloading and loading stations and compared. The loading PMT peak and AUC amplitude were (0.79 ± 0.08) V and (0.094 ± 0.005) mC (mean ± standard deviation), respectively. Unloading PMT and AUC amplitude were (0.79 ± 0.11) V and (0.098 ± 0.014) mC (mean ± standard deviation), respectively. The results during loading and unloading are very similar, demonstrating the transfer efficiency which assures that the SPP/prime/ssDNA complex can be transferred while keeping the same amplitude of emitted photos during DNA sequencing.

7.8 Nucleotide incorporation in homopolymeric stretches

The maximum number of homopolymeric nucleotide additions per single incorporation possible to assess on this platform were also studied (**Figure 62**). This was done by using the sequence B-5‘-ATG GGG GGG GGG ATG GGG GGG GGA TGG GGG GGG ATG GGG GGG ATT GGG GGG TTG GGG GAT

GGG GTC TGG TAT GGA TGT AAA CGC CTG GTA TCT TTA TAG TCC A-3‘ in combination with the sequencing-primer 5‘-GGA CTA TAA AGA TAC CAG GCG TT-3’. This was meant to investigate the limits of the platform by assessing extreme cases such as 10 identical nucleotides in succession.

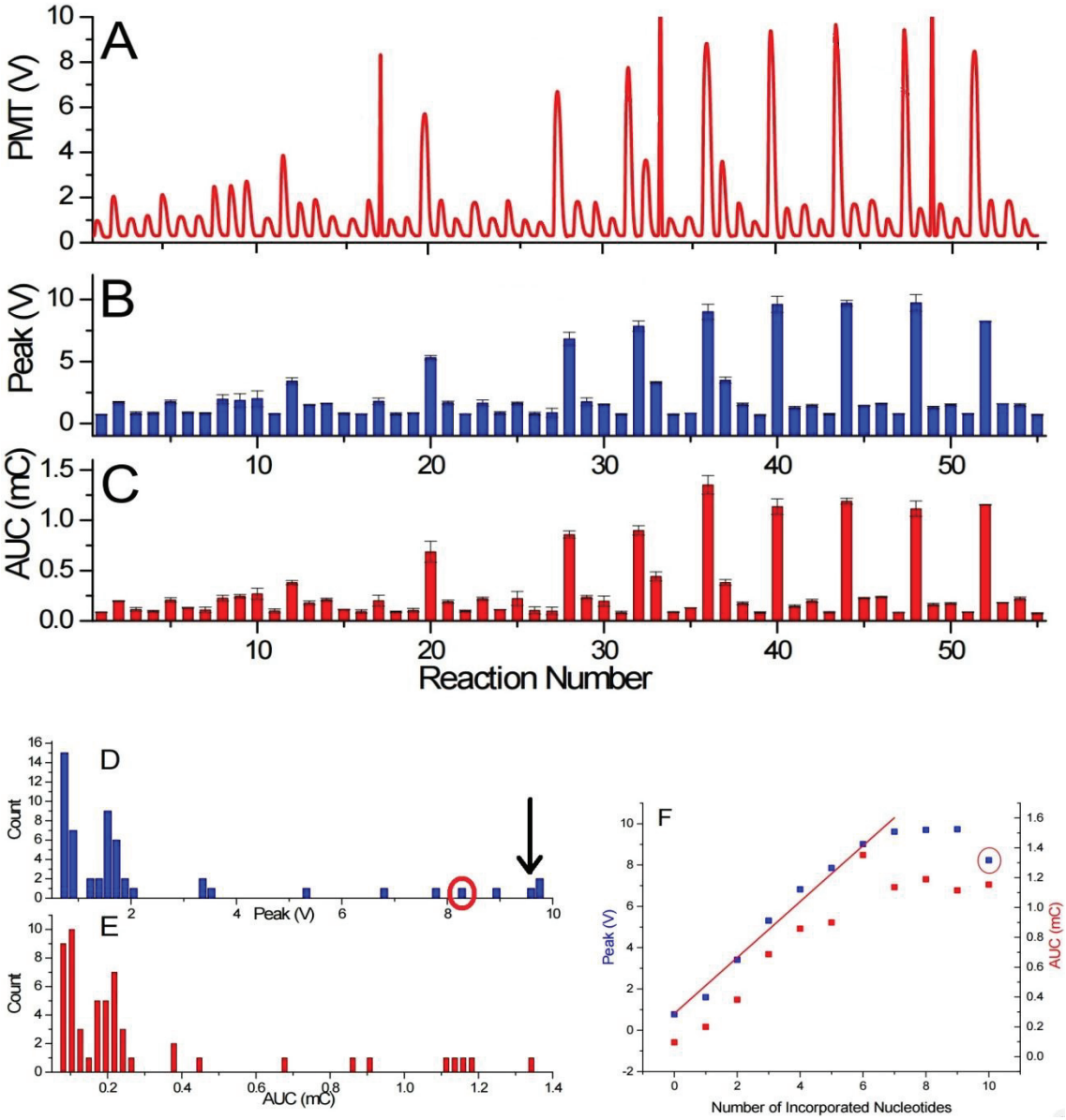

***Figure 62**: (A) Pyrogram showcasing 55 reactions performed on 4 glasses with three changes marked by high intensity peaks around 17th, 34th and 48th reactions. (B) Peak voltages (mean value) with standard error as function of reaction number from two measurements. (C) AUC (value) with standard error as function of reaction number from two measurements. (D) Frequency count of mean peak values manifesting grouping by number of incorporated nucleotides from 0 up to 7 (highlighted by a black arrow). 10 identical incorporated nucleotides in a row results are highlighted with a red circle. (E) Frequency count of mean AUC manifesting grouping according to number of incorporated*

nucleotides from 0 up to 5 showing that the peak values give more consistent data. (F) Peak amplitude (blue) and AUC (red) as function of number of incorporated nucleotides. This has proven that the OSM-sequencing can be used for up to 7 identical serial nucleotides with (1.354 ±0.075) V (mean ± standard deviation) per incorporated nucleotide. Reproduced from Almeida et al. (2015) with permission of Royal Society of Chemistry[264]

The amplitude of emitted light starts was observed to drop after incorporations of more than seven identical nucleotides in a row. Both peak voltages and AUCs amplitude were determined with (1.451 ± 0.067) V and (0.175 ± 0.020) mC (mean ± standard deviation), respectively, per single nucleotide incorporation. Peak voltage amplitude showed more consistent data than the AUC amplitude. The signal level after each wash cycle could be reduced in the reaction complex due to loss or denaturation of either the DNA template or the sequencing primer.

7.9 Resequencing

The platform and experimental design were tested with DNA concentration of 1.25 pmol with a re-sequencing experiment (**Figure 63**). A hydrophobic glass cover slip was prepared with the dNTPs placed in pre-determined order, corresponding to the complementary DNA strand, a 34-mer. The sequence consisted of 21 single, 3 double, 1 triple, and 1 quadruple nucleotide incorporations, and 4 mismatches. We had to use two glass cover slips with one sample transfer from the first glass to the second glass. This system enabled monitoring the emitted photons of the known nucleotide incorporations and to determine the reaction stability as well as reproducibility as displayed in **Figure 63A**. The DNA/primer/SPP complex was moved into a washing droplet in the end of the experiment. The resequencing was performed five times to eliminate random errors and to demonstrate repeatability (error bars in **Figure 63B**). A mismatched event was performed during the sample loading and unloading to determine the background emission as highlighted by the blue ellipses (**Figure 63C**). It was shown that both peak voltages and AUCs amplitude can be utilized for determination of the number of incorporated nucleotides (**Figure 63D and E**, each containing five groups separated from

others). The PMT peak voltage and AUC amplitude are linearly proportional to the number of incorporated nucleotides which demonstrates feasibility of the method as well as little or no loss of SPP, DNA, or primer (**Figure 63F**). The background peak voltage value and AUC amplitudes were only (0.799 ± 0.079) AUC and (0.010 ± 0.012) mC (mean ± standard deviation), respectively, well below the signal for single nucleotide incorporation. The order of reaction stations for resequencing is designed to match the sequence and incorporate nucleotides) in each reaction. Presence of a single nucleotide polymorphism (SNP) is detected as a missing reaction and there will be no nucleotide incorporation once the SNP occurs. The first and last reactions at each glass surface are performed with mismatched nucleotides during sample transfer to detect a background signal and calibrate the system. Once there is a nucleotide mismatch detected during resequencing, the signal will be either stronger than expected (in the case of incorporation of an identical nucleotide), or as intense as the background signal with no incorporation. In the latter case, the pyrosequencing would stop at this point but the user would know that there is at least one SNP in the tested sequence.

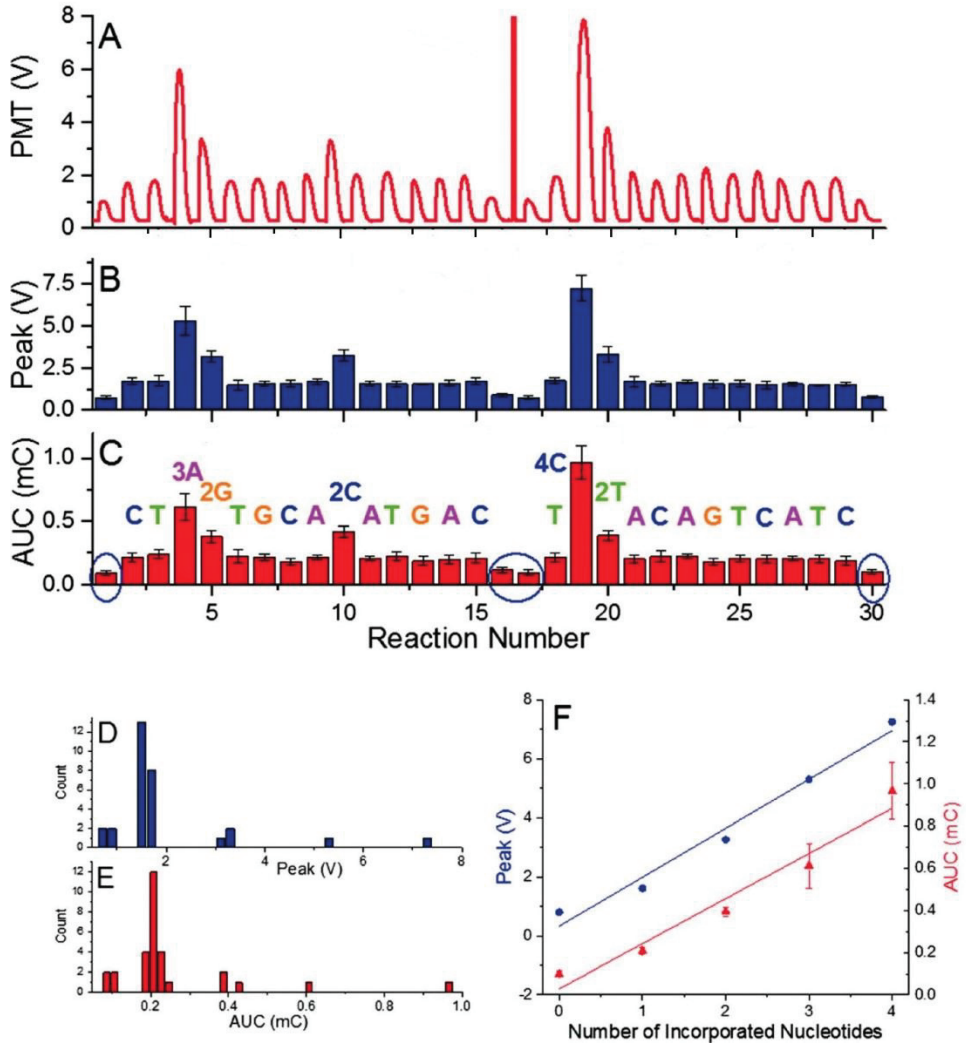

Figure 63 *(A) Pyrogram from the resequencing. (B) Mean value of peak voltage and its standard error as function of reaction number. A mismatched event was performed in the end of the run to determine the background emission (marked by blue ellipses). (C) Mean value of AUC and its standard error as the function of the reaction. Frequency counts of average peak values (D) and AUCs (E) distinguish five groups according to the number of incorporated nucleotides with a nearly perfect linear relationship. (F) Peak amplitude (blue circles) and AUC (red triangles) as a function of the number of incorporated nucleotides with slope of (1.657 ± 0.140) V and (0.214 ± 0.026) mC for peak voltage and AUC, respectively. The nonlinearity is small as the correlation coefficients are 0.972 and 0.944 for peak voltage and AUC, respectively. Reproduced from Almeida et al. (2015) with permission of Royal Society of Chemistry*[264]

7.10 *de novo* sequencing

Proving the feasibility of OSM-sequencing method with unknown samples was carried out by performing *de novo* sequencing with a DNA template with the length of 51 bps. The sequence consisted of 16 single, 9 double, 2 triple, 1 quadruple, and 1 quintuple nucleotide incorporations, and 30 mismatches. We performed the experiment with four nucleotides added in a repeated cyclical fashion comprehending in total 70 reaction stations. The experimental apparatus involved five glass cover slips (**Figure 64A**) and times to avoid random errors. The detected emitted light was processed the same way as in the previous experiments (**Figure 64B and C**). In addition, histograms of both voltage and AUC values (**Figure 64D**) show better grouping for the peak voltage amplitude than that for AUCs (**Figure 64E**). The peak voltage amplitudes in each group (number of identical nucleotides incorporated in a row) are distinct from one another, which should enable an accurate sequence assessment of all 51 bases (**Figure 64F**). The value of peak voltage and AUC amplitude are (1.605 ± 0.068) V and (0.213 ± 0.021) mC (mean ± standard deviation), respectively. Again, the peak voltage signal shows better stability than the AUC as highlighted by the blue ellipse at **Figure 64F**, where the signal for the four identical incorporated nucleotides is practically identical to the one for three identical incorporated nucleotides which means the peak signal amplitude provides more consistent output than the one for AUC.

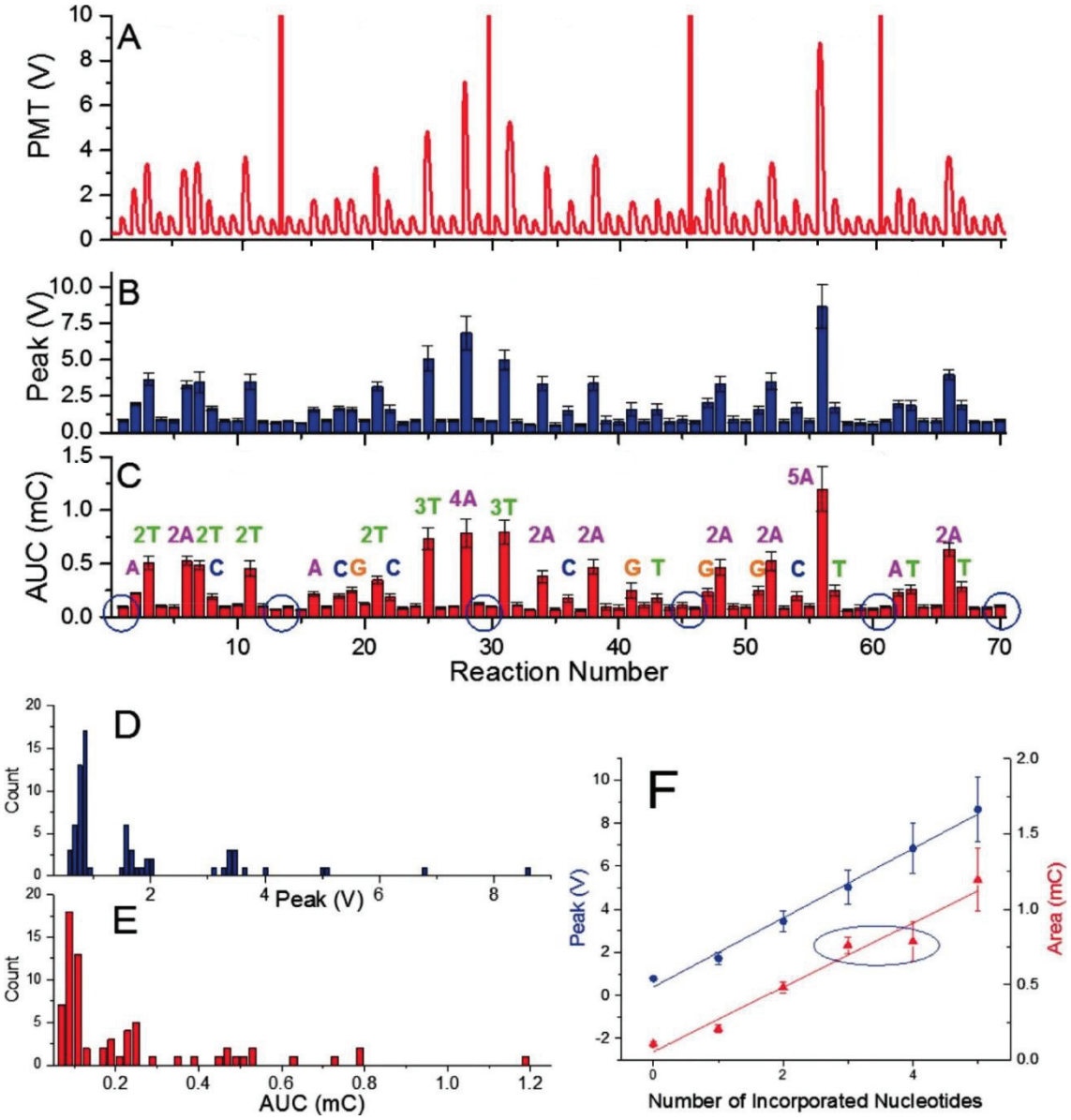

Figure 64 *(A) Pyrogram of de novo sequencing. (B) Mean value of peak voltage and its standard error as function of reaction number. A mismatched event was performed in the end of the run to determine the background emission (marked by blue ellipses). (C) Mean value of AUC and its standard error as function of reaction. Frequency counts of mean peak values (D) distinguish five groups according to the number of incorporated nucleotides and are better defined as AUC values (E) as seen with the blue ellipse marked in (F). (F) Peak amplitude (blue) is linearly proportional to the number of incorporated nucleotides with correlation coefficient of 0.991 and AUC (red) with the same coefficient of 0.953. Reproduced from Almeida et al. (2015) with permission of Royal Society of Chemistry.* [264]

7.11 Longer sequences testing

Furthermore, a sequence with length of 81 nucleotides was carried out with a total of 104 reactions using de novo sequencing configuration. The sequence consisted of 35 single, 8 double, 4 triple, 2 quadruple, and 2 quintuple nucleotide incorporations, and 53 mismatches. The experiment required seven glass cover slips (**Figure 65A**). Peak voltage and AUC amplitudes were (1.495 ± 0.117) V and (0.182 ± 0.027) mC (mean ± standard deviation), respectively (**Figure 65B and C**). The signal per incorporated nucleotide is again well above the background of (0.794 ± 0.117) V and (0.102 ± 0.021) mC (mean ± standard deviation) for peak voltage and AUC amplitudes, respectively (**Figure 65D**). The OSM-sequencing since was able of 81 nucleotides incorporation and, as the PMT signal is has consistent amplitude per nucleotide incorporation, a greater number of nucleotide may be incorporated. The peak amplitude is linearly proportional to the number of incorporated nucleotides with correlation coefficient of 0.944. The same coefficient for AUC is 0.927. As seen before, peak voltage gives more consistent data than AUC (**Figure 65E and F**).

Overall, it was seen that the peak voltage amplitude gave better data than AUC. The peak voltage amplitude per nucleotide incorporation varied between (1.354 ± 0.075) V, (1.657 ± 0.140) V, (1.605 ± 0.068) V and (1.339 ± 0.145) V (mean ± standard deviation) homopolymeric stretches (**Figure 61**), re-sequencing (**Figure 62**), de novo sequencing of 51 (**Figure 63**), and 81 nucleotides (**Figure 64**), respectively. The differences are probably caused by variations in concentration of chemicals due to manual pipetting as well as temperature and humidity conditions fluctuation since most experiments were performed on different days.

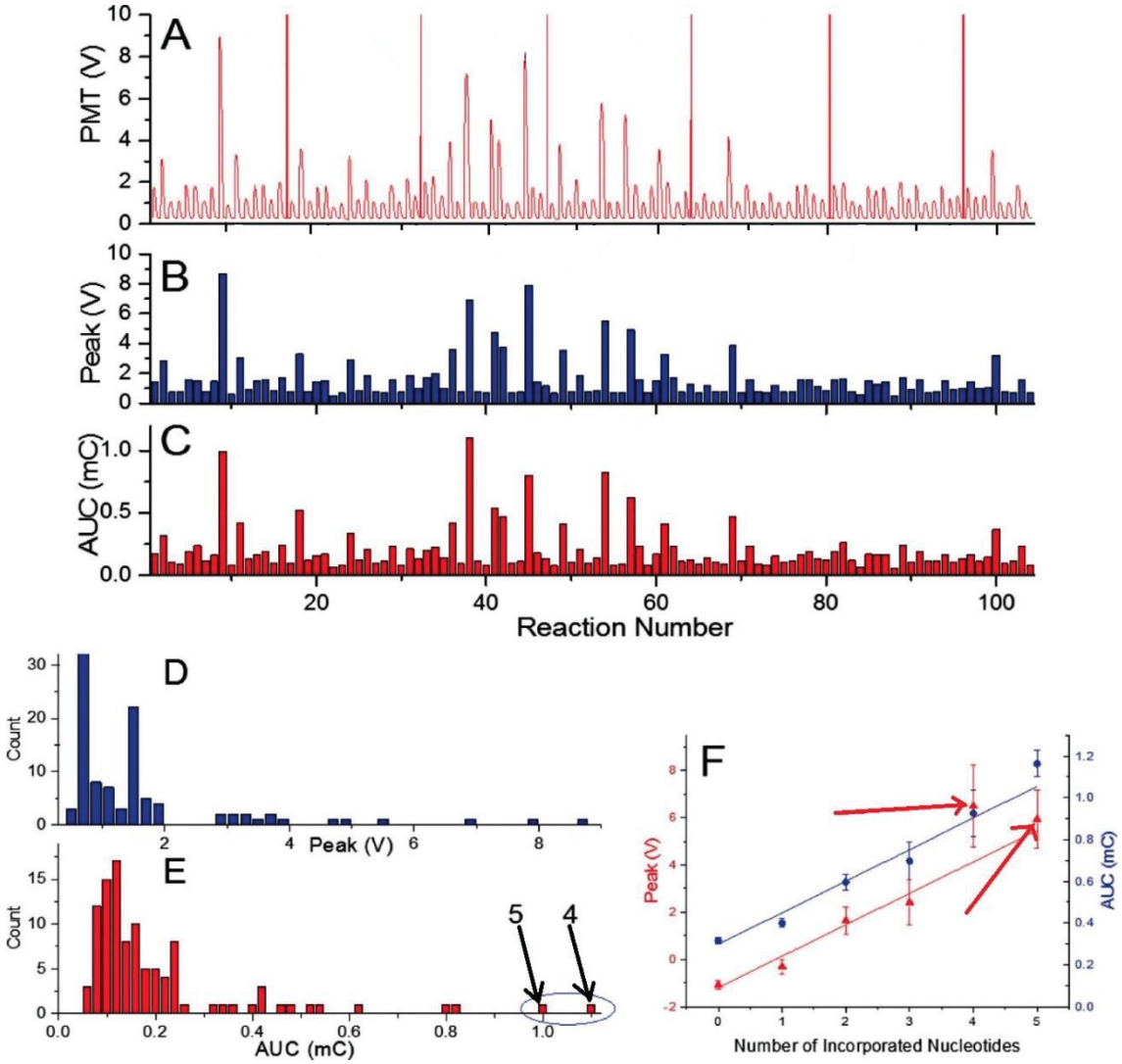

Figure 65 *(A) A pyrogram of long de novo sequencing with 104 reactions. (B) Extracted value of peak voltage as function of reaction number. (C) Extracted mean value of AUC as function of reaction number. Frequency counts of mean peak values (D) distinguish six groups according to the number of incorporated nucleotides. (E) Frequency counts of the AUC are not distinct (arrows). (F) Peak amplitude (blue) and AUC (red) as function of number of incorporated nucleotides. Reproduced from Almeida et al. (2015) with permission of Royal Society of Chemistry*[264]

7.12 Comments on methods

Prior to pyrosequencing, DNA has to be extracted from the sample, purified, and amplified by PCR. Most of these steps are either labor-intensive or require complex robotic systems. Except for pyrosequencing, all other necessary steps have been previously integrated using the OSM concept.[214-215] The system proposed here is compatible with previous work, thus, it may be

included on into a single “sample-to-answer” platform. The pyrosequencing experiments were conducted on a glass cover slip as shown schematically in **Figure 66**. The ssDNA bound to SPP was placed into a first station as shown in (**a**), with a magnet underneath it. The particles are then dragged (**b**) using magnetic force into the first (**E**) enzyme-containing droplet. This droplet is close to the (**S + Nt**) substrate and nucleotide dNTP-containing droplet, that the droplets merge and the pyrosequencing reaction is triggered. The particles are then dragged into the washing droplet. This washing droplet is at a larger distance from the other droplets, so no merging of droplets occurs. The washing steps remove unincorporated or in excess nucleotides were designed which maximizes read length. The washing of SPP/template/primer complex allows removal of nucleotides as well as other reaction byproducts between nucleotide additions. Then, the particles are dragged into another reaction station (**c**) with two droplets, one with enzyme and the other one with substrate and another dNTP. A glass containing eight reaction stations is schematically shown in **Figure 66B** and a photograph of the setup with 16 stations in **Figure 66C** as well as a transfer droplet containing DNA/primer/SPP. The droplets were colored with ink to increase the contrast. The glass with the dimension of 60×20 mm and thickness of 170 μm was treated with 1H,1H,2H,2H-perfluorodecyltriethoxysilane (FAS17), making the surface highly hydrophobic, with a water contact angle of 95°. The glass cover slip was placed on a computer controlled X–Y stage. A disc-shaped neodymium magnet with a diameter of 3 mm, model N45 mm by Supermagnetic, GmbH (Germany) was placed underneath the glass cover slip as previously described in **Chapter 6**.

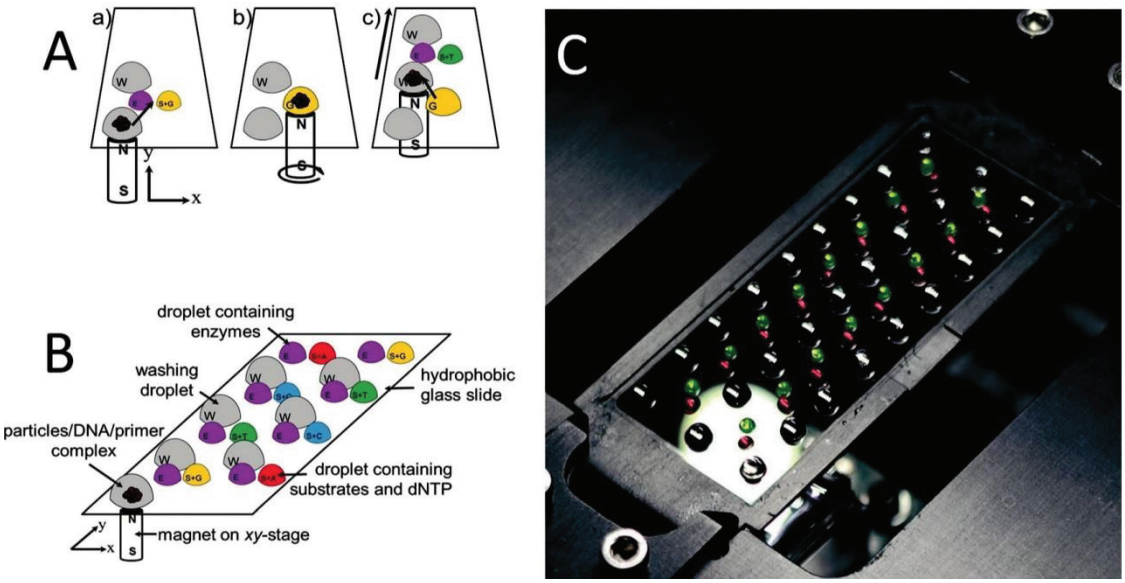

Figure 66 *(A) Representation of a typical nucleotide addition cycle. All droplets are covered with oil, thereby effectively preventing evaporation of water from the sample as well as reagent degradation by oxidation. (a–c) Three phases of pyrosequencing reaction. (B) Components of the experimental setup; (W) washing droplets; (E) droplets containing all the needed enzymes for the pyrosequencing reaction (S + dN). (C) Photograph of the setup consisting of the hydrophobically coated glass cover slip mounted onto a motorized X–Y translation stage with a neodymium–iron–boron magnet fixed beneath the cover slip. The droplets contained color ink to increase the contrast. Reproduced from Almeida et al. (2015) with permission of Royal Society of Chemistry*[264]

The DNA/primer/SPP complex was on moved through the individual reaction/washing stations in the form of droplets using magnetic force. These “stations” were formed by pipetting individual droplets onto the glass covered with mineral oil, thereby preventing water evaporation from reaction droplets. After a series of experiments, the volumes of stations as well as oil covering them are summarized in **Table 3.**

***Table 3**. Ratio between oil and sample volumes stable up to 8 hours (initial and final volumes measured at 0, 2, 4, 6 and 8h)*

	Washing droplet	Enzyme droplet	Substrate and nucleotide droplet
Droplet volume (μL)	≈10	≈3	≈2
Oil volume (μL)	≈2	≈1	≈1

A PMT was placed above the glass aligned with the magnet underneath. Since the sample was always attracted by the magnet and kept on the glass above it, it was also directly below the PMT; thus, all reactions were conducted at the sample location relatively to the PMT. With this setup, both the magnet and the PMT were stationary while the glass was the moving component. The stage with the PMT and magnet was placed in a black box to eliminate ambient light noise. All light emission was recorded and peaks were identified and individually processed to obtain the values of maximum amplitude as well as their areas under the curve (AUC). The AUC unit corresponds to the electrical charge C, as it is time integration of electrical current i from 0 s to t s:

$$AUC \approx \text{const} \int_0^t i\mathrm{d}t,$$

where const is a conversion factor. It consists of a gain of PMT and its transconductance amplifier and PMT efficiency of 105, 1 μA V^{-1}, and 85 mA W^{-1}, respectively for light wavelength of 550 nm.

Chapter 8

Conclusions and outlook

Referring to the objectives of this thesis defined on subchapter **4.2**.

5. To study the potential of droplets as virtual reaction chambers for nucleic acids handling.

    a) The potential of droplets as virtual reaction chambers for nucleic acids handling was investigated and confirmed. For this, the droplets were covered with mineral oil, thereby forming virtual reaction chambers. An oil layer was able to efficiently suppress water evaporation from the sample up to 8 hours of deposition on the glass substrate. (**Table 3**)

    b) Magnetic actuation was successful with DNA loaded superparamagnetic particles, meaning the DNA molecules could be manipulated within and between the virtual reaction chambers without significant degradation. Optical detection was used to make sure the particles aren't being left behind or trapped by adjusting the speed and the trajectory of the magnet. (**Figure 55**)

    c) Was possible to move the particles within fixed droplets and to move the particles with the droplets making possible to merge droplets. (**Figure 56**)

6. To investigate virtual reaction chambers as a platform for pyrosequencing chemistry.

    a) The usage of only one washing station was considered sufficient and the active mixing by moving the particles in a VRC increased the speed of reaction in comparison with just diffusion based mixing. (**Figures 58** and **59**)

7. To investigate the VRC based pyrosequencing platform for DNA sequencing.

   a) DNA sequencing was achieved using pyrosequencing chemistry. The pyrosequencing was performed by having reagents separated in different virtual reaction chambers and moving DNA molecules bound to superparamagnetic particles from droplet to droplet (washing and nucleotide addition) or dragging the droplets for droplet merging (enzymes and substrates real-time mixing). This platform successful determined up to 81 nucleotides long DNA sequences (**Figure 68**) (minimal degradation meaning with discernment of homolorymeric sections).

   b) The effect of DNA concentration bound to articles was tested and the 1.25 pmol of DNA was revealed as the ideal one for DNA loading on the SPP (**Figure 61**).

   c) Base calling in the homopolymeric stretches was studied (u to 6 identical subsequent units) (**Figure 65**)

8. To devise and test the platform for single nucleotide polymorphism analysis which was successful

   a) Single nucleotide polymorphisms were detected within the 55 nucleotide lenght from point 2. (**Figure 66**)

9. Provide scope and perspective for the research trajectory towards more efficient and stable low cost and simple sequencing platforms.

We have demonstrated a simple pyrosequencing system for both de novo (DNA sequencing) and re-sequencing (suitable for SNP detection) using open surface microfluidics with magnetic force actuation on a microscope glass cover slip surface without any surface patterning. Future improvements include an

automated pipetting station followed by a lyophilization step also would make this method more user friendly as operators would only require to dispense an appropriate amount of de-ionized water at pre-defined reaction and washing locations and cover those droplets with mineral oil. The system presented here is compatible with previously designed PCR as well as sample preparation systems. In future, one could create a single complex sample-to-answer system starting with a raw sample, DNA release, its purification, PCR, and pyrosequencing.

Chapter 9

References

[1] E. Bianconi, A. Piovesan, F. Facchin, A. Beraudi, R. Casadei, F. Frabetti, L. Vitale, M. C. Pelleri, S. Tassani, F. Piva, S. Perez-Amodio, P. Strippoli, S. Canaider, *Annals of human biology* **2013**, *40*, 463-471.

[2] C. Human Genome Sequencing, *Nature* **2004**, *431*, 931-945.

[3] J. D. Watson, F. H. C. Crick, *Nature* **1953**, *171*, 737-738.

[4] A. J. Bruce Alberts, Julian Lewis, Martin Raff, Keith Roberts, Peter Walter, *Molecular Biology of the Cell*, 4th edition ed., Garland Science, New York, **2002**.

[5] C. M. G. Reginald H. Garrett, *Biochemistry*, 4th ed ed., Brooks/Cole, Cengage Learning, Belmont, California, **2007**.

[6] M. E. W. Saenger, *Principles of Nucleic Acid Structure*, 1 ed., Springer-Verlag New York, **1984**.

[7] J. D. Watson, *Molecular biology of the gene. Watson, Watson*, Benjamin-Cummings Publishing Company, Boston, **2014**.

[8] E. B. Wilson, **1925**.

[9] S. Sharma, S. Javadekar, M. Pandey, M. Srivastava, R. Kumari, S. Raghavan, *Cell death & disease* **2015**, *6*, e1697.

[10] J. Chen, B. F. Miller, A. V. Furano, *Elife* **2014**, *3*, e02001.

[11] K. Rodgers, M. McVey, *Journal of cellular physiology* **2016**, *231*, 15-24.

[12] J. S. Bertram, *Molecular aspects of medicine* **2000**, *21*, 167-223.

[13] Y. T. Aminetzach, J. M. Macpherson, D. A. Petrov, *Science* **2005**, *309*, 764-767.

[14] V. Burrus, M. K. Waldor, *Research in microbiology* **2004**, *155*, 376-386.

[15] M. Long, E. Betrán, K. Thornton, W. Wang, *Nature Reviews Genetics* **2003**, *4*, 865-875.

[16] P. Hastings, J. R. Lupski, S. M. Rosenberg, G. Ira, *Nature Reviews Genetics* **2009**, *10*, 551-564.

[17] C. Bernstein, A. R. Prasad, V. Nfonsam, H. Bernstein, *New Research Directions in DNA Repair. InTech. doi* **2013**, *10*, 53919.

[18] A. M. Goh, C. R. Coffill, D. P. Lane, *The Journal of pathology* **2011**, *223*, 116-126.

[19] H. L. Rehm, J. S. Berg, L. D. Brooks, C. D. Bustamante, J. P. Evans, M. J. Landrum, D. H. Ledbetter, D. R. Maglott, C. L. Martin, R. L. Nussbaum, *New England Journal of Medicine* **2015**, *372*, 2235-2242.

[20] S. G. V. Ivan Y Iourov, Yuri B Yurov, *eLS* **2012**.

[21] R. Cotton, *Mutation Research/Fundamental and Molecular Mechanisms of Mutagenesis* **1993**, *285*, 125-144.

[22] R. B. Gasser, *International Journal for Parasitology* **1997**, *27*, 1449-1463.

[23] A.-C. Syvänen, *Nature Reviews Genetics* **2001**, *2*, 930-942.

[24] L. Wang, R. Luhm, M. Lei, in *Microarray Technology and Cancer Gene Profiling*, Springer, **2007**, pp. 105-116.

[25] J. Shendure, R. D. Mitra, C. Varma, G. M. Church, *Nature Reviews Genetics* **2004**, *5*, 335-344.

[26] L. T. Franca, E. Carrilho, T. B. Kist, *Quarterly reviews of biophysics* **2002**, *35*, 169-200.

[27] W. J. Ansorge, *New biotechnology* **2009**, *25*, 195-203.

[28] L. Kruglyak, D. A. Nickerson, *Nature genetics* **2001**, *27*, 234-235.

[29] P. L. Ross, K. Lee, P. Belgrader, *Analytical chemistry* **1997**, *69*, 4197-4202.

[30] D. G. Wang, J.-B. Fan, C.-J. Siao, A. Berno, P. Young, R. Sapolsky, G. Ghandour, N. Perkins, E. Winchester, J. Spencer, L. Kruglyak, L. Stein, L. Hsie, T. Topaloglou, E. Hubbell, E. Robinson, M. Mittmann, M. S. Morris, N. Shen, D. Kilburn, J. Rioux, C. Nusbaum, S. Rozen, T. J. Hudson, R. Lipshutz, M. Chee, E. S. Lander, *Science* **1998**, *280*, 1077-1082.

[31] H. Klenow, I. Henningsen, *Proceedings of the National Academy of Sciences of the United States of America* **1970**, *65*, 168-175.

[32] K. B. Mullis, F. A. Faloona, *Methods in enzymology* **1987**, *155*, 335-350.

[33] J. S. Chamberlain, R. A. Gibbs, J. E. Rainer, P. N. Nguyen, C. Thomas, *Nucleic acids research* **1988**, *16*, 11141-11156.

[34] V. Shyamala, G. Ames, *Journal of bacteriology* **1989**, *171*, 1602-1608.

[35] Q. Chou, M. Russell, D. E. Birch, J. Raymond, W. Bloch, *Nucleic Acids Research* **1992**, *20*, 1717-1723.

[36] T. M. Haqqi, G. Sarkar, C. S. David, S. S. Sommer, *Nucleic acids research* **1988**, *16*, 11844-11844.

[37] H. A. Erlich, D. Gelfand, J. J. Sninsky, *Science* **1991**, *252*, 1643-1651.

[38] R. Don, P. Cox, B. Wainwright, K. Baker, J. Mattick, *Nucleic acids research* **1991**, *19*, 4008.

[39] P. M. Holland, R. D. Abramson, R. Watson, D. H. Gelfand, *Proceedings of the National Academy of Sciences* **1991**, *88*, 7276-7280.

[40] U. Gibson, C. A. Heid, P. M. Williams, *Genome research* **1996**, *6*, 995-1001.

[41] C. A. Heid, J. Stevens, K. J. Livak, P. M. Williams, *Genome research* **1996**, *6*, 986-994.

[42] C. T. Wittwer, M. G. Herrmann, A. A. Moss, R. P. Rasmussen, *Biotechniques* **1997**, *22*, 130-139.

[43] M. U. Kopp, A. J. De Mello, A. Manz, *Science* **1998**, *280*, 1046-1048.

[44] I. M. Mackay, K. E. Arden, A. Nitsche, *Nucleic acids research* **2002**, *30*, 1292-1305.

[45] F. Sanger, S. Nicklen, A. R. Coulson, *Proceedings of the National Academy of Sciences of the United States of America* **1977**, *74*, 5463-5467.

[46] W. Ansorge, B. S. Sproat, J. Stegemann, C. Schwager, *Journal of biochemical and biophysical methods* **1986**, *13*, 315-323.

[47] J. M. Prober, G. L. Trainor, R. J. Dam, F. W. Hobbs, C. W. Robertson, R. J. Zagursky, A. J. Cocuzza, M. A. Jensen, K. Baumeister, *Science* **1987**, *238*, 336-341.

[48] L. M. Smith, J. Z. Sanders, R. J. Kaiser, P. Hughes, C. Dodd, C. R. Connell, C. Heiner, S. B. Kent, L. E. Hood, *Nature* **1986**, *321*, 674-679.

[49] W. Ansorge, H. Voss, S. Wiemann, C. Schwager, B. Sproat, J. Zimmermann, J. Stegemann, H. Erfle, N. Hewitt, T. Rupp, *Electrophoresis* **1992**, *13*, 616-619.

[50] X. C. Huang, M. A. Quesada, R. A. Mathies, *Analytical chemistry* **1992**, *64*, 967-972.

[51] E. M. Southern, *Journal of molecular biology* **1975**, *98*, 503-517.

[52] P. Lysov Iu, V. L. Florent'ev, A. A. Khorlin, K. R. Khrapko, V. V. Shik, *Doklady Akademii nauk SSSR* **1988**, *303*, 1508-1511.

[53] R. Drmanac, S. Drmanac, I. Labat, R. Crkvenjakov, A. Vicentic, A. Gemmell, *Electrophoresis* **1992**, *13*, 566-573.

[54] R. Drmanac, S. Drmanac, Z. Strezoska, T. Paunesku, I. Labat, M. Zeremski, J. Snoddy, W. Funkhouser, B. Koop, L. Hood, *Science* **1993**, *260*, 1649-1652.

[55] R. J. Melamede, *U.S. Patent 4863849* **1985**.

[56] B. Canard, R. S. Sarfati, *Gene* **1994**, *148*, 1-6.

[57] M. L. Metzker, R. Raghavachari, S. Richards, S. E. Jacutin, A. Civitello, K. Burgess, R. A. Gibbs, *Nucleic Acids Research* **1994**, *22*, 4259-4267.

[58] P. Nyrén, *Analytical Biochemistry* **1987**, *167*, 235-238.

[59] E. D. Hyman, *Anal Biochem* **1988**, *174*, 423-436.

[60] P. Nyrén, *Journal of bioluminescence and chemiluminescence* **1994**, *9*, 29-34.

[61] M. Ronaghi, M. Uhlén, P. Nyrén, *Science* **1998**, *281*, 363-365.

[62] P. Nyrén, S. Karamohamed, M. Ronaghi, *Analytical biochemistry* **1997**, *244*, 367-373.

[63] P. Nyren, Google Patents, **2001**.

[64] M. Ronaghi, S. Karamohamed, B. Pettersson, M. Uhlén, P. Nyrén, *Analytical Biochemistry* **1996**, *242*, 84-89.

[65]

[66] S. J. Benkovic, C. E. Cameron, *Methods in enzymology* **1994**, *262*, 257-269.

[67] S. Karamohamed, J. Nilsson, K. Nourizad, M. Ronaghi, B. Pettersson, P. Nyrén, *Protein expression and purification* **1999**, *15*, 381-388.

[68] V. Espinosa, A. M. Kettlun, A. Zanocco, E. Cardemil, M. Valenzuela, *Phytochemistry* **2003**, *63*, 7-14.

[69] N. Nourizad, M. Ehn, B. Gharizadeh, S. Hober, P. Nyrén, *Protein expression and purification* **2003**, *27*, 229-237.

[70] P. Nyrén, A. Lundin, *Analytical biochemistry* **1985**, *151*, 504-509.

[71] A. Ahmadian, J. Lundeberg, *Biotechniques* **2002**, *32*, 1122-1124, 1126, 1128 passim.

[72] P.-Y. Kwok, *Annual review of genomics and human genetics* **2001**, *2*, 235-258.

[73] R. B. Wallace, J. Shaffer, R. Murphy, J. Bonner, T. Hirose, K. Itakura, *Nucleic acids research* **1979**, *6*, 3543-3558.

[74] M. Jobs, *Nature Biotechnology* **1999**, *17*, 87-88.

[75] L. G. Lee, C. R. Connell, W. Bloch, *Nucleic acids research* **1993**, *21*, 3761-3766.

[76] K. J. Livak, S. Flood, J. Marmaro, W. Giusti, K. Deetz, *Genome Research* **1995**, *4*, 357-362.

[77] U. Landegren, R. Kaiser, J. Sanders, L. Hood, *Science* **1988**, *241*, 1077-1080.

[78] F. Barany, *Proceedings of the National Academy of Sciences* **1991**, *88*, 189-193.

[79] J. Banér, M. Nilsson, M. Mendel-Hartvig, U. Landegren, *Nucleic acids research* **1998**, *26*, 5073-5078.

[80] P. M. Lizardi, X. Huang, Z. Zhu, P. Bray-Ward, D. C. Thomas, D. C. Ward, *Nature genetics* **1998**, *19*, 225-232.

[81] M. Nilsson, K. Krejci, J. Koch, M. Kwiatkowski, P. Gustavsson, U. Landegren, *Nature genetics* **1997**, *16*, 252-255.

[82] M. Nilsson, H. Malmgren, M. Samiotaki, M. Kwiatkowski, B. P. Chowdhary, U. Landegren, *Science* **1994**, *265*, 2085-2088.

[83] P. D. Grossman, W. Bloch, E. Brinson, C. C. Chang, F. A. Eggerding, S. Fung, S. Woo, E. S. Winn-Deen, *Nucleic acids research* **1994**, *22*, 4527-4534.

[84] D. A. Nickerson, R. Kaiser, S. Lappin, J. Stewart, L. Hood, U. Landegren, *Proceedings of the National Academy of Sciences* **1990**, *87*, 8923-8927.

[85] A.-C. Syvänen, K. Aalto-Setälä, L. Harju, K. Kontula, H. Söderlund, *Genomics* **1990**, *8*, 684-692.

[86] A.-C. Syvänen, *Human mutation* **1999**, *13*, 1-10.

[87] K. Mullis, F. Faloona, S. Scharf, R. Saiki, G. Horn, H. Erlich, *Cold Spring Harbor symposia on quantitative biology* **1986**, *51 Pt 1*, 263-273.

[88] C. Newton, A. Graham, L. Heptinstall, S. Powell, C. Summers, N. Kalsheker, J. Smith, A. Markham, *Nucleic acids research* **1989**, *17*, 2503-2516.

[89] H. Okayama, D. T. Curiel, M. L. Brantly, M. D. Holmes, R. G. Crystal, *J Lab Clin Med* **1989**, *114*, 105-113.

[90] D. Y. Wu, L. Ugozzoli, B. K. Pal, R. B. Wallace, *Proceedings of the National Academy of Sciences* **1989**, *86*, 2757-2760.

[91] S. S. Sommer, J. D. CASSADY, J. L. SOBELL, C. D. BOTTEMA, in *Mayo Clinic Proceedings, Vol. 64*, Elsevier, **1989**, pp. 1361-1372.

[92] J. P. Day, F. Barany, D. Bergstrom, R. P. Hammer, *Nucleic acids research* **1999**, *27*, 1810-1818.

[93] A. Ahmadian, B. Gharizadeh, D. O'Meara, J. Odeberg, J. Lundeberg, *Nucleic acids research* **2001**, *29*, e121-e121.

[94] V. Lyamichev, A. L. Mast, J. G. Hall, J. R. Prudent, M. W. Kaiser, T. Takova, R. W. Kwiatkowski, T. J. Sander, M. de Arruda, D. A. Arco, *Nature biotechnology* **1999**, *17*, 292-296.

[95] J. G. Hall, P. S. Eis, S. M. Law, L. P. Reynaldo, J. R. Prudent, D. J. Marshall, H. T. Allawi, A. L. Mast, J. E. Dahlberg, R. W. Kwiatkowski, *Proceedings of the National Academy of Sciences* **2000**, *97*, 8272-8277.

[96] Z. Tsuchihashi, N. Dracopoli, *The pharmacogenomics journal* **2002**, *2*, 103-110.

[97] D. J. Beebe, G. A. Mensing, G. M. Walker, *Annual review of biomedical engineering* **2002**, *4*, 261-286.

[98] T. Chován, A. Guttman, *TRENDS in Biotechnology* **2002**, *20*, 116-122.

[99] S. C. Jakeway, A. J. de Mello, E. L. Russell, *Fresenius' journal of analytical chemistry* **2000**, *366*, 525-539.

[100] A. J. Tüdős, G. A. Besselink, R. B. Schasfoort, *Lab on a Chip* **2001**, *1*, 83-95.

[101] E. Verpoorte, *Electrophoresis* **2002**, *23*, 677-712.

[102] X. C. Huang, M. A. Quesada, R. A. Mathies, *Analytical chemistry* **2002**, *64*, 2149-2154.

[103] T. Vo-Dinh, B. Cullum, *Fresenius' journal of analytical chemistry* **2000**, *366*, 540-551.

[104] A. Manz, N. Graber, H. á. Widmer, *Sensors and actuators B: Chemical* **1990**, *1*, 244-248.

[105] T. McCreedy, *TrAC Trends in Analytical Chemistry* **2000**, *19*, 396-401.

[106] T. McCreedy, *Analytica chimica acta* **2001**, *427*, 39-43.

[107] H. Shadpour, M. L. Hupert, D. Patterson, C. Liu, M. Galloway, W. Stryjewski, J. Goettert, S. A. Soper, *Analytical chemistry* **2007**, *79*, 870-878.

[108] L. Martynova, L. E. Locascio, M. Gaitan, G. W. Kramer, R. G. Christensen, W. A. MacCrehan, *Analytical chemistry* **1997**, *69*, 4783-4789.

[109] J. A. Thompson, H. H. Bau, *Journal of Chromatography B* **2010**, *878*, 228-236.

[110] J.-M. Mermet, M. Otto, M. Valcarcel Cases, **2004**.

[111] H. Becker, L. E. Locascio, *Talanta* **2002**, *56*, 267-287.

[112] A. De Mello, *Lab on a Chip* **2002**, *2*, 31N-36N.

[113] R. M. McCormick, R. J. Nelson, M. G. Alonso-Amigo, D. J. Benvegnu, H. H. Hooper, *Analytical chemistry* **1997**, *69*, 2626-2630.

[114] H. Becker, U. Heim, *Sensors and materials* **1999**, *11*, 297-304.

[115] H. Qi, T. Chen, L. Yao, T. Zuo, *Optics and Lasers in Engineering* **2009**, *47*, 594-598.

[116] D. C. Duffy, J. C. McDonald, O. J. Schueller, G. M. Whitesides, *Analytical chemistry* **1998**, *70*, 4974-4984.

[117] J. R. Anderson, D. T. Chiu, H. Wu, O. Schueller, G. M. Whitesides, *Electrophoresis* **2000**, *21*, 27-40.

[118] P. Atkins, *Oxford University Press, Oxford* **2002**.

[119] E. Verpoorte, *Lab on a Chip* **2003**, *3*, 60N-68N.

[120] H. Kawaguchi, *Progress in Polymer Science* **2000**, *25*, 1171-1210.

[121] M. B. Meza, *Drug Discovery Today* **2000**, *5*, 38-41.

[122] L. B. Bangs, *Pure and applied chemistry* **1996**, *68*, 1873-1879.

[123] D. S. Peterson, *Lab on a Chip* **2005**, *5*, 132-139.

[124] C. Lim, Y. Zhang, *Biosensors and Bioelectronics* **2007**, *22*, 1197-1204.

[125] A.-C. Syvänen, G. R. Taylor, *Human mutation* **2004**, *23*, 401-405.

[126] L. Directed, *Science* **1991**, *251*, 767.

[127] D. Shalon, S. J. Smith, P. O. Brown, *Genome research* **1996**, *6*, 639-645.

[128] A. Marshall, J. Hodgson, *Nature biotechnology* **1998**, *16*, 27-32.

[129] R. K. Saiki, P. S. Walsh, C. H. Levenson, H. A. Erlich, *Proceedings of the National Academy of Sciences* **1989**, *86*, 6230-6234.

[130] T. T. Nikiforov, Y.-H. Rogers, *Analytical biochemistry* **1995**, *227*, 201-209.

[131] R. D. Mitra, G. M. Church, *Nucleic Acids Research* **1999**, *27*, e34-e39.

[132] A. Oliphant, D. L. Barker, J. R. Stuelpnagel, M. S. Chee, *Biotechniques* **2002**, *32*, 56-58.

[133] A. C. Pease, D. Solas, E. J. Sullivan, M. T. Cronin, C. P. Holmes, S. Fodor, *Proceedings of the National Academy of Sciences* **1994**, *91*, 5022-5026.

[134] J. G. Hacia, *Nature genetics* **1999**, *21*, 42-47.

[135] E. Southern, U. Maskos, J. Elder, *Genomics* **1992**, *13*, 1008-1017.

[136] N. Tibanyenda, S. H. De Bruin, C. A. Haasnoot, G. A. van der Marel, J. H. van Boom, C. W. Hilbers, *European journal of biochemistry / FEBS* **1984**, *139*, 19-27.

[137] T. Pastinen, A. Kurg, A. Metspalu, L. Peltonen, A. C. Syvanen, *Genome Res* **1997**, *7*, 606-614.

[138] K. Lindroos, S. Sigurdsson, K. Johansson, L. Rönnblom, A. C. Syvänen, *Nucleic acids research* **2002**, *30*, e70-e70.

[139] J. M. Shumaker, A. Metspalu, C. T. Caskey, *Human mutation* **1996**, *7*, 346-354.

[140] S. Dubiley, E. Kirillov, A. Mirzabekov, *Nucleic Acids Research* **1999**, *27*, e19-i-e19-vi.

[141] D. O'Meara, A. Ahmadian, J. Odeberg, J. Lundeberg, *Nucleic acids research* **2002**, *30*, e75-e75.

[142] K. L. Gunderson, X. C. Huang, M. S. Morris, R. J. Lipshutz, D. J. Lockhart, M. S. Chee, *Genome research* **1998**, *8*, 1142-1153.

[143] M. Chee, R. Yang, E. Hubbell, A. Berno, X. C. Huang, D. Stern, J. Winkler, D. J. Lockhart, M. S. Morris, S. P. Fodor, *Science* **1996**, *274*, 610-614.

[144] C. F. Edman, D. E. Raymond, D. J. Wu, E. Tu, R. G. Sosnowski, W. F. Butler, M. Nerenberg, M. J. Heller, *Nucleic Acids Research* **1997**, *25*, 4907-4914.

[145] S. C. Jacobson, R. Hergenroder, L. B. Koutny, J. M. Ramsey, *Analytical chemistry* **1994**, *66*, 1114-1118.

[146] A. Manz, D. J. Harrison, E. M. Verpoorte, J. C. Fettinger, A. Paulus, H. Lüdi, H. M. Widmer, *Journal of Chromatography A* **1992**, *593*, 253-258.

[147] D. J. Harrison, K. Fluri, K. Seiler, Z. Fan, C. S. Effenhauser, A. Manz, *SCIENCE-NEW YORK THEN WASHINGTON-* **1993**, *261*, 895-895.

[148] K. B. Jacobson, H. F. Arlinghaus, M. V. Buchanan, C. Chung-Hsuan, G. L. Glish, R. L. Hettich, S. A. McLuckey, *Genetic Analysis: Biomolecular Engineering* **1991**, *8*, 223-229.

[149] V. Dolník, S. Liu, S. Jovanovich, *Electrophoresis* **2000**, *21*, 41-54.

[150] J. Li, P. Thibault, N. H. Bings, C. D. Skinner, C. Wang, C. Colyer, J. Harrison, *Analytical chemistry* **1999**, *71*, 3036-3045.

[151] P. F. Gavin, A. G. Ewing, *Analytical chemistry* **1997**, *69*, 3838-3845.

[152] P. F. Gavin, A. G. Ewing, *Journal of Microcolumn Separations* **1998**, *10*, 357-364.

[153] U. Backofen, F.-M. Matysik, C. E. Lunte, *Analytical chemistry* **2002**, *74*, 4054-4059.

[154] S. Liu, Y. Shi, W. W. Ja, R. A. Mathies, *Analytical chemistry* **1999**, *71*, 566-573.

[155] R. A. Mathies, P. C. Simpson, A. T. Woolley, in *Micro Total Analysis Systems' 98*, Springer, **1998**, pp. 1-6.

[156] P. C. Simpson, D. Roach, A. T. Woolley, T. Thorsen, R. Johnston, G. F. Sensabaugh, R. A. Mathies, *Proceedings of the National Academy of Sciences* **1998**, *95*, 2256-2261.

[157] A. T. Woolley, G. F. Sensabaugh, R. A. Mathies, *Analytical chemistry* **1997**, *69*, 2181-2186.

[158] B. M. Paegel, C. A. Emrich, G. J. Wedemayer, J. R. Scherer, R. A. Mathies, *Proceedings of the National Academy of Sciences* **2002**, *99*, 574-579.

[159] B. M. Paegel, L. D. Hutt, P. C. Simpson, R. A. Mathies, *Analytical chemistry* **2000**, *72*, 3030-3037.

[160] I. Kheterpal, J. R. Scherer, S. M. Clark, A. Radhakrishnan, J. Ju, C. L. Ginther, G. F. Sensabaugh, R. A. Mathies, *Electrophoresis* **1996**, *17*, 1852-1859.

[161] J. R. Scherer, I. Kheterpal, A. Radhakrishnan, W. W. Ja, R. A. Mathies, *Electrophoresis* **1999**, *20*, 1508-1517.

[162] A. P. Sassi, A. Paulus, I. D. Cruzado, T. Bjornson, H. H. Hooper, *Journal of Chromatography A* **2000**, *894*, 203-217.

[163] Y.-H. Chen, W.-C. Wang, K.-C. Young, T.-T. Chang, S.-H. Chen, *Clinical chemistry* **1999**, *45*, 1938-1943.

[164] M. A. Northrup, M. Ching, R. White, R. Watson, in *Transducers, Vol. 93*, **1993**, pp. 924-926.

[165] P. Wilding, M. A. Shoffner, L. J. Kricka, *Clinical Chemistry* **1994**, *40*, 1815-1818.

[166] M. A. Northrup, B. Benett, D. Hadley, P. Landre, S. Lehew, J. Richards, P. Stratton, *Analytical chemistry* **1998**, *70*, 918-922.

[167] M. A. Burns, C. H. Mastrangelo, T. S. Sammarco, F. P. Man, J. R. Webster, B. Johnsons, B. Foerster, D. Jones, Y. Fields, A. R. Kaiser, *Proceedings of the National Academy of Sciences* **1996**, *93*, 5556-5561.

[168] S. C. Jacobson, J. M. Ramsey, *Analytical chemistry* **1996**, *68*, 720-723.

[169] A. T. Woolley, D. Hadley, P. Landre, A. J. deMello, R. A. Mathies, M. A. Northrup, *Analytical chemistry* **1996**, *68*, 4081-4086.

[170] M. A. Burns, B. N. Johnson, S. N. Brahmasandra, K. Handique, J. R. Webster, M. Krishnan, T. S. Sammarco, P. M. Man, D. Jones, D. Heldsinger, *Science* **1998**, *282*, 484-487.

[171] T. Thorsen, S. J. Maerkl, S. R. Quake, *Science* **2002**, *298*, 580-584.

[172] A. Y. Fu, H.-P. Chou, C. Spence, F. H. Arnold, S. R. Quake, *Analytical chemistry* **2002**, *74*, 2451-2457.

[173] C. L. Hansen, E. Skordalakes, J. M. Berger, S. R. Quake, *Proceedings of the National Academy of Sciences* **2002**, *99*, 16531-16536.

[174] S. Quake, *Electrophoresis* **2002**, *23*, 1531-1536.

[175] M. C. Needels, D. G. Jones, E. H. Tate, G. L. Heinkel, L. M. Kochersperger, W. J. Dower, R. W. Barrett, M. A. Gallop, *Proceedings of the National Academy of Sciences* **1993**, *90*, 10700-10704.

[176] R. J. Fulton, R. L. McDade, P. L. Smith, L. J. Kienker, J. R. Kettman, *Clinical chemistry* **1997**, *43*, 1749-1756.

[177] A. W. Czarnik, *Current opinion in chemical biology* **1997**, *1*, 60-66.

[178] B. Armstrong, M. Stewart, A. Mazumder, *Cytometry* **2000**, *40*, 102-108.

[179] H. Cai, P. S. White, D. Torney, A. Deshpande, Z. Wang, B. Marrone, J. P. Nolan, *Genomics* **2000**, *66*, 135-143.

[180] J. Chen, M. A. Iannone, M.-S. Li, J. D. Taylor, P. Rivers, A. J. Nelsen, K. A. Slentz-Kesler, A. Roses, M. P. Weiner, *Genome research* **2000**, *10*, 549-557.

[181] M. A. Iannone, J. D. Taylor, J. Chen, M. S. Li, P. Rivers, K. A. Slentz-Kesler, M. P. Weiner, *Cytometry* **2000**, *39*, 131-140.

[182] K. V. Rao, P. W. Stevens, J. G. Hall, V. Lyamichev, B. P. Neri, D. M. Kelso, *Nucleic acids research* **2003**, *31*, e66-e66.

[183] K. L. Michael, L. C. Taylor, S. L. Schultz, D. R. Walt, *Analytical chemistry* **1998**, *70*, 1242-1248.

[184] F. J. Steemers, J. A. Ferguson, D. R. Walt, *Nature biotechnology* **2000**, *18*, 91-94.

[185] J.-B. Fan, X. Chen, M. K. Halushka, A. Berno, X. Huang, T. Ryder, R. J. Lipshutz, D. J. Lockhart, A. Chakravarti, *Genome Research* **2000**, *10*, 853-860.

[186] D. R. Greaves, R. K. Patient, *The EMBO journal* **1985**, *4*, 2617-2626.

[187] J. H. Leamon, W. L. Lee, K. R. Tartaro, J. R. Lanza, G. J. Sarkis, A. D. deWinter, J. Berka, K. L. Lohman, *Electrophoresis* **2003**, *24*, 3769-3777.

[188] H. Craighead, *Nature* **2006**, *442*, 387-393.

[189] R. Daw, J. Finkelstein, *Nature* **2006**, *442*, 367-367.

[190] A. J. deMello, *Nature* **2006**, *442*, 394-402.

[191] J. El-Ali, P. K. Sorger, K. F. Jensen, *Nature* **2006**, *442*, 403-411.

[192] D. Janasek, J. Franzke, A. Manz, *Nature* **2006**, *442*, 374-380.

[193] P. Yager, T. Edwards, E. Fu, K. Helton, K. Nelson, M. R. Tam, B. H. Weigl, *Nature* **2006**, *442*, 412-418.

[194] M. J. Swickrath, S. D. Burns, G. E. Wnek, *Sensors and Actuators B: Chemical* **2009**, *140*, 656-662.

[195] D. S. Kim, S. W. Lee, T. H. Kwon, S. S. Lee, *Journal of micromechanics and microengineering* **2004**, *14*, 798.

[196] M. Abdelgawad, M. W. Watson, A. R. Wheeler, *Lab on a Chip* **2009**, *9*, 1046-1051.

[197] G. M. Walker, D. J. Beebe, *Lab on a Chip* **2002**, *2*, 131-134.

[198] M. Tokeshi, T. Minagawa, K. Uchiyama, A. Hibara, K. Sato, H. Hisamoto, T. Kitamori, *Analytical chemistry* **2002**, *74*, 1565-1571.

[199] M. Marques, P. Fernandes, J. Cabral, P. Žnidaršič-Plazl, I. Plazl, *Chemical Engineering Journal* **2010**, *160*, 708-714.

[200] B. D. Piorek, S. J. Lee, J. G. Santiago, M. Moskovits, S. Banerjee, C. D. Meinhart, *Proceedings of the National Academy of Sciences* **2007**, *104*, 18898-18901.

[201] L. Hong, T. Pan, *Lab on a Chip* **2010**, *10*, 3271-3276.

[202] L. Hong, T. Pan, *Journal of Microelectromechanical Systems* **2010**, *19*, 246-253.

[203] G. M. Whitesides, *Nature* **2006**, *442*, 368-373.

[204] D. R. Reyes, D. Iossifidis, P.-A. Auroux, A. Manz, *Analytical chemistry* **2002**, *74*, 2623-2636.

[205] P.-A. Auroux, D. Iossifidis, D. R. Reyes, A. Manz, *Analytical chemistry* **2002**, *74*, 2637-2652.

[206] T. Vilkner, D. Janasek, A. Manz, *Analytical chemistry* **2004**, *76*, 3373-3386.

[207] J. West, M. Becker, S. Tombrink, A. Manz, *Analytical chemistry* **2008**, *80*, 4403-4419.

[208] R. Mukhopadhyay, *Analytical chemistry* **2006**, *78*, 1401-1404.

[209] S.-Y. Teh, R. Lin, L.-H. Hung, A. P. Lee, *Lab on a Chip* **2008**, *8*, 198-220.

[210] R. B. Fair, *Microfluidics and Nanofluidics* **2007**, *3*, 245-281.

[211] V. Srinivasan, V. K. Pamula, R. B. Fair, *Lab on a Chip* **2004**, *4*, 310-315.

[212] J. A. Schwartz, J. V. Vykoukal, P. R. Gascoyne, *Lab on a Chip* **2004**, *4*, 11-17.

[213] U. Lehmann, C. Vandevyver, V. K. Parashar, M. A. M. Gijs, *Angewandte Chemie International Edition* **2006**, *45*, 3062-3067.

[214] J. Pipper, M. Inoue, L. F. P. Ng, P. Neuzil, Y. Zhang, L. Novak, *Nat Med* **2007**, *13*, 1259-1263.

[215] J. Pipper, Y. Zhang, P. Neuzil, T.-M. Hsieh, *Angewandte Chemie International Edition* **2008**, *47*, 3900-3904.

[216] A. A. Garcia, A. Egatz-Gómez, S. A. Lindsay, P. Dominguez-Garcia, S. Melle, M. Marquez, M. A. Rubio, S. Picraux, D. Yang, P. Aella, *Journal of Magnetism and Magnetic Materials* **2007**, *311*, 238-243.

[217] J. Schneider, A. Egatz-Gómez, S. Melle, S. Lindsay, P. Dominguez-Garcia, M. Rubio, M. Marquez, A. A. García, *Colloids and Surfaces A: Physicochemical and Engineering Aspects* **2008**, *323*, 19-27.

[218] T. Ohashi, H. Kuyama, N. Hanafusa, Y. Togawa, *Biomed Microdevices* **2007**, *9*, 695-702.

[219] N.-T. Nguyen, K. M. Ng, X. Huang, *Applied Physics Letters* **2006**, *89*, 052509.

[220] N.-T. Nguyen, A. Beyzavi, K. M. Ng, X. Huang, *Microfluidics and Nanofluidics* **2007**, *3*, 571-579.

[221] Y. Sun, N.-T. Nguyen, Y. C. Kwok, *Analytical chemistry* **2008**, *80*, 6127-6130.

[222] Y. Sun, Y. C. Kwok, N.-T. Nguyen, *Lab on a Chip* **2007**, *7*, 1012-1017.

[223] M. Shikida, N. Nagao, R. Imai, H. Honda, M. Okochi, H. Ito, K. Sato, *Journal of Micromechanics and Microengineering* **2008**, *18*, 035034.

[224] M. Shikida, K. Takayanagi, H. Honda, H. Ito, K. Sato, *Journal of Micromechanics and Microengineering* **2006**, *16*, 1875.

[225] M. Shikida, K. Takayanagi, K. Inouchi, H. Honda, K. Sato, *Sensors and Actuators B: Chemical* **2006**, *113*, 563-569.

[226] U. Lehmann, D. de Courten, C. Vandevyver, V. Parashar, M. Gijs, *Microelectronic engineering* **2007**, *84*, 1669-1672.

[227] U. Lehmann, S. Hadjidj, V. K. Parashar, C. Vandevyver, A. Rida, M. A. Gijs, *Sensors and Actuators B: Chemical* **2006**, *117*, 457-463.

[228] Z. Long, A. M. Shetty, M. J. Solomon, R. G. Larson, *Lab on a Chip* **2009**, *9*, 1567-1575.

[229] H. Tsuchiya, M. Okochi, N. Nagao, M. Shikida, H. Honda, *Sensors and Actuators B: Chemical* **2008**, *130*, 583-588.

[230] N. Pamme, *Lab on a Chip* **2006**, *6*, 24-38.

[231] H.-Y. Kim, H. J. Lee, B. H. Kang, *Journal of colloid and interface science* **2002**, *247*, 372-380.

[232] S. Hodges, O. Jensen, J. Rallison, *Journal of Fluid Mechanics* **2004**, *512*, 95-131.

[233] Y. Zhang, T.-H. Wang, *Advanced Materials* **2013**, *25*, 2903-2908.

[234] I. A. Eydelnant, U. Uddayasankar, M. W. Liao, A. R. Wheeler, *Lab on a Chip* **2012**, *12*, 750-757.

[235] L. K. Fiddes, V. N. Luk, S. H. Au, A. H. Ng, V. Luk, E. Kumacheva, A. R. Wheeler, *Biomicrofluidics* **2012**, *6*, 014112.

[236] D. Witters, N. Vergauwe, S. Vermeir, F. Ceyssens, S. Liekens, R. Puers, J. Lammertyn, *Lab on a Chip* **2011**, *11*, 2790-2794.

[237] J. Gong, *Lab on a Chip* **2008**, *8*, 898-906.

[238] Y. Zhang, S. Park, K. Liu, J. Tsuan, S. Yang, T.-H. Wang, *Lab on a Chip* **2011**, *11*, 398-406.

[239] N.-T. Nguyen, G. Zhu, Y.-C. Chua, V.-N. Phan, S.-H. Tan, *Langmuir* **2010**, *26*, 12553-12559.

[240] Y. Zhang, D. J. Shin, T.-H. Wang, *Lab on a chip* **2013**, *13*, 4827-4831.

[241] L. Chen, A. Manz, P. J. Day, *Lab on a Chip* **2007**, *7*, 1413-1423.

[242] J. K.-K. Ng, H. Feng, W.-T. Liu, *Analytica chimica acta* **2007**, *582*, 295-303.

[243] K.-Y. Lien, C.-J. Liu, Y.-C. Lin, P.-L. Kuo, G.-B. Lee, *Microfluidics and Nanofluidics* **2009**, *6*, 539-555.

[244] R. Elghanian, J. J. Storhoff, R. C. Mucic, R. L. Letsinger, C. A. Mirkin, *Science* **1997**, *277*, 1078-1081.

[245] W.-F. Fang, W.-J. Chen, J.-T. Yang, *Sensors and Actuators B: Chemical* **2014**, *192*, 77-82.

[246] C. J. Huang, W. F. Fang, M. S. Ke, H. Y. E. Chou, J. T. Yang, *Lab on a Chip* **2014**, *14*, 2057-2062.

[247] D. J. Boles, J. L. Benton, G. J. Siew, M. H. Levy, P. K. Thwar, M. A. Sandahl, J. L. Rouse, L. C. Perkins, A. P. Sudarsan, R. Jalili, V. K. Pamula, V. Srinivasan, R. B. Fair, P. B. Griffin, A. E. Eckhardt, M. G. Pollack, *Analytical chemistry* **2011**, *83*, 8439-8447.

[248] E. R. F. Welch, Y.-Y. Lin, A. Madison, R. B. Fair, *Biotechnology Journal* **2011**, *6*, 165-176.

[249] A. M. Borman, C. J. Linton, D. Oliver, M. D. Palmer, A. Szekely, E. M. Johnson, *Journal of Clinical Microbiology* **2010**, *48*, 3648-3653.

[250] J. D. Watson, F. H. Crick, *Annals of the New York Academy of Sciences* **1995**, *758*, 13-14.

[251] E. S. Lander, L. M. Linton, B. Birren, C. Nusbaum, M. C. Zody, J. Baldwin, K. Devon, K. Dewar, M. Doyle, W. FitzHugh, *Nature* **2001**, *409*, 860-921.

[252] J. C. Venter, M. D. Adams, E. W. Myers, P. W. Li, R. J. Mural, G. G. Sutton, H. O. Smith, M. Yandell, C. A. Evans, R. A. Holt, *science* **2001**, *291*, 1304-1351.

[253] M. O. Altmeyer, A. Manz, P. Neužil, *Analytical chemistry* **2015**, *87*, 5997-6003.

[254] C. D. Ahrberg, A. Manz, *RSC Advances* **2016**, *6*, 42076-42080.

[255] Z. Guttenberg, H. Müller, H. Habermüller, A. Geisbauer, J. Pipper, J. Felbel, M. Kielpinski, J. Scriba, A. Wixforth, *Lab on a Chip* **2005**, *5*, 308-317.

[256] P. Neuzil, J. Pipper, T. M. Hsieh, *Molecular bioSystems* **2006**, *2*, 292-298.

[257] P. Neuzil, C. Zhang, J. Pipper, S. Oh, L. Zhuo, *Nucleic acids research* **2006**, *34*, e77-e77.

[258] P. Neuzil, L. Novak, J. Pipper, S. Lee, L. F. Ng, C. Zhang, *Lab on a Chip* **2010**, *10*, 2632-2634.

[259] C. D. Ahrberg, B. R. Ilic, A. Manz, P. Neužil, *Lab on a Chip* **2016**, *16*, 586-592.

[260] C. D. Ahrberg, P. Neužil, *Scientific Reports* **2015**, *5*, 12595.

[261] C. D. Ahrberg, A. Manz, P. Neužil, *Analytical chemistry* **2016**, *88*, 4803-4807.

[262] C. D. Ahrberg, B. R. Ilic, A. Manz, P. Neuzil, *Lab on a Chip* **2016**, *16*, 586-592.

[263] A. Přibylka, A. V. Almeida, M. O. Altmeyer, J. Petr, J. Ševčík, A. Manz, P. Neužil, *Lab on a Chip* **2013**, *13*, 1695-1698.

[264] A. V. Almeida, A. Manz, P. Neuzil, *Lab on a Chip* **2016**, *16*, 1063-1071.

[265] M. Abdelgawad, A. R. Wheeler, *Advanced Materials* **2009**, *21*, 920-925.

[266] M. G. Pollack, V. K. Pamula, V. Srinivasan, A. E. Eckhardt, *Expert Review of Molecular Diagnostics* **2011**, *11*, 393-407.

[267] S. K. Cho, H. Moon, *Biochip Journal* **2008**, *2*, 79-96.

[268] N.-T. Nguyen, *Microfluidics and Nanofluidics* **2012**, *12*, 1-16.

[269] S. K. Cho, H. Moon, C.-J. Kim, *Journal of microelectromechanical systems* **2003**, *12*, 70-80.

[270] C. Sung Kwon, F. Shih-Kang, M. Hyejin, K. Chang-Jin, in *Technical Digest. MEMS 2002 IEEE International Conference. Fifteenth IEEE International Conference on Micro Electro Mechanical Systems (Cat. No.02CH37266)*, **2002**, pp. 32-35.

[271] P. Neužil, W. Sun, T. Karásek, A. Manz, *Applied Physics Letters* **2015**, *106*, 024104.

[272] J. Pipper, Y. Zhang, P. Neuzil, T. M. Hsieh, *Angewandte Chemie International Edition* **2008**, *47*, 3900-3904.

[273] P. Neužil, W. Sun, T. Karasek, A. Manz, *Applied Physics Letters* **2015**, *106*, 024104.

[274] J. Pipper, M. Inoue, L. F. Ng, P. Neuzil, Y. Zhang, L. Novak, *Nature medicine* **2007**, *13*, 1259-1263.